Interim Report No. 65-2

STUDY OF FLUID TRANSIENTS IN CLOSED CONDUITS

Contract: NAS 8 11302

Interim Report No.: 65-2

Contractor: Oklahoma State University, Stillwater, Oklahoma

Segment Generating Report: School of Mechanical Engineering
Fluid Power and Controls Laboratory

STUDY OF FLUID TRANSIENTS IN CLOSED CONDUITS

Contract: NAS 8 11302

Control Number: DCN-1-4-50-01153-01(IF)
CPB 02-1209-64

Date: 18 March 1965

Prepared for: George C. Marshall Space Flight Center, Huntsville, Alabama

Prepared by: E. C. Fitch, Project Co-director
J. D. Parker, Project Co-director
C. R. Gerlach, Project Leader
H. C. Hewitt, Research Assistant
G. Maples, Research Assistant
E. Mitwally, Research Assistant
R. Stuntz, Research Assistant

Approved:

E. C. Fitch

J. D. Parker

TABLE OF CONTENTS

LIST OF FIGURES

LIST OF TABLES

LIST OF SYMBOLS

a	Thermal diffusivity
$\frac{a_v}{a_l}$	Cavitation form parameter based on areas
A	Constant at integration Conduit cross-sectional area
B	Constant of integration
c	Speed of sound in fluid
c_o	Isentropic speed of sound in fluid
c_v	Specific heat, constant volume
C_1	Chord length
C_2	369 nT ft-#f
C_e	Electrically equivalent capacitance
C_p	Pressure coefficient
C_{P_l}	Specific heat of the liquid
$C_{P_{min_s}}$	Minimum pressure coefficient of a smooth surface
C_q	Conduit capacitance based on flow rate
C_v	Conduit capacitance based on velocity
C_w	Conduit capacitance based on weight flow rate
D	Conduit diameter
$\frac{D}{D_t}$	Substantial derivative
D_i	Conduit inside diameter
D_o	Conduit outside diameter

D^*	Critical bubble diameter
e_j	Voltage at point j
f	Tube wall factor, Equation (2.44) Parameter defined by Equation (6.53)
F_L	Froude's number
g	Acceleration due to gravity
h	Height of roughness element Tube wall thickness
h(z,s)	A function of integration
H	Boundary layer shape parameter
i	Imaginary unit, $\sqrt{-1}$
i_j	Electrical current at point j
I_q	Fluid inertance based on flow rate
I_v	Fluid inertance based on velocity
I_w	Fluid inertance based on weight flow rate
$J_o(x)$	Bessel function of order zero and argument x
$J_1(x)$	Bessel function of order one and argument x
k	Coefficient of heat conduction Parameter defined by Equation (6.25)
K	Cavitation number
K_o	Cavitation number evaluated at reference plane "o"
$\overline{K_o}$	Modified cavitation number, Equation (4.9)
K_d	Desinent cavitation number evaluated at plane of desinent cavitation
K_i	Incipient cavitation number evaluated at plane of incipient cavitation
K_{do}	Desinent cavitation number evaluated at reference plane "o"
K_{io}	Incipient cavitation number evaluated at reference plane "o"

K_{ro}	Incipient cavitation number of roughness element evaluated at reference plane "o"
L	Conduit length
L_l	Length or linear dimension
L_e	Electrically equivalent inductance
L_v	Heat of vaporization
n	Number of moles of gas Index number
N	Number of nuclei per unit volume of the fluid
$p = p(t)$	Fluid stream pressure, function of time
p_b	Back pressure
p_d	Stream pressure at plane of desinent cavitation
p_e	Exit pressure
p_g	Partial pressure of gas
p_i	Stream pressure at plane of incipient cavitation
p_v	Vapor pressure
p_{do}	Stream pressure for desinent cavitation evaluated at reference "o"
p_{io}	Stream pressure for incipient cavitation evaluated at reference "o"
p^*	$(p-p_v)$ min.
p_∞	Pressure at a distance from a bubble
P(s)	Transformed pressure, function of s
$P_j(s)$	Transformed pressure at point j
P_e	Pecle't number
q	Fluid flow rate
$\dot{q}$	Heat generated per second per unit volume
q_b	Heat flux density across vapor - liquid interface

$\bar{q}$	Vector heat flow rate
$Q(x)$	Heat liberated at bubble radius
r	Radial coordinate position
$\mathbf{r}$	Unit vector in radial direction
r_o	Conduit inner radius
R	Bubble radius
$R(v)$	Conduit resistance
R_1	Resistance coefficient, Equation (2.16)
$\bar{R}$	Radius of centerline of elbow
R_e	Reynolds number Electrically equivalent resistance
R^*	Critical bubble radius
s	Laplace variable
t	Time
$\bar{t}_{max.}$	Maximum thickness of hydrofoil
T	Temperature
T_o	Initial temperature
T_s	Saturation temperature at a given pressure
T_{rs}	Temperature of saturated vapor
$T_{\infty s}$	Saturation temperature away from the bubble
T_{ws}	Saturation temperature at the wall
T_∞	Temperature away from any bubbles
T_w	Wall temperature
ΔT	$T_\infty - T_s$
v	Axial velocity
v_c	Conduit wall velocity
v_ℓ	Specific volume of liquid

v_o	Steady flow velocity
v_r	Radial velocity
v_v	Specific volume of vapor
v_z	Axial velocity
$\bar{v}$	Vector velocity (see Figure 2.1)
V(s)	Transformed velocity
V	Stream velocity
$V_c(s)$	Transformed conduit wall velocity
V_o	Stream velocity at reference "o"
V_t	Stream velocity at throat
W	Weber number
x	Distance measured along hydrofoil centerline
z	Axial coordinate
Z_c	Characteristic impedance (see Equation 2.26)
Z_c'	Characteristic impedance (see Equation 6.37)
α	Air content
α/α_s	Relative air content
β	Parameter
$\bar{\beta}$	1.03 psi/ppm
β^*	$R/2\sqrt{at}$
Γ	Propagation constant
δ	Boundary layer thickness
δ^*	Displacement thickness
ϵ	Parameter defined by Equation (2.22)
θ	Momentum thickness
θ	Coordinate angle
$\boldsymbol{\theta}$	Unit vector in $\boldsymbol{\theta}$ direction
κ	Bulk modulus of elasticity of fluid
μ	Absolute viscosity

ν	Kinematic viscosity
ξ	Parameter defined by Equation (2.20)
ρ	Mass density
ρ_L	Liquid mass density
ρ_o	Average mass density
ρ_v	Vapor mass density
σ	Surface tension
σ_o	Prandtl number
φ	Scalor field
φ_f	Scalor field related to body force, see Equation (6.45)
φ_1	Scalor field
$\hat{\varphi}_1$	Transformed φ_1
Φ	Dissipation function
$\bar{\psi}$	Vector field
$\bar{\psi}_1$	Vector field
ψ_1	Related to $\bar{\psi}_1$ by $\bar{\psi}_1 = \Theta\ \psi_1$
$\bar{\psi}_f$	Vector field related with body force, see Equation (6.45)
$\hat{\psi}_1$	Transformed ψ_1
ω	Angular frequency
∇	Vector operator del

CHAPTER I

Introduction

This report covers the work performed since the writing of Interim Report No. 64-1 as authorized by contract NAS 8 11302.

Scope of Work

The original scope of work for this study may be broken down into four phases as follows:

A. Complete a comprehensive review of past literature.

B. Develop a mathematical model which describes the transients in fluid conduits and shows the effects of fluid inertance, fluid capacitance, and fluid resistance. Develop an analog model based on the mathematical model which will simulate the fluid transients in a cryogenic closed conduit.

C. Conduct an experimental study to verify the conduit simulation models. Make necessary modifications in the models to achieve appropriate agreement with laboratory data.

D. Study the effects of components, derive their associated transfer functions, and add this input to the paragraph C above to obtain the effects of added components.

In order to most effectively accomplish this work, the project personnel were divided into two teams with one team concentrating

their efforts on the study of two-phase phenomena as concerned with cryogenic fluids. The other team is studying transient fluid conduits with emphasis on one-phase fluids. The efforts of both teams are being combined to study the effects of two-phase fluids on the characteristics of flow in fluid conduits.

Summary of Progress to Date

The work which has been done to date toward the successful completion of the work objective as indicated in the scope may be summarized as follows:

A. An exhaustive survey of previous investigations has been completed for both the single-phase and two-phase areas of the study.

B. A detailed transfer function model for a viscous, two-dimensional, single-phase conduit has been derived and appears to be capable of extension to cover preliminary two-phase and cavitation studies. This model has been experimentally verified for the single-phase case.

C. A conduit model showing the effects of body forces and system vibration has been derived. The equipment necessary to experimentally verify this model for single-phase flow is being constructed.

D. An investigation of the nonlinear effects associated with conduit dynamics has been made using a linearized second-order equation of motion.

E. The design of a hydrodynamic tunnel capable of handling liquid nitrogen has been completed and construction is about to begin.

F. A bubble observation chamber, suitable for studies with liquid nitrogen, has been designed and constructed.

The following chapters of this report give a detailed account of this work.

Summary of Proposed Work

The work proposed for the remainder of the contract period may be summarized as follows:

A. Further extend the single-phase conduit model to include the effects of components.

B. Investigate the applicability of analog solutions for the lumped-parameter model.

C. Verify experimentally the component, body-force, and nonlinear models.

D. Investigate possible extensions of single-phase conduit models to cover preliminary two-phase and cavitation studies.

E. Complete construction of the hydrodynamic tunnel and use it to study the effect of acceleration on relaxation time in both limited and profuse cavitation, the conditions for cavity formation, and the effect of flow patterns on cavitation in bends.

F. Bubble growth and collapse in nitrogen will be observed in the bubble observation chamber using a high speed camera. Both static and transient pressure conditions will be studied.

Recommendations for Future Investigations

Although the work which will be accomplished in this first year of study represents a significant contribution in the field of conduit dynamics, we feel that due to the experience and knowledge gained during this period we will be at a stage where we can undertake more specific and practical problems of interest to NASA. Areas which it is felt deserve further study and will be rewarding to the space program include:

A. Study the formation and behavior of bubbles in conduit systems subject to vibrations.

B. Extend the concepts of the present conduit models to incorporate tubulence, bubbles and cavitation effects.

C. Continue the analytical and experimental investigation of the significance of the nonlinear effects in conduits and their components.

D. Investigate experimentally the effect of flow patterns upon cavitation for flow in bends and other geometries using liquid nitrogen and other flowing fluids.

CHAPTER II

Review of the Literature for Single-Phase Conduit Systems

2.1 Definition of the Problem

The problems associated with the design or analysis of fluid systems are challenging, particularly for systems involving unsteady flows. A typical system may contain many components such as pumps, valves, actuators, reservoirs, motors, etc. generally connected together in some manner by fluid lines. A complete analysis of such a system must involve not only the components but also the fluid lines. This is particularly true for unsteady conditions where the effects of the fluid lines have in some cases caused otherwise well designed systems to be inoperable.

In general, the area of study associated with the flow of fluids through conduits is called "Conduit Dynamics". A rigorous application of Conduit Dynamics to the study of a fluid line involves a complete study of the fluid itself plus a study of the effect which the pipe or conduit has upon the fluid. For example, in making computations involving the effect of fluid compressibility we may make large errors if we do not include the compressibility effect due to the elasticity of the pipe walls. Conduit Dynamics includes fluid studies which are associated with the two areas known as "water hammer" and "surge".

The complete description of a fluid line in which the effects of compressibility, fluid inertia, viscosity and heat transfer are important involves the simultaneous solution of the following equations:

1) Equations of Motion (Navier-Stokes equations)

2) Continuity equation

3) Energy equation

4) Equation of state of fluid

5) Dynamical equation of motion of tube or conduit

Also, application of the boundary and initial conditions is necessary in order that answers may be arrived at for particular cases of interest. An exact description, i.e. an exact solution of the governing equations, is nearly impossible. However, by means of various simplifying assumptions, it is possible to arrive at solutions which yield rather good quantitative descriptions of the system being analyzed. In many cases these simplifying assumptions are questionable. By means of the discussions which follow, an effort will be made to present, in an organized manner, the work which has been accomplished by previous investigators. Indications will be made, where possible, of the application and limitation of the ideas.

2.2 Lumped and Distributed Systems

The physical properties of all real systems are distributed with respect to time and space. The extent or influence of this distributive effect varies greatly, depending on the particular system being studied. For the case of the fluid systems which will concern us, this distributive effect may or may not need be considered. In general, those physical systems which are described by relations involving distributed

parameters are called distributed parameter systems. The dynamical equations for distributed systems are generally partial differential equations. Those systems which do not involve distributed parameters are called lumped parameter systems. The dynamical equations for lumped systems are generally ordinary differential equations. If we take a distributed parameter system, average the effect of the distributed parameter(s), and concentrate this average at some point then we say that we have "lumped" the system. The validity of approximating a distributed system by a lumped system or systems depends upon the operating conditions of the system and also upon the manner in which the lumping is performed.

The distributed effects of fluid systems which will concern us are those due to compressibility, inertia and resistance. In the literature, those studies which involve compressibility and inertia are called "water hammer studies" while those involving mainly inertia effects are called "surge studies."

2.3 Linear Distributed Models - No Conduit Wall Effects

For the purposes of this discussion, consider a fluid conduit system to be describable in terms of a cylindrical coordinate system as shown in Figure 2.1. Unless otherwise indicated we will assume laminar, axi-symmetric flow. Also, for brevity, we will use vector notation where applicable (a summary of vector notation was given in Interim Report No. 64-1 or see reference 1).

As indicated in the introduction, a complete description of the system involves solving the following equations.

A) The Navier-Stokes Equations [2, 3]*

Assuming a fluid of constant viscosity, we may write

$$\rho \frac{D\bar{v}}{Dt} = -\nabla p + \mu\left\{\frac{4}{3}\nabla(\nabla\cdot\bar{v}) - \nabla(\nabla\times\bar{v})\right\} \tag{2.1}$$

B) The Continuity Equation

$$\frac{\partial \rho}{\partial t} + \nabla\cdot(\rho\bar{v}) = 0 \tag{2.2}$$

C) The Energy Equation

Assuming the fluid to have constant specific heat and viscosity we have

$$\rho g c_v \frac{DT}{Dt} - \frac{Dp}{Dt} = \mu\Phi - \nabla\cdot\bar{q} \tag{2.3}$$

where Φ is the dissipation function [2] and $\bar{q}$ is the vector heat flow rate.

D) Equation of State of Fluid

The equation of state of a fluid is the functional relationship between its pressure, density and temperature (i.e. its state variables). For a liquid it is given by

$$dp = \kappa \frac{d\rho}{\rho} \tag{2.4}$$

where κ is the bulk modulus of elasticity of the fluid.

In this chapter we will be mainly concerned with those conduit models which are describable in terms of first-order or linearized governing equations. When this is done the nonlinear convective inertia terms which appear in the substantial derivative D/D_t are removed. Also, where ρ appears alone it is replaced by an average

*Brackets denote references at end of report.

density ρ_0 . We will also neglect temperature effects unless it is otherwise specified. Under these stipulations the governing relations become,

$$\rho_0 \frac{\partial \bar{v}}{\partial t} = -\nabla p + \mu \left\{ \frac{4}{3} \nabla(\nabla \cdot \bar{v}) - \nabla(\nabla \times \bar{v}) \right\} \tag{2.5}$$

for the first-order equation of motion,

$$\frac{\partial \rho}{\partial t} + \rho_0 \nabla \cdot \bar{v} = 0 \tag{2.6}$$

for the continuity equation, and

$$dp = \chi \frac{d\rho}{\rho_0} \tag{2.7}$$

for the liquid equation of state. The quantities $\bar{v}$ and p now represent small perturbations from some steady condition. We must also restrict ourselves to perturbations about a mean or net velocity, $v_0 \ll c_0$. These restrictions are important to remember. In Section 2.7 we will discuss briefly the effect of violation of these assumptions.

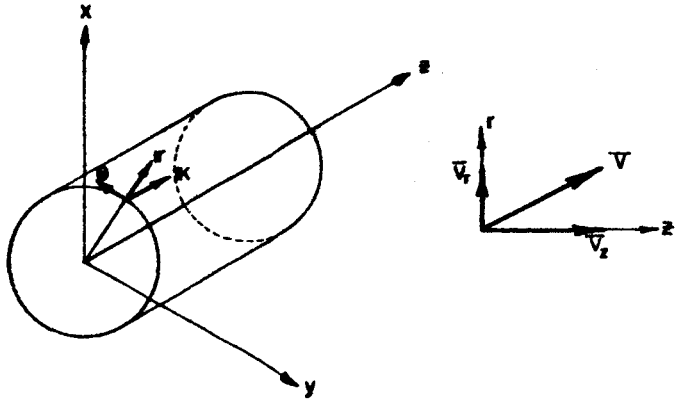

Figure 2.1 Coordinate System

Frictionless Model

The starting point for studies of conduit dynamics is the one-dimensional wave equation which was first derived by d'Alembert in about 1750 in connection with his studies of vibrating strings. Joukowsky [4] and Allievi [5] are generally credited as first associating wave phenomena with water hammer problems in order that studies of the wave equation could be used in explaining pressure transients in conduits. The wave equation for a compressible liquid is derivable from Equations (2.5), (2.6), and (2.7) if one assumes that the viscous effects are negligible. The result is

$$\frac{\partial^2 v}{\partial t^2} = c_o^2 \nabla^2 v \tag{2.8}$$

where c_o is the isentropic speed of sound in the fluid and is given, for a fluid, by

$$c_o = \sqrt{\frac{K}{\rho_o}}. \tag{2.9}$$

v represents the fluid disturbance velocity in the direction of propagation. Solutions to Equation (2.8) predict sinusoidal pressure and velocity disturbances propagating unattenuated with respect to space and time with a velocity c_o. If Equation (2.8) is solved for the case of a suddenly closed valve on one end of a line with a constant pressure reservoir at the other end, Figure 2.2a, then the disturbance pressure will be of the form

$$P(t) = \rho_o c_o v_o \left(\frac{4}{\pi}\right) \sum_{n=1}^{\infty} \left(\frac{1}{2n-1}\right) \sin\left\{\frac{\pi c_o}{2L}(2n-1)t\right\} \tag{2.10}$$

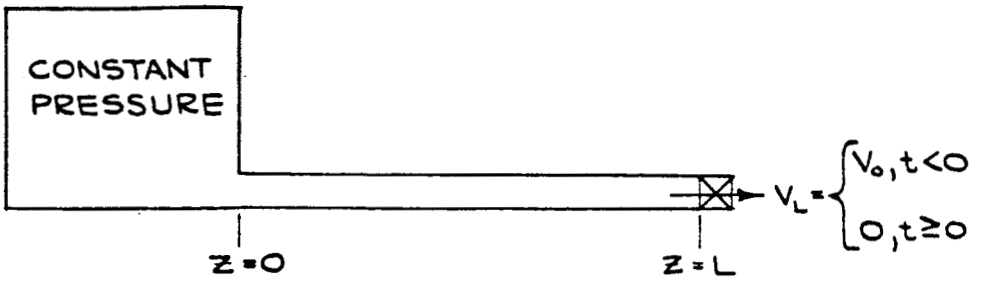

(a) Conduit with Suddenly Closed Valve at One End, Reservoir Other End

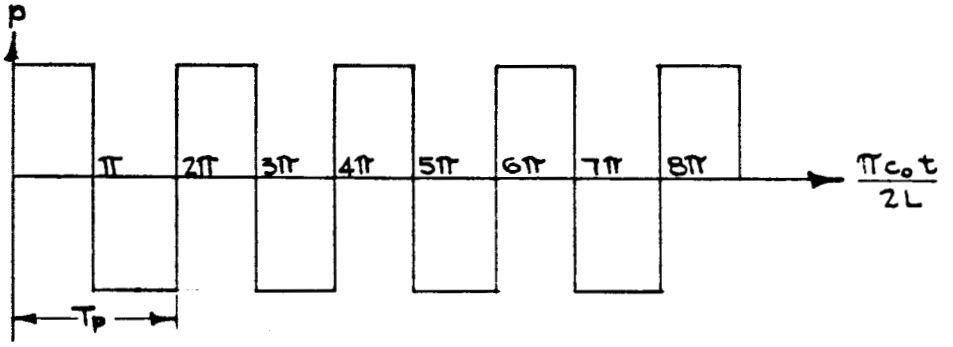

(b) Square Wave Pressure Variation at Suddenly Closed Valve

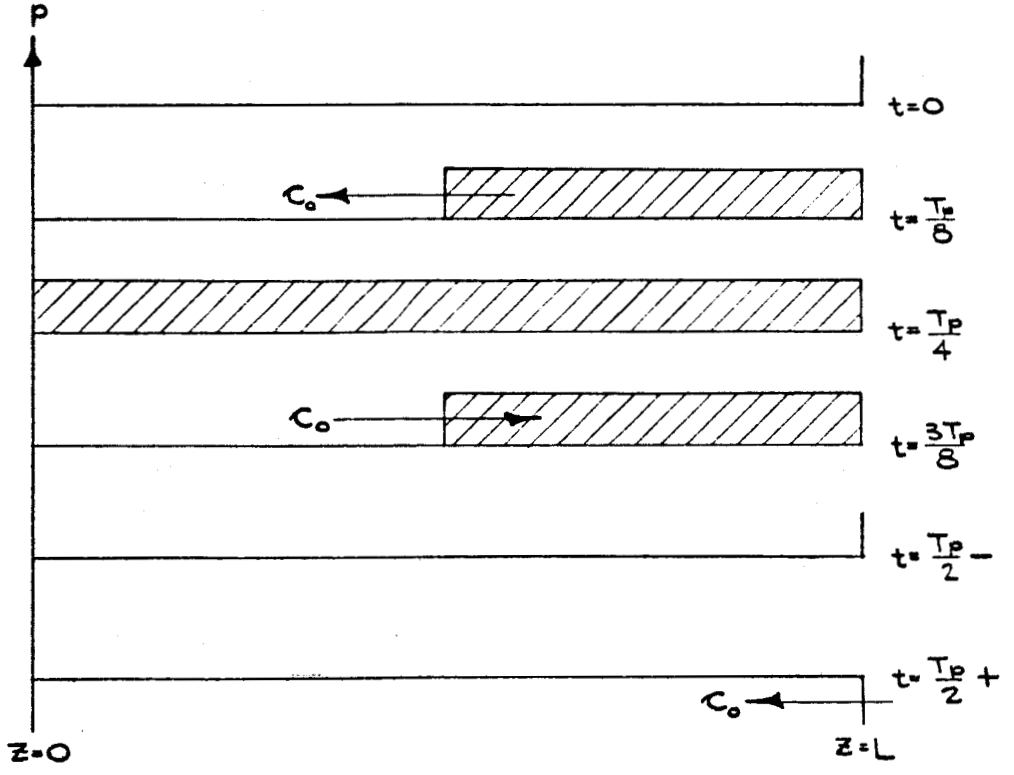

(c) Pressure History of Waves in Conduit for One Half Period

Figure 2.2 Suddenly Closed Valve - Classical Water Hammer Problem

where v_o is the initial mean velocity in the pipe before flow stoppage. Equation (2.10) is the mathematical expression for a square wave with period $(4L/c_o)$, see Figure 2.2b. Now examine the physical chain of events which result in this pressure square wave. At the instant of valve closure the fluid at $z = L$ is instantly stopped and the kinetic energy of the fluid is converted instantaneously (no friction) to potential energy (pressure). This positive pressure wave propagates toward $z = 0$ with velocity c_o and reflects back to $z = L$ with zero pressure, see Figure 2.2c. The pressure wave then becomes negative and propagates again to $z = 0$ where it reflects with zero pressure back again to $z = L$, thus completing one cycle of the pressure wave.

It is evident from this discussion that the conduit of Figure 2.2 has a characteristic "natural" frequency of oscillation $fc = c_o/4L$. A critical analysis of Equation (2.10), however, shows that this particular disturbance actually consists of an infinite number of discrete characteristic frequencies $fc = c_o(2n-1)/4L$. In general, we may say that a conduit will have an infinite number of characteristic frequencies, whose values depend not only upon c_o and L but also upon the end conditions for the conduit. When we excite this system with some form of time variant non-sinusoidal disturbance, the system response will be the sum of the response of each characteristic frequency. The extent to which a given characteristic frequency will be "excited" depends on the type of disturbance. In general, the "sharper" the disturbance, the greater will be the extent to which the high frequency terms are excited. It is important to

realize that the above results are very idealized and include neither the effects of friction or of pipe wall elasticity (these topics will be discussed later on). The results, however, indicate the upper limit of amplitude for a given disturbance. Extensive treatments of the application of this simple theory to practical problems may be found in references [6, 7, 24]. These applications, in general, involve a graphical or numerical solution of the wave equation.

Friction Effects

When researchers [e.g., 12] performed experiments on models demonstrating water hammer they found considerable discrepancy between the simple plane wave theory and actual results. They found that when sudden flow changes were effected, the resulting pressure transients changed shape with time similar to the diagram in Figure 2.3.

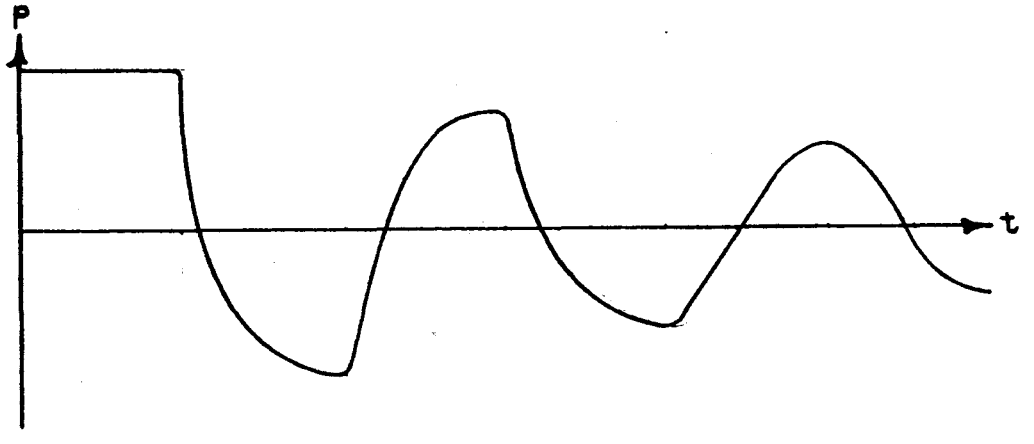

Figure 2.3 Actual Pressure vs. Time Plot for Suddenly Closed Valve

We see that in the actual case, the sharp corners of the pressure trace are being "rounded off" and the amplitude is decaying with time. This phenomena results from dispersive and dissipative effects which are a consequence of viscosity, pipe wall effects, etc. In general, they result from friction effects. It is interesting to note that the greatest dispersion and dissipation occurs on the high frequency terms which are those terms responsible for the sharp corners of the pressure trace. To account for all dispersive and dissipative effects would require an exact solution of the governing equations. However, past researchers have obtained useful results by means of approximate solutions.

Plane Wave Viscous Model

It was demonstrated by Stokes that plane or unbounded waves do not satisfy the simple one-dimensional wave equation, but rather due to viscosity must satisfy

$$\frac{\partial^2 v}{\partial t^2} = c_o^2 \frac{\partial^2 v}{\partial z^2} + \frac{4}{3} \nu \frac{\partial^3 v}{\partial z^2 \partial t} . \tag{2.11}$$

Equation (2.11) may be obtained from Equations (2.5), (2.6), and (2.7) by assuming one-dimensional effects only. Solutions to Equation (2.11) may be represented by

$$v = v_o e^{\pm \Gamma z + i\omega t} \tag{2.12}$$

where Γ is a complex constant called the propagation constant or propagation factor and is given, in general by

$$\Gamma = \Gamma_r + i \Gamma_c . \tag{2.13}$$

The quantity Γ_r is the spatial attenuation factor since the term $e^{\pm \Gamma_r z}$ represents the spatial decay or attenuation of the wave. The quantity ω/Γ_c is called the phase velocity and is the actual velocity of propagation of the disturbance. In general, the phase velocity <u>does not</u> equal c_o. The value of Γ for the solution given in Equation (2.9) is

$$\Gamma = \frac{i\omega}{c_o\sqrt{1+\frac{4}{3}\frac{i\omega\nu}{c_o^2}}} \cdot \tag{2.14}$$

ω represents the angular frequency of the disturbance.

Solutions to Equation (2.11) have been obtained by some researchers [8] in an effort to account for dispersion and dissipation effects in water hammer. These solutions, however, greatly underestimate the viscous effect because Equation (2.11) accounts for shear only in the direction of propagation (the z direction). Much greater viscous effects are acting in the radial direction due to the fact that the fluid velocity must go to zero at the pipe wall. We must conclude then that solutions to Equation (2.11) will not adequately describe the viscous effects in conduit dynamics.

<u>Linear Resistance Model</u>

The approach that a great number of researchers [6, 7, 9, 10, 11, 12, 13, 14] have used is to modify Equation (2.5) by substituting in place of the viscosity dependent terms a friction term which is proportional to the velocity. The resulting equation of motion is

$$\frac{\partial v}{\partial t} = -\frac{1}{\rho_o}\frac{\partial p}{\partial z} - R_1 v \cdot \tag{2.15}$$

R_1 is a resistance or friction coefficient often given by the laminar flow resistance value, or

$$R_1 = \frac{8\nu}{r_o^2}, \tag{2.16}$$

r_o being the pipe radius. When Equation (2.15) is solved simultaneously with the continuity equation and the equation of state, we obtain the same solution as in Equation (2.12) except Γ now has the value

$$\Gamma = \frac{i\omega}{c_o}\sqrt{\frac{R_1}{i\omega} + 1}\ . \tag{2.17}$$

If the solution to Equation (2.15) is obtained for the case of a suddenly closed valve, the pressure versus time plot at the valve will look similar to Figure 2.4.

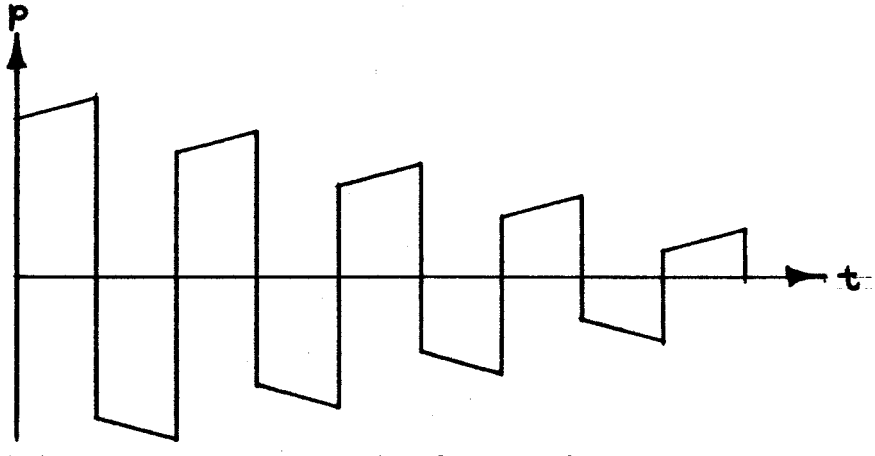

Figure 2.4 Pressure for Suddenly Closed Valve from Linear Friction Model

Although this linear friction model does not give the exact answer, especially over a wide frequency range, it has good utility when experimental values of R_1 may be determined and when the frequency range is limited.

Two-Dimensional Viscous Model-Longitudinal Mode Only

A model reported in the literature [17, 18] which more exactly describes the first-order viscous effects for the longitudinal mode of vibration only is a result of the solution of the following reduced form of the equation of motion

$$\rho_0 \frac{\partial v}{\partial t} = -\frac{\partial p}{\partial z} + \mu\left\{\frac{\partial^2 v}{\partial r^2} + \frac{1}{r}\frac{\partial v}{\partial r}\right\}. \tag{2.18}$$

The resulting propagation factor is

$$\Gamma = \frac{\left(\frac{i\omega}{c_0}\right)}{\left\{1 - \frac{2J_1(\xi r_0)}{\xi r_0 J_0(\xi r_0)}\right\}^{1/2}} \tag{2.19}$$

where

$$\xi^2 = -\frac{i\omega}{\nu} \tag{2.20}$$

and where $J_1(\xi r_0)$ and $J_0(\xi r_0)$ are, respectively, the first and zeroth order Bessel functions [19] of the argument ξr_0. Brown [17] has obtained the pressure history for the case of a suddenly closed valve using the solution to Equation (2.18). His results have much the same general shape as that of the experimental results of other authors, but the results are inconclusive since no supporting experimental results were included with the theoretical predictions. We can conclude, however, that Equation (2.18) is a better representation of the true physical situation than the models previously discussed. From the standpoint of frequency response chracteristics as reported by Oldenberger and Goodson [10], this theory follows very closely the experimental results. Brown [17] and two other authors [15, 16] have solved Equation (2.18) for a fluid in which the heat transfer

may not be neglected, thus it must be solved simultaneously with the energy, continuity and state equations. This results in a propagation factor

$$\Gamma = \frac{i\omega}{c_0} \left\{ \frac{1 + (\gamma - 1)\frac{2 J_1(\epsilon r_0)}{\epsilon r_0 J_0(\epsilon r_0)}}{1 - \frac{2 J_1(\xi r_0)}{\xi r_0 J_0(\xi r_0)}} \right\} \tag{2.21}$$

where now

$$\epsilon^2 = - \frac{i\omega}{\nu} \sigma_0 \tag{2.22}$$

and σ_0 is the Prandtl number [2] and γ is the ratio of specific heats for the fluid. This model has not been experimentally verified by researchers so its validity must be regarded, at this time, as undetermined.

Exact Linear Model

A model based on the exact solution of Equations (2.5), (2.6), and (2.7) was presented in Interim Report No. 64-1. This model predicts an infinite number of discrete modes of propagation instead of only one mode as the previously discussed models predict. In a given situation, the fundamental or longitudinal mode usually predominates but there may be some circumstances under which neglecting the higher modes leads to errors in the analysis. This more elaborate model needs to be verified experimentally before any definite conclusions can be reached. It is interesting to note that the zeroth mode propagation factor for this model coincides with that given by Equation (2.19) for the simpler model which has been proven experimentally to give good results in predicting the frequency response for this mode.

Discussions of analytical and experimental investigations of the higher modes of propagation in connection with inviscid flow or wave propagation are extensive throughout the acoustics literature [27, 28, 29, etc.]. To the best knowledge of the writer, however, an exact treatment of these higher modes with respect to viscous propagation is nonexistent in the literature except for the presentation in Interim Report No. 64-1.

2.4 Fluid Transmission Line Concept - Transfer Equations

So far we have been discussing only time domain solutions to our equations. If we were to begin the exact study of a fluid system in which several components were involved, then the time domain approach would be exceedingly difficult and we would probably get completely lost in the mathematics. A useful and simple approach when dealing with the frequency analysis of fluid conduits (or any fluid component) is that of the fluid transmission line [7, 10, 20]. Consider the fluid line to be representable as shown in Figure 2.5 as a four-terminal system. If we solve the system equations for

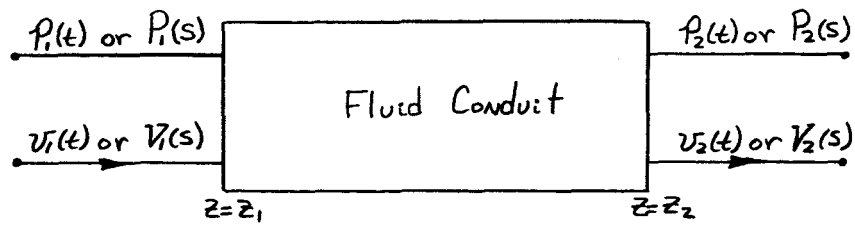

Figure 2.5 Four-Terminal Representation of Fluid Conduit

our conduit in the Laplace transform domain then we obtain a rather simple set of equations relating the four transformed variables, thus

$$P_2(s) = P_1(s) \cosh \Gamma L - Z_c V_1(s) \sinh \Gamma L \tag{2.23}$$

and

$$V_2(s) = V_1(s) \cosh \Gamma L - \frac{P_1(s)}{Z_c} \sinh \Gamma L \quad . \tag{2.24}$$

In Equations (2.23) and (2.24) $V_1(s)$, $V_2(s)$, $P_1(s)$ and $P_2(s)$ represent the Laplace transform of the respective time functions and s is the Laplace variable. Also,

$$L = Z_2 - Z_1 \tag{2.25}$$

and

$$Z_c = \frac{\rho_0 c_0^2 \Gamma}{s} \, . \tag{2.26}$$

Z_c is called the characteristic impedance of the conduit. The Γ which appears in Equations (2.23), (2.24) and (2.26) is identical with previous Γ's except that here $i\omega = s$, the Laplace variable. The value of Γ, of course, depends upon the model. It is important to note that this form of the transfer equations is the same for all of the previous models discussed, only the value of Γ varies. The transfer equations for the four-terminal representation of Figure 2.5 will change, in general, when there is motion of the pipe wall and when we include the higher modes of propagation. Note also that the fluid velocities represented here are average values, that is they have been integrated over the cross-section; thus they are only dependent on time and the axial coordinate.

The utility of valid transfer equations in the frequency analysis of a conduit system cannot be over emphasized. If four-terminal transfer equations can be written for each element of a fluid system, then the total system performance may be analyzed by combining the equations into a new set of transfer equations which represent the entire system. Suppose, for example, that we have two components of a fluid system arranged in series as shown in Figure 2.6.

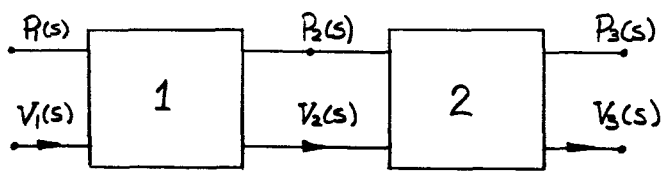

Figure 2.6 Series Arrangement of Two-Fluid Components

Suppose that the transfer equations for element 1 may be expressed in the form

$$P_2(s) = A_1(s)\, P_1(s) + B_1(s)\, V_1(s) \tag{2.27}$$

and

$$V_2(s) = C_1(s)\, P_1(s) + D_1(s)\, V_1(s). \tag{2.28}$$

Writing Equation (2.28) in matrix form gives

$$\begin{bmatrix} P_2 \\ V_2 \end{bmatrix} = \begin{bmatrix} A_1 & B_1 \\ C_1 & D_1 \end{bmatrix} \cdot \begin{bmatrix} P_1 \\ V_1 \end{bmatrix} \tag{2.29}$$

In a similar manner we may write for element 2,

$$\begin{bmatrix} P_3 \\ V_3 \end{bmatrix} = \begin{bmatrix} A_2 & B_2 \\ C_2 & D_2 \end{bmatrix} \cdot \begin{bmatrix} P_2 \\ V_2 \end{bmatrix} . \tag{2.30}$$

Substitution of (2.29) into (2.30) yields

$$\begin{bmatrix} P_3 \\ V_3 \end{bmatrix} = \begin{bmatrix} A_2 & B_2 \\ C_2 & D_2 \end{bmatrix} \cdot \begin{bmatrix} A_1 & B_1 \\ C_1 & D_1 \end{bmatrix} \cdot \begin{bmatrix} P_1 \\ V_1 \end{bmatrix} \tag{2.31}$$

or, by matrix multiplication

$$\begin{bmatrix} P_3 \\ V_3 \end{bmatrix} = \begin{bmatrix} (A_1A_2 + B_2C_1) & (A_2B_1 + B_2D_1) \\ (A_1C_2 + C_1D_2) & (B_1C_2 + D_1D_2) \end{bmatrix} \cdot \begin{bmatrix} P_1 \\ V_1 \end{bmatrix} . \tag{2.32}$$

We might for convenience write

$$\begin{bmatrix} P_3 \\ V_3 \end{bmatrix} = \begin{bmatrix} A_3 & B_3 \\ C_3 & D_3 \end{bmatrix} \cdot \begin{bmatrix} P_1 \\ V_1 \end{bmatrix} \tag{2.33}$$

so that, effectively we have combined elements 1 and 2 into a new element 3. We may represent the new element as shown in Figure 2.7.

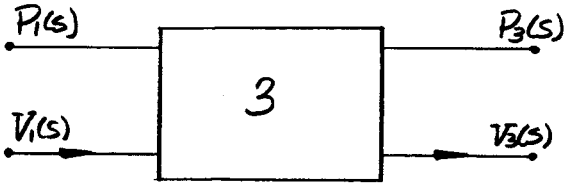

Figure 2.7 Combined Series Elements

Methods similar to this have been employed to great advantage in the analysis of noise transmission in complex fluid systems which involve series and parallel elements [22]. The matrix theory for four-terminal elements has been worked out by Pipes [23] for various types of arrangements of the elements.

In general, the matrix method approach is ideally suited to frequency analysis studies of a conduit system. It allows very complex systems to be analyzed easily with a digital computer.

2.5 Lumped Models

Up to now we have been discussing distributed parameter models of conduit systems. We found such models to be expressible in terms of transfer relations which lend themselves well to frequency analysis. In general, these distributed models are difficult to deal with in the time domain. This is a major handicap for many technically interesting problems such as problems involving conduit systems which contain valves closing or opening arbitrarily with time. In cases such as this we may want only the time response of the system. In terms of the distributed parameter models, this means that the transfer relations for the system of interest must be transformed from the Laplace domain back into the time domain, or that some numerical or graphical procedure must be used to solve the system describing equations. The transformation of the transfer relations is very formidable; on the other hand, the graphical or numerical procedures are rather simple ways to analyze a system but lack the degree of generality usually desired in system analysis. Due to these drawbacks in the application of the distributed parameter models, lumped parameter approximations are often used in conduit system analysis. These models also have drawbacks which much be kept in mind. The major restriction which must be imposed on the lumped model of a distributed system is that it is valid only at low frequency. The method has been found to be valid, in most instances, only if the frequencies involved are not

greater than about one-eighth of the first critical frequency of the lumped element. The exception to this restriction would be a system which has sufficient damping so that compressibility may be neglected. Now examine some typical ways in which conduit systems are lumped; first, we need to consider the basic lumped elements, i.e., inertance, capacitance and resistance [7, 20, 25].

Fluid Inertance

Consider the fluid line shown in Figure 2.8. We will assume that only the pressure and inertia forces are important and that compressibility may be neglected.

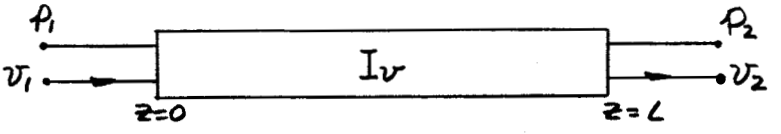

Figure 2.8 Lumped Model Inertance Element

Writing the equation of motion for this case gives

$$p_1 - p_2 = \rho_0 \ell \frac{dv}{dt} = I_v \frac{dv}{dt} \tag{2.34a}$$

where $v_1 = v_2 = v$ since the flow is incompressible. The quantity $\rho_0 L$ represents a fluid inertance. Before proceeding, it should be noted that Equation (2.34a) is often found in various other forms in the literature. It may be found also as

$$p_1 - p_2 = \frac{\rho_0 \ell}{A} \frac{dq}{dt} = I_q \frac{dq}{dt} \tag{2.34b}$$

where q is the flow rate and A is the cross-sectional area. For this case the fluid inertance is $\rho_0 L/A$. Another form of Equation (2.34a) is

$$p_1 - p_2 = \frac{\ell}{Ag} \frac{dw}{dt} = I_w \frac{dw}{dt} \tag{2.34c}$$

where w is the weight flow rate. Notice that the inertance, I, is not the same in each case. Notice also that these equations are valid only for constant area lines.

Fluid Capacitance

Now consider a fluid line in which only compressibility effects are important, i.e., inertia or inertance effects and resistance effects are unimportant. With respect to Figure 2.9, applying the

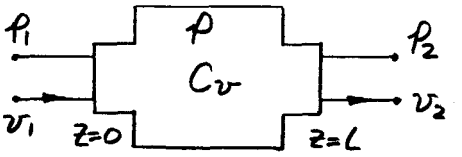

Figure 2.9 Lumped Model Capacitance Element

continuity and state equations we have, since $p_1 = p_2 = p$

$$v_1 - v_2 = \frac{L}{K}\frac{dp}{dt} = C_v \frac{dp}{dt}. \qquad (2.35a)$$

Again, as was true for Equation (2.34) we could have just as well have written Equation (2.35) in terms of q or w, but the value of C would also have been different, thus

$$q_1 - q_2 = \frac{AL}{K}\frac{dp}{dt} = C_q \frac{dp}{dt} \qquad (2.35b)$$

and also

$$w_1 - w_2 = \frac{\rho g AL}{K}\frac{dp}{dt} = C_w \frac{dp}{dt}. \qquad (2.35c)$$

Fluid Resistance

Because of the large number of parameters which may effect the fluid resistance, it becomes more difficult in this case to write

a valid theoretical relationship which holds for a wide range of flow and pressure variations. The usual approach, therefore, is to treat fluid resistance semi-empirically by defining the pressure drop due to resistance between points 1 and 2 of a lumped resistive element as

$$p_1 - p_2 = R(v)\, v \tag{2.36}$$

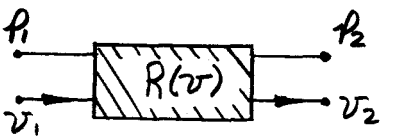

Figure 2.10 Lumped Model Resistive Element

where $v_1 = v_2 = v$ and $R(v)$ is an experimentally determined function of velocity. Of course if the pressure and velocity are steady, then $R(v)$ is well known from information contained in standard fluid mechanics textbooks. For the case of oscillating flow only (no net flow), we can get a good value for the resistance coefficient by considering a low frequency approximation of the two-dimensional viscous distributed parameter model. This will be shown later in this section.

Fundamental Lumped Model

If we now combine our three basic elements together, we have the fundamental representation of a lumped line. If we combine Equations (2.34a) and (2.36) and consider also Equation (2.35a), then we may

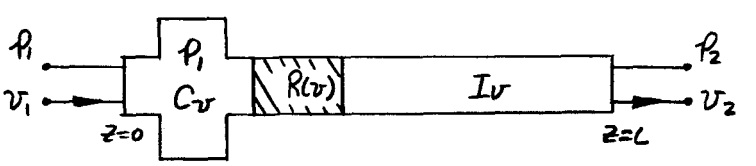

Figure 2.11 Fundamental Representation of Lumped Line

write for the fundamental representation

$$P_1 - P_2 = I_v \frac{dv_2}{dt} + R(v)\, v_2 \tag{2.37}$$

and

$$v_1 - v_2 = C_v \frac{dP_1}{dt}. \tag{2.38}$$

Now take the Laplace transformation of (2.37) and (2.38), thus

$$P_1(s) - P_2(s) = s I_v V_2(s) + R(v)\, V_2(s) \tag{2.39}$$

and

$$V_1(s) - V_2(s) = s C_v P_1(s). \tag{2.40}$$

Writing these last two equations in our standard transfer form gives,

$$P_2(s) = P_1(s)\left\{1 + s C_v [s I_v + R(v)]\right\} - V_1(s)\left\{s I_v + R(v)\right\} \tag{2.41}$$

and

$$V_2(s) = V_1(s) - s C_v P_1(s). \tag{2.42}$$

In Chapter VI we will further discuss these last two relations with reference to the exact or distributed parameter models.

There are many possible ways of representing a conduit with lumped elements other than the representation of Figure 2.11.

Equivalent Electrical Circuits

One motivation for using lumped models, other than simplicity, is that they readily yield to simulation on an analog computer. Using a pressure-voltage analogy the electrical equivalent of the

fundamental lumped model becomes that shown in Figure 2.12. The values

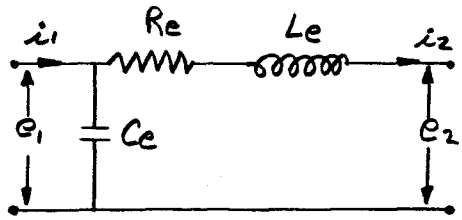

Figure 2.12 Electrical Analogy for Fundamental Lumped Conduit with Friction

of Re, Le and Ce depend upon what is made to be the analog of electrical current. Table 2.1 shows the analogous quantities for three possible analogs. Other circuits which are often used in an effort to improve

Electrical Quantity	Voltage e	Current i	Resistance Re	Inductance Le	Capacitance Ce
Analogous	p	v	R(v)	$\rho_o L$	L/χ
Conduit System	p	q	$\frac{R(v)}{A}$	$\frac{\rho_o L}{A}$	AL/χ
Quantity	p	w	$\frac{R(v)}{\rho_o Ag}$	$\frac{L}{Ag}$	$\frac{\rho_o gAL}{\chi}$

Table 2.1 Electrical Analogs

the accuracy of representation are shown in Figure 2.13.

Method for Improving Lumped Model

We stated previously that a lumped model generally is valid only if the frequencies involved are not greater than about one-eighth of the first critical frequency of the lumped element. We can conveniently get around this restriction by using several "lumps" to simulate a conduit. Suppose, for example, that the highest frequency encountered

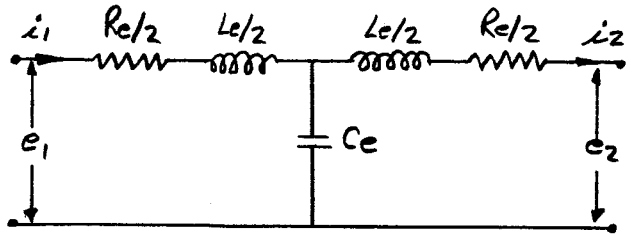

T Representation

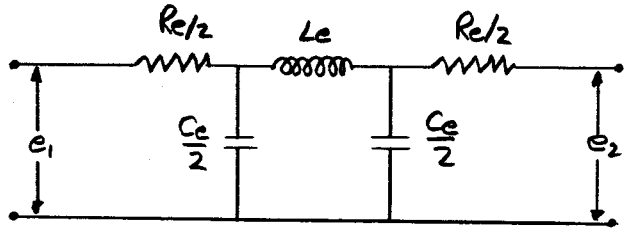

π Representation

Figure 2.13 Variations of Electrical Analogs

is about ten times too high for valid lumping; then, if we use ten electrically equivalent circuits in series (after reducing Re, Le and Ce by a factor of ten) we are able to circumvent the original restriction. Figure 2.14 shows the electrical analog for an n-segmented lumped model.

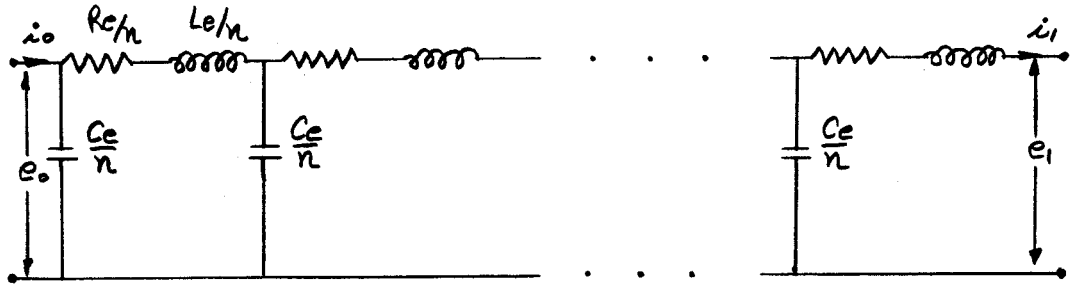

Figure 2.14 Analog for n-Segmented Lumped Conduit with Friction

It is worth mentioning at this time that if a conduit has enough resistance then the high frequency terms are damped enough that the above mentioned restrictions can be relaxed to some degree. No quantitative information is available at this time on this subject.

2.6 Conduit Wall Effects

Thus far in our developments we have been overlooking the effects which the conduit wall may have upon the fluid dynamics. Depending upon the operating parameters of the system being analyzed, accounting for the effects of the wall may be very simply achieved or, on the other hand, may require an extensive mathematic treatment in order to get reasonable answers. Fortunately, most problems with which we will be concerned can be handled with the simple treatment. Problems demanding a complex analysis usually occur only when dealing with extremely high operating frequencies.

Simplified Analysis

Korteweg in 1878 showed that wave propagation was dependent upon both the elasticity of the fluid and of the conduit wall and that the resultant propagation velocity must be equal to or less than c_o. It has been shown (see for example Reference 7) that the actual sound velocity is

$$c = \frac{c_o}{\sqrt{1 + \kappa f / E_t}} \tag{2.43}$$

where E_t is Young's modulus for the tube material and f is given by

$$f = \begin{cases} D_o/h, & \text{thin-walled tube} \\ 2\left(\dfrac{D_o^2 + D_i^2}{D_o^2 - D_i^2}\right), & \text{thick-walled tube} \end{cases} \tag{2.44}$$

In Equation (2.44) D_o represents the conduit outside diameter and D_i represents the inside diameter. All that is required in the simplified analysis is that we replace c_o with the c of Equation (2.43) in our analysis.

More Exact Analysis

There have been a large number of papers written pertaining to the effect of conduit wall elasticity on the transmission characteristics of fluid within the conduit. Basically, conduits may be divided into two types with regard to the elastic characteristics of their walls; elastic flexible and elastic stiff. For a conduit with elastic flexible walls we assume that pressure variations within the conduit can cause radial deformations which do not cause corresponding axial disturbances in the conduit wall, i.e. all disturbances in the wall are localized and cannot propagate axially along the conduit wall. For elastic stiff walls, on the other hand, disturbances can propagate axially along the pipe wall. Some of the authors who have made contributions on the effects of conduit elasticity are Lamb [26], Jacobi [27], Morgan [28], Lin and Morgan [29] and Skalak [30]. None of these authors have treated exactly a viscous fluid in this connection. An exact treatment of both flexible and stiff walls for a viscous fluid was presented in Interim Report No. 64-1.

In general, the relations expressing the propagation velocity variation with frequency have trends as shown sketched in Figure 2.14. Notice that only one mode transmits for all frequencies for the case of an elastic flexible wall, whereas two modes transmit at all frequencies for an elastic stiff wall. Note also that the limiting value for small

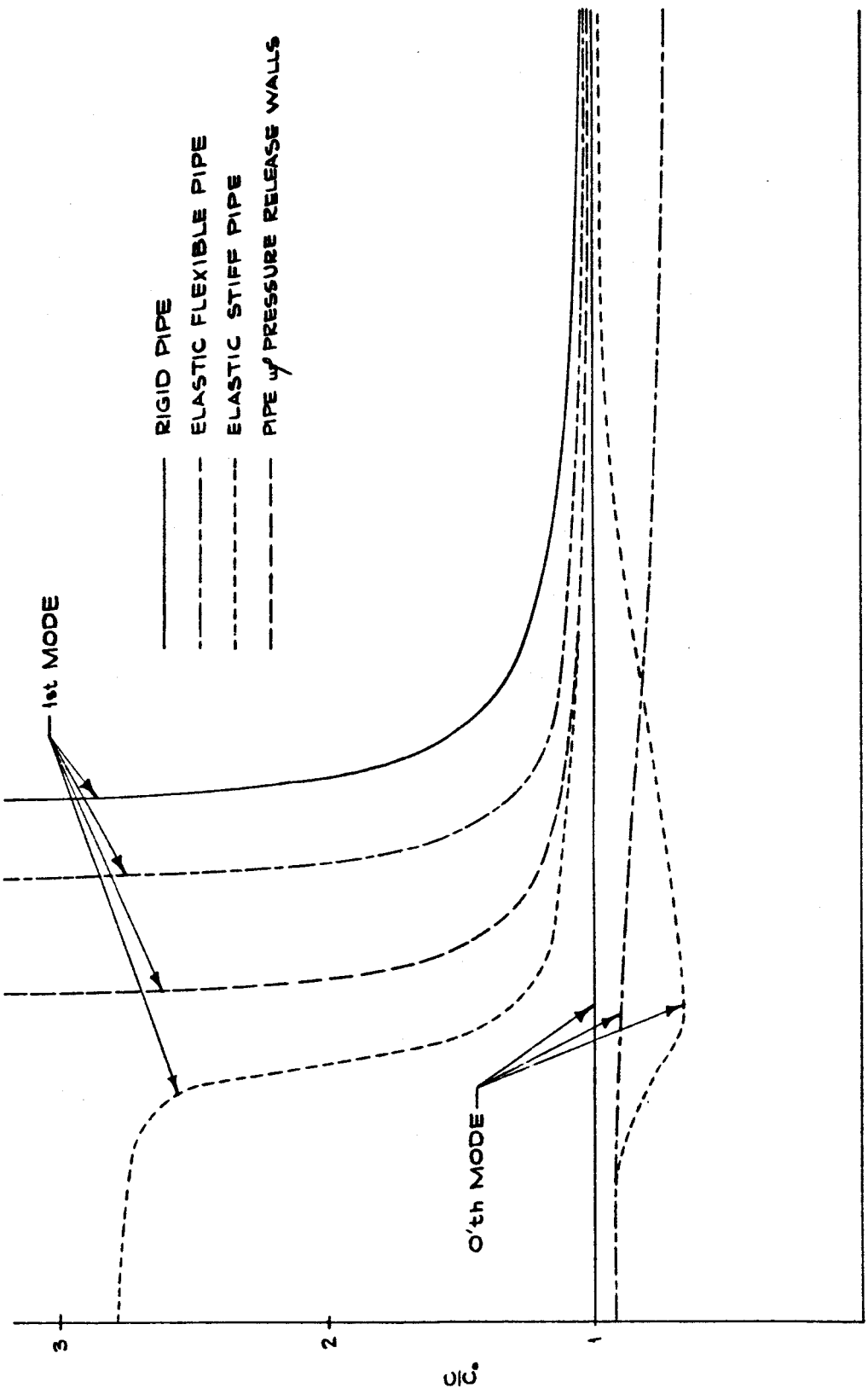

Figure 2.15 Propagation Velocity vs. Frequency

frequency in both cases approaches the same value, c/c_o. This is the same value as predicted by the simplified analysis from Equation (2.43). We see then that the simplified analysis is exact for low frequencies for the zeroth mode.

2.7 Nonlinear Effects

Thus far in our discussion we have been limited to problems involving small perturbations about some steady flow condition where the steady velocity component is much less than c_o. The reason for imposing these restrictions stems from the fact that in the previous developments the nonlinear terms of the equations of motion were neglected. Consider again the exact form of the Navier-Stokes equations (for a constant viscosity fluid) given by Equation (2.1), or

$$\rho \frac{D\bar{v}}{Dt} = -\nabla p + \mu \left\{ \frac{4}{3} \nabla(\nabla \cdot \bar{v}) - \nabla(\nabla \times \bar{v}) \right\}. \qquad (2.1)$$

The difficult nonlinear terms are contained in the substantial derivative, $D\bar{v}/Dt$. For the velocity component in the z direction, we have (assuming axisymmetric flow),

$$\frac{Dv_z}{Dt} \equiv \frac{\partial v_z}{\partial t} + v_r \frac{\partial v_z}{\partial r} + v_z \frac{\partial v_z}{\partial z} . \qquad (2.45)$$

There seem to be two main conditions, with respect to problems of conduit dynamics, under which we must account to some degree for the nonlinear terms of the equations of motion. These conditions are:

1) Case where there is a large steady flow component but small unsteady components.

2) Case where the unsteady terms are large and the steady flow terms may or may not be large.

We will now discuss each case in more detail.

Case 1

We assume in this case that we may write for the velocity

$$v_z = v_{z_0} + v_{z_1} \tag{2.46}$$

where v_{z_0} is the steady flow term, i.e. independent of time, and v_{z_1} is the time variant perturbation or disturbance velocity. We assume also that $|v_{z_1}| \ll |v_{z_0}|$. Based upon these assumptions we may approximate Equation (2.45) by (after neglecting the small order terms)

$$\frac{Dv_z}{Dt} \approx \frac{\partial v_{z_1}}{\partial t} + v_{z_0} \frac{\partial v_{z_1}}{\partial z} . \tag{2.47}$$

Since v_{z_0} will be a known quantity as a result of solving the steady-state hydrodynamical equations, this means Equation (2.47) is linear; thus, we have linearized the substantial derivative for this case.

Regetz [31] utilized a linearization such as this to enable an analytical description of the response characteristics of hydraulic lines with a net flow. Regetz' analytical work is for nonviscous flow.

Considerable work has been done along these same lines by one of the project members and is reported on in Chapter VI.

Case 2

If the unsteady perturbations are of sufficiently large magnitude then a linearization procedure will not work and one has to contend with the nonlinear equations. This area of study needs much work before

generally applicable methods of solution are availabe. In many cases the method of characteristics [32] may be used if we do not have to contend with viscosity.

2.8 Component Effects

A discussion of fluid conduits would be hardly complete without some mention of components commonly associated with them.

Orifices

A treatment of the unsteady flow of a liquid through an orifice in a conduit is due to Goodson [33]. In this method the describing partial differential equations are reduced by integration to a linear ordinary differential equation in time relating flow, pressure drop and area of the orifice. Now follow his development.

We will assume the following conditions to hold:

(1) The conduit length is much greater than its diameter so that wave effects associated with the orifice may be neglected.

(2) Tube wall effects are negligible in the vicinity of the orifice.

(3) Viscous effects are negligible.

(4) Density changes are small.

If we average the equation of motion, Equation (2.1), across the cross-section, considering the above conditions, then we may write

$$\frac{\partial q}{\partial t} + \frac{\partial [q v_m]}{\partial z} + \frac{A}{\rho_0} \frac{\partial p}{\partial z} = 0 \qquad (2.48)$$

for the one-dimensional equation of motion, and

$$\frac{\partial[\rho A]}{\partial t} + \rho_o \frac{\partial q}{\partial z} = 0 \tag{2.49}$$

for the continuity relation. Here, $q = q(z,t)$ is the flow rate; $v_m = v_m(z,t)$ is the average axial velocity over the cross-section; and $A = A(z,t)$ is the orifice area. We now define an effective length ℓ_o of the orifice, as shown in Figure 2.15, to account for the effect of the orifice on the flow patterns in the vicinity of the orifice. Goodson has simultaneously integrated Equation (2.48) and (2.49) from 0 to ℓ_o which results in an ordinary differential equation relating flow rate and pressure drop in terms of a time variant area for the case of a compressible liquid. For many purposes the compressibility effects may be neglected which much simplifies

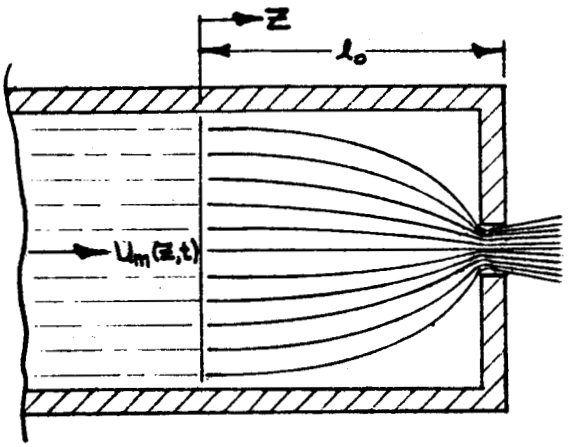

Figure 2.16 Flow Patterns Near Orifice

the resulting differential equation to

$$b_1 \frac{dq(0)}{dt} + b_2 q(0)^2 = \frac{\Delta p(t)}{\rho_o} \tag{2.50}$$

where $q(0)$ is the flow rate at $z = 0$ and $\Delta p(t)$ is the pressure drop across the orifice. Also,

$$b_1 = \int_0^{\ell_0} \frac{dz}{A(z,t)} \tag{2.51}$$

and

$$b_2 = \int_0^{\ell_0} \frac{dz}{A(z,t)} \cdot \frac{\partial}{\partial z}\left(\frac{1}{A(z,t)}\right). \tag{2.52}$$

We can express Equation (2.50) in a more convenient form by letting $q = q_0 + q_1$ where q_0 is a steady flow term and q_1 is the perturbed flow. We then have, assuming q_1 is small

$$b_1 \frac{dq_1}{dt} + 2b_2 q_0 q_1 = \Delta p_1(t) \tag{2.53}$$

where $p = p_0 + p_1$ and p_0 is the steady pressure and p_1 is the perturbed pressure. No experimental evidence is presented by Goodson specifically verifying this orifice model. This model is interesting from the standpoint of accounting for the nonlinear characteristics of orifices and also in allowing the orifice area to be variable in time.

Notice that, in view of the discussion of Section 2.5, Equation (2.53) demonstrates the pressure drop to be composed of an inertance term plus a resistive term; thus we may rewrite Equation (2.53) in the form

$$I_q \frac{dq_1}{dt} + R(q)\, q_1 = \Delta p_1(t). \tag{2.54}$$

I_q is the inertance for the orifice and $R(q)$ is the resistance.

A considerable amount of experimental work has been performed by Thurston and Martin [34] pertaining to orifice flow. Figure 2.16 shows sketches typical of their results. Notice the nonlinearity of I_q and $R(q)$ for large values of the volume flow.

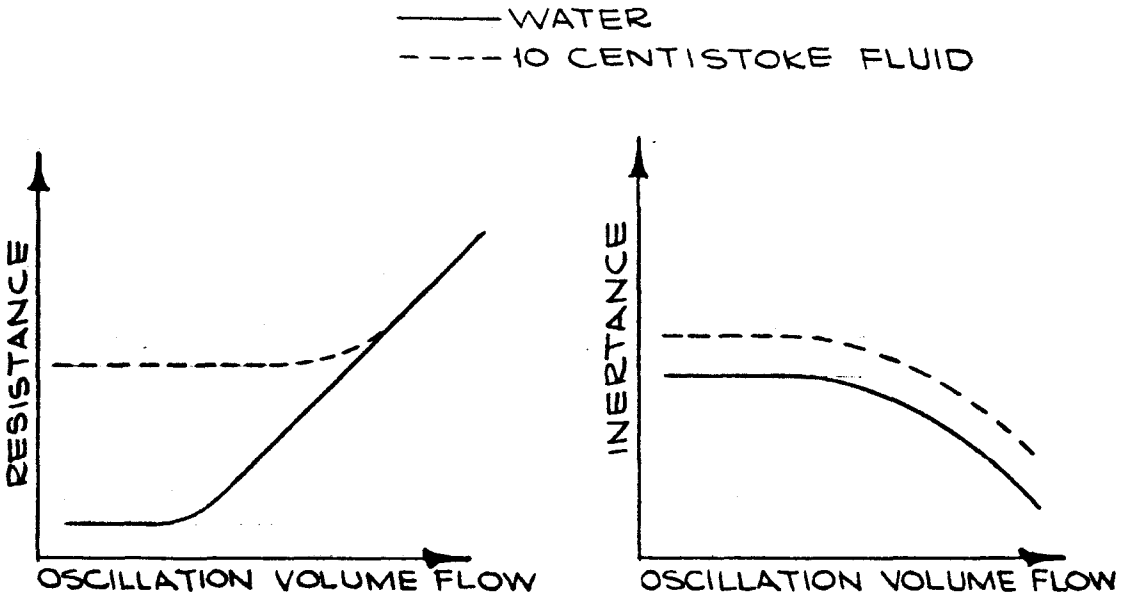

Figure 2.17 Inertance and Resistance vs. Volume Flow for Oscillating Flow Through Orifice

Other Components

There are many other types of components commonly associated with conduits which may have effects upon the transmission characteristics. Not enough articles concerning various components have been found in order that quantitative information can be given at this time.

CHAPTER III

Two-Phase Flow

Discussion of Two-Phase Flow

This chapter will be limited to a discussion of one component, liquid-vapor, two-phase flow. This is the type of flow which would normally be of concern in the flow of a cryogenic fluid through conduits.

The amount of material published on the subject of two-phase flow has increased tremendously over the past decade. According to Reference [35], over 400 publications on two-phase gas-liquid flow phenomena appeared during the year 1963. These publications do not include the subjects of atomization, cavitation, and condensation. With such a large number of publications appearing each year on this subject, it is difficult to thoroughly review all of the material. Several recent documents have attempted to compile a list of important publications on the subject of two-phase flow, Reference [36], [37], [38], [39]. It has been said that it may soon be necessary to have a bibliography on two-phase flow bibliographies.

Basically, the analytical treatment of two-phase flow is no different from that of single-phase flow. The fundamental concepts of conservation of mass, conservation of momentum, and the first

and second laws of thermodynamics hold for two-phase flow as they do for single-phase flow. These basic laws may be expressed in differential form leading to the differential equations of conservation of mass, conservation of momentum and conservation of energy. A difficulty arises in the solution of these equations however since the differential equations must be written for each phase and solved simultaneously. The difficulty is in attempting to write the necessary boundary and initial conditions for these equations. The complexities involved in such an approach have limited the usefulness of this method. A number of simplifying assumptions have been put forward in the literature to permit some accomplishments in predicting two-phase flow behavior.

Perhaps the most common assumption that has been made is the recognition of distinct flow patterns that exist in two-phase flow. A study of these individual flow patterns or flow regimes has allowed some simplifications to be made in the analysis of each regime. There is some disagreement in the description of the various flow regimes. However most attempts at describing the flow patterns begin with distinguishing the flow as either horizontal or vertical. In horizontal flow the flow patterns normally described in the literature include spray or mist flow, annular flow, slug flow, wavey flow, stratified flow, plug flow, and bubble flow. (The flow patterns are listed in order of decreasing gas or vapor to liquid flow rate). In vertical flow the patterns are usually described as mist flow, spray-annular flow, annular flow, slug, churn, or plug flow and bubble or froth flow. A number of flow

regime maps have been given in the literature for a prediction of the conditions under which the various flow regimes exist. Several of these flow regime maps are given in Reference [35].

Since the area of study involved in this contract includes situations where only a small amount of vapor formation will be permitted, the bubble or froth flow regime was considered to be the most important regime for intense study. This placed a limit upon the amount of literature which had to be carefully reviewed and permitted a narrowing down of the techniques of solution of the two-phase problem. Bubble or froth flow lends itself to certain mathematical treatment not useful in many of the other two-phase flow regimes. The assumptions of isotropic and homogeneous behavior are fairly realistic ones for the bubble flow regime.

The most important information needed for any bubble flow study is that on the behavior of the individual bubbles. An adequate description of bubble formation and growth is needed in order to complete the description of the behavior of two-phase flow involving the bubble or froth flow regime. Bubble formation and bubble dynamics has long been of interest to persons studying the phenomena of boiling heat transfer. Much of the current literature being studied and utilized has come from this field.

Another important fact that has been realized during the course of the investigation is that the presence of the bubbles in the liquid has a very outstanding effect on the velocity of sound. At mass ratios of vapor to liquid which exist in the bubble

flow regime, the effect on the sonic velocity is considerable. This can be seen in Figure 3.1 and Figure 3.2 taken from Reference [40]. The speed of sound has been shown in Interim Report 64-1 to be an important parameter in certain single-phase flow problems. It would be expected that similar effects would carry over into the two-phase flow problems. Ability to estimate the sonic velocity of various mixtures of vapor and liquid must be acquired before any great degree of success can be accomplished in this area.

The prediction of pressure drop in steady two-phase flow is not too difficult using rather well-established methods, first developed in Reference [41]. The transient two-phase flow problem, however, has been given only a minimum amount of study. A very recent survey on the problem of flow oscillations in two-phase systems is given in Reference [42]. It is felt that some of this material will be useful in the continuing study of transient two-phase systems.

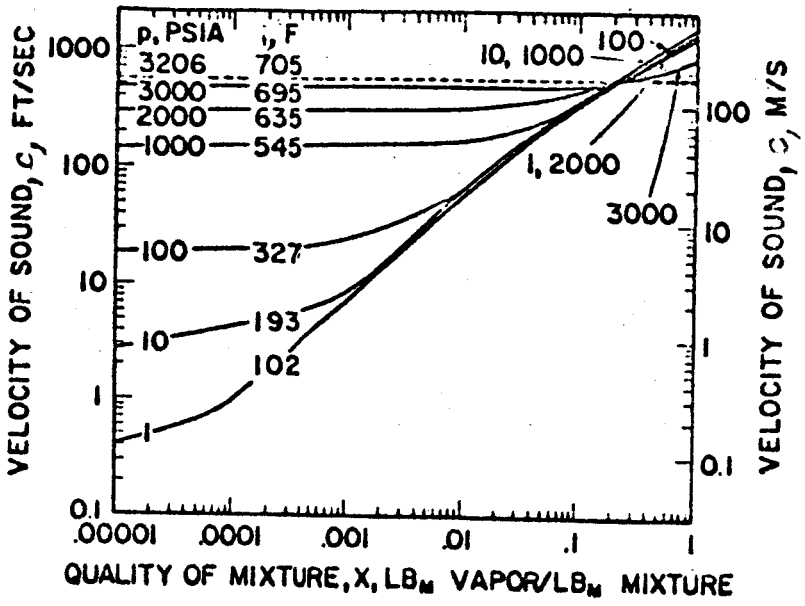

Figure 3.1 Velocity of Sound in Steam-Water Mixtures as a Function of Mixture Quality

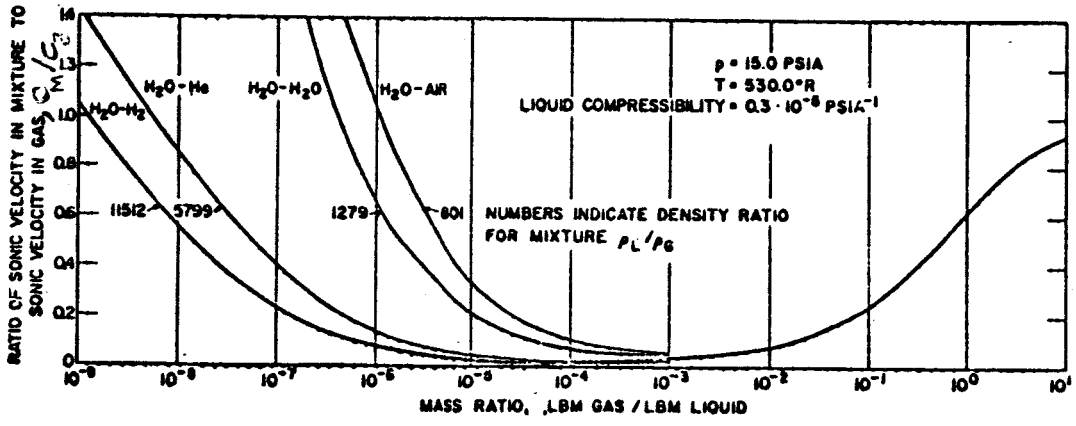

Figure 3.2 Ratio of Adiabatic Sonic Velocity in Mixture to Sonic Velocity in Gas Phase Versus the Ratio of Mass of Gas to Mass of Liquid for Several Gas-Liquid Combinations

CHAPTER IV

Cavitation Literature Survey

4.1 Introduction

Cavitation is the formation and subsequent collapse of cavities in a liquid when the local static pressure at some point decreases to or below the vapor pressure and then increases as the fluid progresses downstream. This can easily occur when a fluid, near its saturation pressure, is flowing through conduits which are equipped with components. Whenever cavitation occurs the complexity of the flow problem is increased several times because of the formation of two-phase flow. Two-phase flow is often undesirable not only because of the increased complexity of the flow problem but also because of the unsteadiness often caused by its formation. Therefore, before a complete analysis of two-phase single component flow through conduits can be attempted, we must be able to predict the conditions at which two-phase flow starts and the conditions under which these cavities will collapse.

The literature on cavitation has grown to great proportions since studies began in the late nineteenth century. This is due to the large number of variables involved and to the wide range of the aspects of cavitation any one of which may happen to be of prime interest to investigators in different fields. The

literature reviewed on cavitation will be directed toward vaporous cavitation as might be expected to occur in fluids flowing through conduits.

In order to clearly bring out the problem to be discussed it is necessary to distinguish between two broad types of cavitation. Vaporous cavitation is the sudden expansion of a vapor bubble due to vaporization of the liquid at the bubble wall whereas gaseous cavitation is the relatively slow expansion of a gas bubble due to diffusion. Strasberg [43] showed that the critical pressure needed for vaporous cavitation would be equal to or less than the vapor pressure whereas gaseous cavitation could occur at pressures above the vapor pressure.

Vaporous Cavitation, a phenomenon caused by a decrease in the stream pressure, may occur as a result of any one or combination of: (1) friction in the conduit, (2) decreasing the flow area, (3) centrifugal effects (flow in bends), (4) vibration and etc. However, pressure alone does not specify the conditions under which a flowing fluid will cavitate. It might be said that pressures below the vapor pressure is a necessary condition for vaporous cavitation; however, this is not sufficient because of other variables.

4.2 Variables Affecting Cavitation

The variables which affect the onset of cavitation may be divided into four major groups. These groups together with the individual group variables are:

I. Fluid Properties

1. Vapor pressure
2. Surface tension
3. Wettability of liquid
4. Viscosity
5. Thermal conductivity
6. Mass diffusion coefficient
7. Pressure

II. Foreign Variables

1. Dissolved gases
2. Undissolved gases
3. Impurities (solids, dissolved solids, etc.)

III. Conduit Variables

1. Surface roughness
2. Material of conduit

IV. Dynamic Variables

1. Turbulence level
2. Pressure distribution
3. Velocity
4. Vibration

Because of the large number of varibles involved, the efforts to find similarity or scaling laws encompassing all of these variables has not been successful.

The problem of determining the conditions under which a fluid will cavitate is not impossible because of the relatively minor role most of these variables play and the dominant role of a few. Vapor pressure is the most important single variable because it gives an indication of the pressure necessary to cause cavitation. Several investigators have considered the nuclei present in the fluid and conduit as an important variable. The role of the nuclei in producing cavitation will be discussed in a following section.

4.3 Incipient and Desinent Cavitation

Incipient cavitation is defined as that phenomena which occurs when the stream pressure progresses from a condition of no cavitation to one supporting cavitation. It marks the onset of cavitation. Desinent cavitation, on the other hand, identifies the condition

when the stream passes from a condition supporting cavitation to one wherein there is no cavitation. It defines the cessation of cavitation. Many investigators in the past called both the beginning and the cessation "incipient" cavitation. Holl [44] in 1960 named these two different occurrences of cavitation.

For incipient cavitation there will correspond a particular value of p called the "inception pressure" p_i, whereas for desinent cavitation there is the "desinence presure" p_d. From these definitions there follows the incipient-cavitation number K_{i_o} and desinent-cavitation number K_{d_o} defined by

$$K_{i_o} = \frac{p_{i_o} - p_v}{\frac{1}{2} \rho_o V_o^2} \tag{4.1}$$

and

$$K_{d_o} = \frac{p_{d_o} - p_v}{\frac{1}{2} \rho_o V_o^2} \cdot \tag{4-2}$$

The subscript "o" designates a reference state which is usually taken upstream of the minimum pressure section.

The experimental investigation of Lehman and Young [45] and Kermeen [46] indicate that the desinence pressure, p_d, is greater than or equal to the inception pressure, p_i. The pressure difference $p_d - p_i$ is often referred to as the "cavitation hysteresis." Thus, for the same vapor pressure, we can write the following relation between Equations (4.1) and (4.2),

$$K_{d_o} \geq K_{i_o} \cdot \tag{4.3}$$

For a given flow condition K_{d_o} appears to be the upper limit for K_{i_o}. Holl [44] pointed out that investigators, in the past, called desinent cavitation as incipient cavitation because of its repeatable nature. However, in some cases, there is no difference between incipient and desinent cavitation except in the definitions.

4.4 The Inception of Cavitation

A. Nuclei Theory for Cavitation Inception

It is now the generally accepted view that the inception of cavitation in ordinary liquids is associated with the growth of nuclei containing vapor, undissolved gas, or both, which are present either within the liquid or in crevices on bounding walls. On the basis of physical arguments made by Eisenberg [47], it is unlikely that completely dissolved gases can play a dominant role in inception, although in certain cases such dissolved gases may become important during the inception process. The work of Harvey, McElroy and Whiteley [48] is of particular importantce in this connection, having demonstrated that water, saturated with air, when "denucleated" by prior application of large pressures exhibited very high fracture strength. Thus, the pressure of such nuclei is taken to account for cavitation onset at pressures of the order of vapor pressure.

Cavitation inception is a dynamic phenomenon; however, the basic principles can be revealed by a static analysis. For static equilibrium the following equation, for a spherical bubble, must be satisfied:

$$P_v + P_g = P + \frac{2\sigma}{R} . \qquad (4.4)$$

For a constant weight of a perfect gas at constant temperature $p_g = \frac{C_1}{R^3}$, where C_1 is proportional to the number of molecules or weight of the gas and R refers to the radius of the sphere. Hence, Equation (4.4) becomes

$$p - p_v = \frac{C_1}{R^3} - \frac{2\sigma}{R} . \tag{4.5}$$

The minimum value of $p - p_v = p^*$ occurs at a radius

$$R = R^* = \left(\frac{3C_1}{2\sigma}\right)^{1/2}$$

or

$$(p - p_v)_{min} = -\frac{4\sigma}{3R^*} . \tag{4.6}$$

In this relation the negative sign indicates that the critical fluid pressure is actually below the vapor pressure. If the pressure is decreased slightly from the condition of $(p - p_v)_{min} = p^*$ at $R = R^*$, the bubble becomes unstable and tends to grow without bound. At pressures greater than the critical pressure, the bubble is stable and assumes an equilibrium radius satisfying Equation (4.4). The relation between $p - p_v$ and diameter for different values of C_1 and assuming a surface tension value of 0.005 lbs. per ft. for 68 F water are shown in Figure 4.1. The corresponding relation between pressure and critical diameter is shown in Figure 4.2.

It may be observed from Equation (4.6) that the critical radius for a bubble containing only vapor ($C_1 = 0$) is zero and consequently the fluid pressure must be infinitely negative in order to cavitate such a bubble. This requirement for infinite pressure to cause

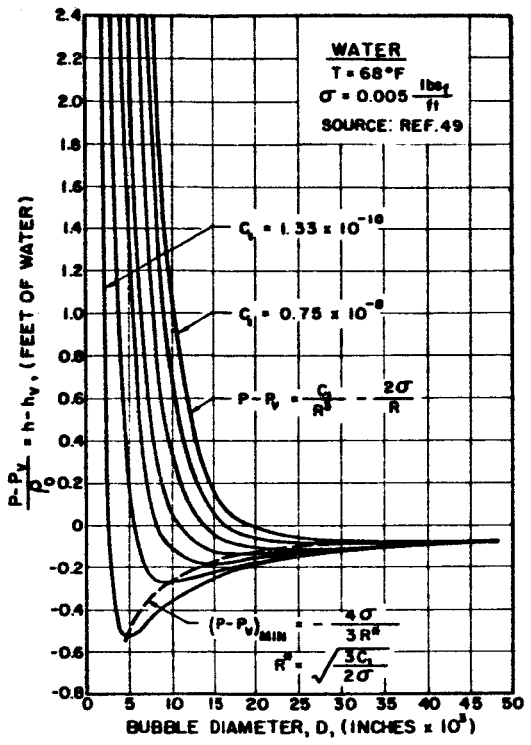

Figure 4.1 Pressure as a Function Bubble Size

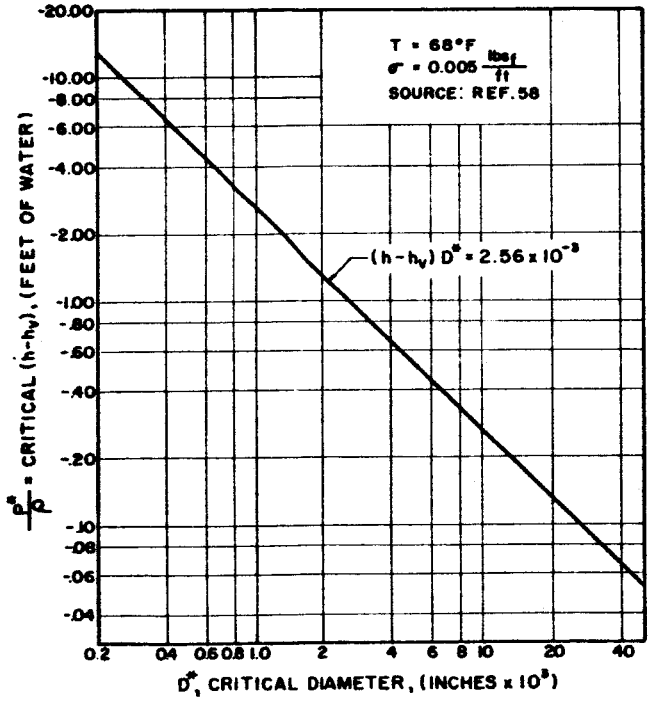

Figure 4.2 Pressure Required to Cause Instability of Critical-Size Gas Nuclei

instability of a vapor must be modified when the bubble radius approaches molecular size and the continuum theory becomes invalid.

The previous analysis has considered only the static stability of the cavitation nuclei. It appears reasonable to expect that if nuclei are subjected to transient pressure reductions that the critical pressure for instability might be considerably less than the value given by Equation (4.6). Noltingk [50] was able to show, in the majority of cases, that the critical pressure predicted by the static analysis is not significantly altered by the duration of the transient. Noltingk's investigation revealed that the pressure need only stay at the critical pressure for a time slightly greater than the natural period of oscillation of the bubble. For a bubble diameter of 0.001 inches, the pressure need remain at the critical value for approximately 10 microseconds. On the other hand, cavitation experiments conducted at high velocities on small scale models with short low pressure regions (flow through venturi type nozzles) can be misleading if it is assumed that dynamic effects do not influence the critical nuclei size and pressure.

B. Sources of Nuclei

In the previous section a spherical gas bubble was assumed as the nuclei for cavitation. Such nuclei do exist near the surface of agitated liquids as continuously entrained air bubbles. However, at greater depths, or in a confined fluid, it appears that the gas should dissolve in the fluid. The partial pressure of the gas within the bubble is higher than the surrounding fluid pressure because of surface

tension and thus some gas should diffuse into the liquid. The loss of gas decreases the size of the bubble, and thus increases the surface tension pressure which increases the gas partial pressure and increases the rate of diffusion into the liquid, and so forth. From Equation (4.6) we have seen that stable spherical vapor nuclei cannot exist. Consequently, some nuclei source other than free gas bubbles must be postulated in order to explain the cavitation that is observed in fluids in which free gas bubbles of the required size for instability are not observed.

When new glass which has been cleaned with acid is immersed in water, the water tends to fill all the microscopic cracks and crevices. Such a surface is often referred to as hydrophyllic. Schweitzer and Szebehely [51] ran some gas evolution test by placing the fluid to be tested in steel and lucite containers. No precaution was made to chemically clean the containers. With water they were unable to produce any appreciable supersaturation without observing bubble formation. However, with petroleum hydrocarbons, which wet both steel and lucite, they observed considerable supersaturations (100 percent) without bubble release, provided the liquid was kept in a static state. Thus, this illustrates that the properties of the liquid are important when studying cavitation.

A material in which water does not tend to fill microscopic cracks and crevices is classified as hydrophobic. This type of material includes almost everything and thus gas volumes are easily contained in the crevices of foreign particles entrained

in the fluid or in the crevices of the boundary material itself. It is presently believed that the nuclei needed for the cavitation process (other than free gas bubbles) are located in the crevices and cracks of such hydrophobic materials. Harvey, McElroy, and Whiteley [48] were able to show that in a crevice of a hydrophobic material it is possible to have contact angles between the liquid, solid, and gas, such that the surface tension pressure is considerably reduced and tends to decrease rather than increase the cavity pressure. Under these circumstances, it is possible to postulate an equilibrium condition in which gas neither diffuses into or out of the gas trapped in the crevice, and it is these microscopic gas volumes that are currently believed to be the nuclei needed for cavitation inception.

Knapp [52] explained the difference between a pure liquid's ability to cavitate and a liquid that cavitates as soon as the pressure drops below the vapor pressure in terms of "weak spots." The findings of Knapp agreed with those of Harvey et.al. [48] in that weak spots which initiate cavitation usually occur on solid surfaces in contact with liquids. Knapp observed that normal cleaning methods were inadequate to remove weak spots from metal surfaces. This is probably due to the presence of innumerable cracks in the metal surface.

In summary, there are three distinct sources of nuclei. Each source is capable of causing the phenomena of cavitation. These are:

1. The free undissolved gas bubble, usually macroscopic in size.
2. The nuclei that exist in the crevices of foreign particles.
3. The nuclei that exist in the boundary material. Kermeen, McGraw and Parkin [53] were able to take pictures of this source of nuclei during a cavitation study.

The interpretation of cavitation tests, in which cavitation is actually produced in the test facility, is effected by the nuclei present. To properly extrapolate such test results to the prediction of prototype cavitation, the relevant scaling factors must be considered.

C. Cavitation Scale Effects

If the occurrence of cavitation were uncluttered by the appearance of scale effects, the experimental study of cavitation would be fairly easy. The test of a given shape over a range of K_o values would give the desired information. An indication of such an idealized cavitation behavior is presented with the aid of Figure 4.3.

The streamlines and pressure coefficient, for potential flow past a simple shape, are shown in Figure 4.3(a) and 4.3(b) respectively. At some point on the body, the minimum pressure occurs. The absolute value of this pressure is dependent only on the relative flow velocity, V_o, the reference pressure, p_o, and the exact shape of the body. This minimum pressure value for the given body is thus uniquely characterized by $C_{p_{min}}$, the minimum value of the conventional pressure coefficient in which

$$C_p = \frac{p - p_o}{\frac{1}{2} \rho_o V_o^2} \tag{4.7}$$

In the idealized situation, no cavitation test would be required because the value of K_o at which cavitation would first appear is simply $-C_{p_{min}}$. If the pressure could be measured at the proper location, $C_{p_{min}}$ could be found by a noncavitating test with water, or even air, as the test medium. However, as a result of scale effects, cavitation tests are required.

The manner in which a cavitation test would verify the K_{i_o} prediction, in the idealized cavitation situation, is shown in Figure 4.3(c). A cavitation test is normally conducted with the initial operation of the test facility at a high K_o value, for which there is no possibility of cavitation. The operating K_o

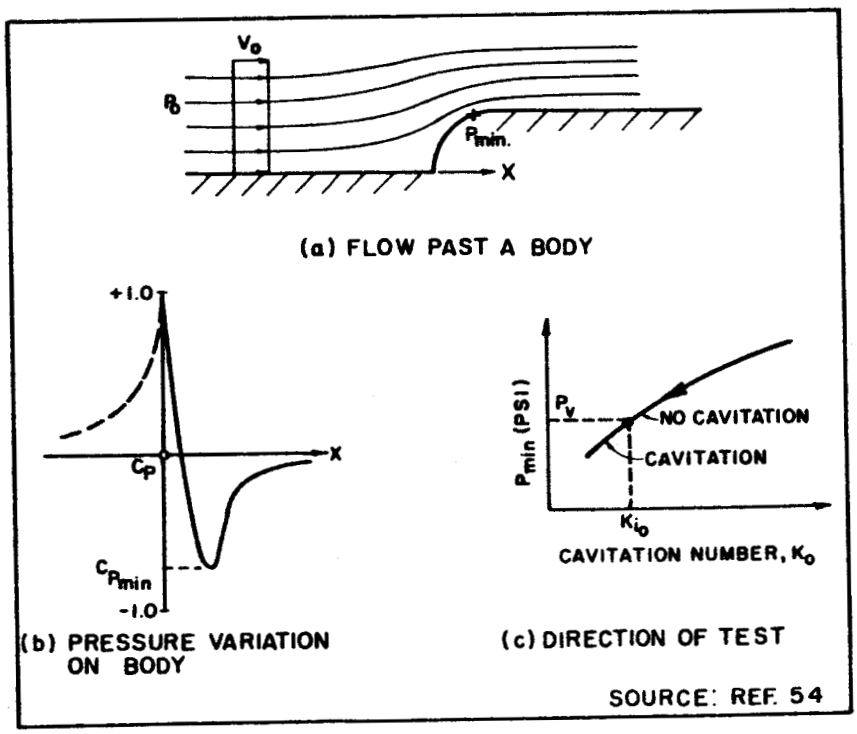

Figure 4.3 Body Flow Dynamics and Idealized Cavitation Test Behavior

value is then reduced, either by raising V_o or lowering p_o, with an associated decrease in the absolute pressure p_{min}, until the value $p_{min} = p_v$ is reached. The reduction of K_o below the inception value (K_{i_o}) has no further effect on p_{min}, which remains equal to p_v. However, the nature of cavitation is changed as K_o is reduced below K_{i_o}. At the inception point, the cavitation consists of small bubbles that quickly collapse with tremendous noise as they proceed into regions of higher pressure. At K_o values below K_{i_o}, larger cavities may form which change the flow and force relations for the object or conduit.

Unfortunately, little is known about how the conditions, at the beginning of a cavity, change with the degree of cavitation. Thus, a detail study of this could provide useful information.

From this discussion of the idealized cavitation occurence situation scale effects may be defined as any flow phenomena which will cause deviations from the idealized occurrence. Thus, if the pressure distribution over the body varies with the nature of the flow, this represents one kind of scale effect. If cavitation does not always start when p_v is reached, then another type of scale effect is represented. The pressure distribution on a body is affected by such factors as fluid viscosity, surface roughness and etc. The pressure at which cavitation occurs depends on such factors as nuclei present, surface tension, pressure distribution and etc.

Holl and Wislicenus [55] pointed out that the idealized similarity relation of cavitation ($K_o = P_o - P_v/\frac{1}{2}\rho_o V_o^2$) is based on certain assumptions. These are:

1. All pressure differences in the flow are proportional to ρV^2.
2. Geometric similarity includes surface irregularities of the flow boundaries.
3. The vapor pressure in the flow field is constant and the pressure at which cavitation takes place is the equilibrium vapor pressure.
4. Cavitation takes place instantaneously whenever the vapor pressure is reached.

The correct similarity relations, which are needed to describe cavitation, are unknown. However, Holl and Wislicenus [55] listed several similarity relations which may help describe cavitation. These are given in Table 1. The classical relation, included in Table 1, must always be satisfied together with the requirement of geometric and kinematic similarity.

4.5 The Investigations of Cavitation Inception

In the following sections we will discuss the experimental and theoretical investigations of cavitation inception for unseparated flow past streamlined bodies, separated flow past non-streamlined bodies, and flow through venturi type nozzles, orifices, and tubes.

A. Unseparated Flow Past Streamlined Bodies

A streamlined body is a body in which the curvatures are sufficiently mild to permit nearly ideal flow (that is, flow without boundary layer separation). The pressure distribution on this body, as obtained from potential flow theory, would be expected to be in

TABLE 4-1 [55]

	No.	Forces And Characteristics	General Similarity Requirements	Similarity Requirements For Same Fluid Properties	Probable Effects On K of Changes in V and L_1 Only
Ideal Flow	1	Inertia Forces Only (Classical Theory)	$K = \frac{p - p_v}{\frac{1}{2}\rho V^2} = \text{Const.}$	$p - p_v$ proportional to V^2	No Effects K = Const.
Hydrodynamic Scale Effects On The Fluid Pressure	2	Viscosity And Inertia Forces	Reynolds' Law of Similarity $Re = VL/\nu = \text{Const.}$	$VL_1 = \text{Const.}$	K Increases With VL_1
	3	Gravity And Inertia Forces	Froude's Law of Similarity $F_L = V/\sqrt{gL_1} = \text{Const.}$	$V/\sqrt{gL_1} = \text{Const.}$	Vertical Differences In Cavitation Decrease With Increasing $V/\sqrt{L_1}$
	4	Elastic And Inertia Forces (Compressibility)	Law of Constant Mach Number $M = V/c = \text{Const.}$	V = Const.	Not Predictable. Probably Effective Only With Extensive Cavitation
	5	Effects of Surface Irregularities	$h/\delta = \text{Const.}$ for $R_e = \text{Const.}$: $h/L_1 = \text{Const.}$	SAME	K Increases With h/L_1. K decreases with increasing L_1 if h increases slower than L_1.
Thermodynamic Scale Effects	6	Effects of Vapor Pressure	$p_v/p = \text{Const.}$	p = Const. Therefore V = Const.	K increases with V
	7	Effects of Vaporization And Heat Transfer	$\frac{1}{p}\frac{\partial p_v}{\partial T}\frac{s_v}{s_\ell}\frac{v_\ell}{v_v}\frac{L_v}{c_{p_\ell}}$ $P_e^{n_1} = \text{Const.}$ Peclet Number, $P_e = \frac{c_{p_\ell} VL_1}{v_\ell k}$	$VL_1 = \text{Const.}$	K decreases with increasing VL_1
		(6) and (7) may be neglected if p_v/p is very small (e.g. for Cold Water)			
Molecular And Other Microscopic Scale Effects	8	Surface Tension And Inertia Forces	Law of Constant Weber Number $W = \rho V^2 L_1/\sigma = \text{Const.}$	$V^2L_1 = \text{Const.}$	K increases with V^2L_1
	9	Number of Nuclei	$\sqrt[3]{N} \cdot L_1 = \text{Const.}$ (Only if nearly all nuclei form centers of cavitation)	$L_1 = \text{Const.}$	K increases with L_1 (for N = Const.)

Table 4.1 Cavitation Similarity Relations

good agreement with experimental measurements if the boundary layer displacement thickness is small compared with the body diameter. This condition is usually met if the Reynolds number is sufficiently high to produce a fully developed turbulent boundary layer. [56]

Knapp and Hollander [57] made a high-speed photographic (20,000 pictures per second) study of the formation and collapse of individual bubbles during the flow of water past a 1.5 caliber Ogive-Nosed body. The life of the bubble from the instant it was large enough to be detected until the completion of its first collapse was only about 0.003 seconds. The formation period required about three fourths of this time, leaving one fourth for the collapse period. The conditions of the water tunnel were: V_o = 40 fps, p_v = 0.40 psia, and p_o = 4 psia.

In many of the pictures taken, it was obvious that the collapse of one bubble had a major effect on the collapse of its neighbor. Furthermore, as the severity of the cavitation was increased, the bubble concentration built up very rapidly, so that rarely if ever could a single bubble be seen to form and collapse without interference.

Kermeen, McGraw, and Parkin [53] investigated several geometrically similar hemispherical and 1.5-caliber Ogive-Nosed bodies for cavitation inception at various water tunnel speeds. The results of this investigation are shown in Figure 4.4. Figure 4.4 illustrates that the measured incipient cavitation numbers were less than $|C_{p_{min}}|$ and depended on both the model size and the test velocity. However, the data indicates that the incipient cavitation number does approach

$|C_{p_{min}}|$ for large size bodies and high tunnel speeds. It is suggested that the scale effects shown in Figure 4.4 are primarily caused by the low concentration of nuclei and the small nuclei sizes present in the test water. [58] The curves shown in Figure 4.4 are average curves drawn through the data.

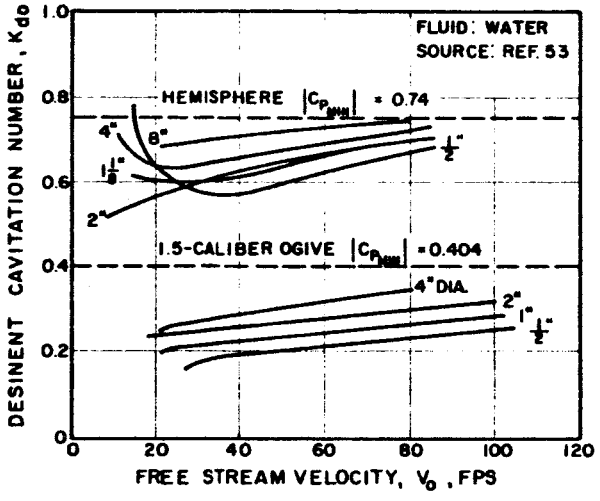

Figure 4.4 Incipient Cavitation Number as a Function of Free-Stream Velocity for Bodies With Hemispherical Noses and 1.5-Caliber Ogive Noses

Figure 4.5 shows how the desinent cavitation number varies with the Reynolds number for the flow of water past Joukowski hydrofoils. For a given size the desinent cavitation number increases with the Reynolds number. Furthermore, for a given Reynolds number, the desinent cavitation number decreases with increasing size. On the other hand, the NACA 16012 hydrofoil data shown in Figure 4.6 differ markedly from the trend shown in Figures 4.4 and 4.5. In Figure 4.6 the cavitation number decreases for a given size with

increasing Reynolds number (with increasing velocity) and increases for a given Reynolds number with increasing size. This unique behavior goes together with the flat pressure distribution of these profiles at 0-degree angle of attack (see Figure 4.7) in contrast to the peaked minimum pressure of other streamlined bodies treated. Calehuff and Wislicenus [61] reported that cavitation on the profiles with flat pressure distribution had the form of traveling bubbles, whereas with peaked under-pressures cavitation appeared to be attached to the surface.

In Figures 4.5 and 4.6 the scale effects can be seen. Also, the effect of pressure distribution on the inception of cavitation is shown to have an important influence.

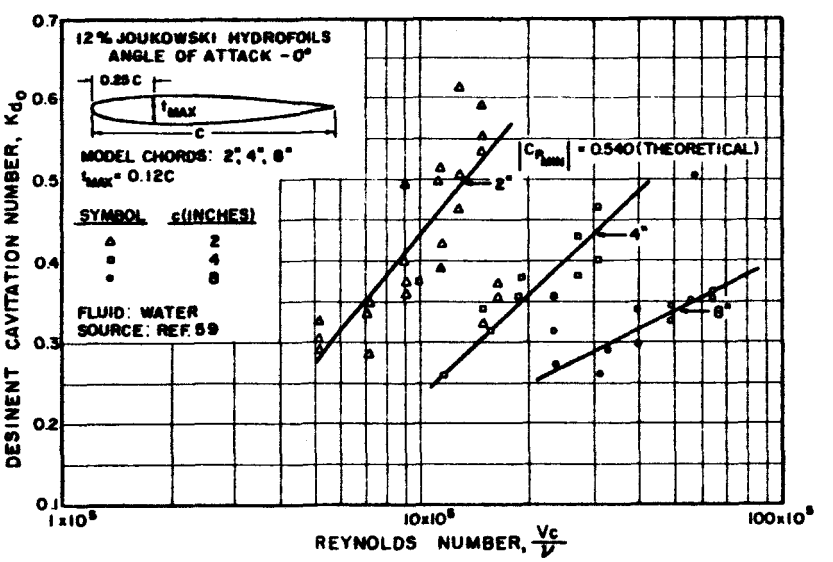

Figure 4.5 Desinent Cavitation Number as a Function of Reynolds Number for Water Flowing Past Joukowski Hydrofoils

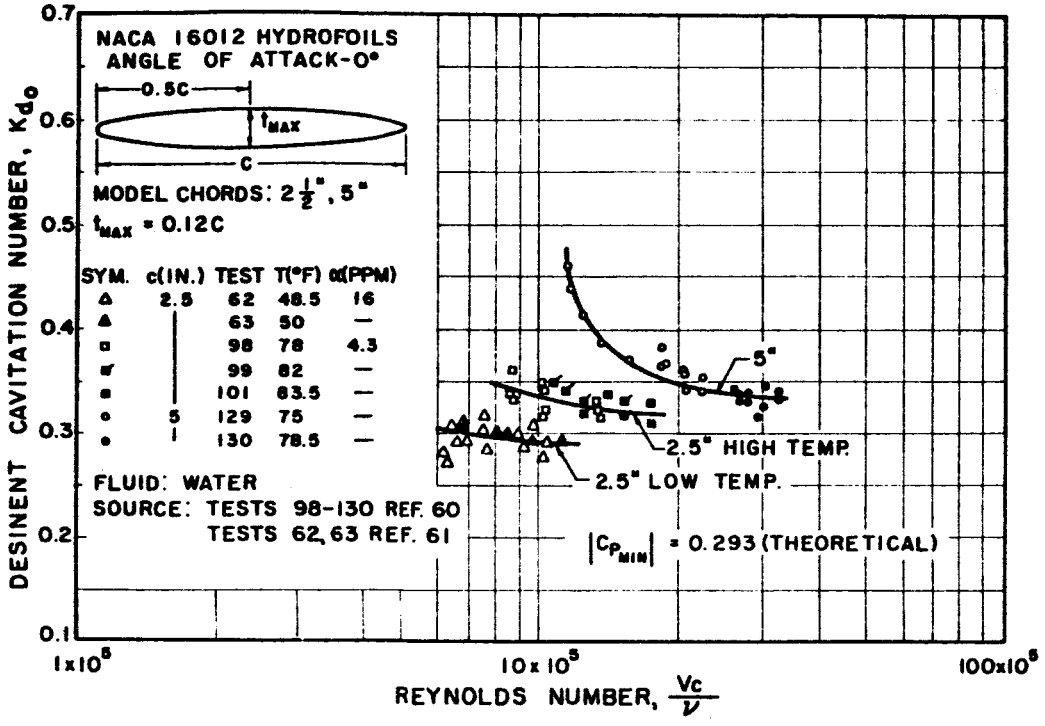

Figure 4.6 Desinent Cavitation Number as a Function of Reynolds Number for Water Flowing Past NACA 16012 Hydrofoils

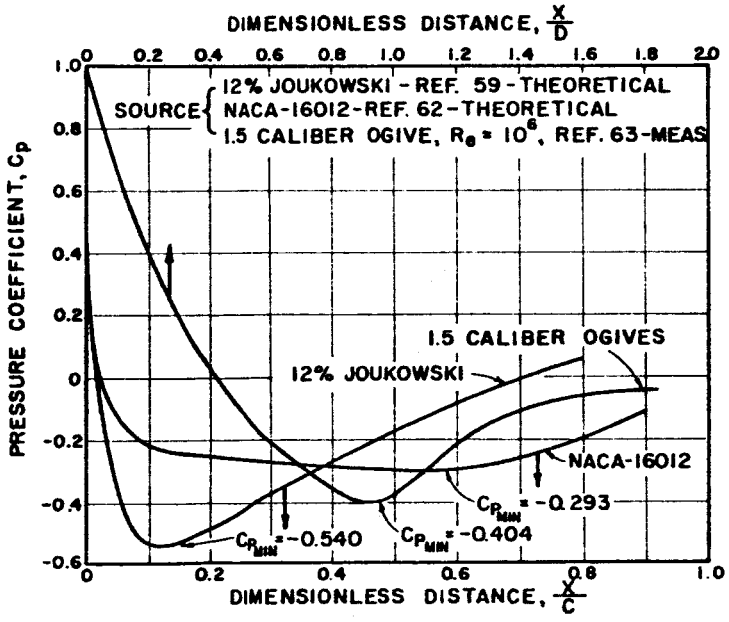

Figure 4.7 Pressure Distributions for Streamlined Bodies

The type of flow in the boundary-layer has an important effect on the inception of cavitation. Daily and Johnson [58] investigated the effects of a turbulent boundary-layer on the inception of cavitation for the flow of water through a two-dimensional nozzle. The flow in the boundary-layer was rotational and the minimum pressure did not occur on the wall (for large body curvatures) but slightly away from it in the center of the eddies that compose the boundary-layer. Thus cavitation can actually begin at values of K_o that are slightly greater than $|C_{p_{min}}|$ because of the additional pressure reduction caused by turbulence. However, Daily and Johnson pointed out that the boundary layer turbulence effect is small and can usually be neglected at the high velocities that are normally encountered in hydraulic structures where cavitation is expected.

The effect of air content on the occurrence of cavitation, for water flowing past hydrofoils, was investigated by Holl [44]. These hydrofoils were tested at various angles of attach. Figure 4.8 shows the results of these tests.

Holl [44] observed that two types of desinent cavitation could be determined. As the pressure was increased causing the cavitation to disappear, a pressure was reached where the cavitation disappeared uniformly across the span. This was referred to as areal cavitation.. However, it was observed that several cavitation bubbles still clung to the surface and continued to do so up to very high ambient pressures. These spots of cavitation were manifest on the NACA 16012 hydrofoils at angles of attack above the critical angle.

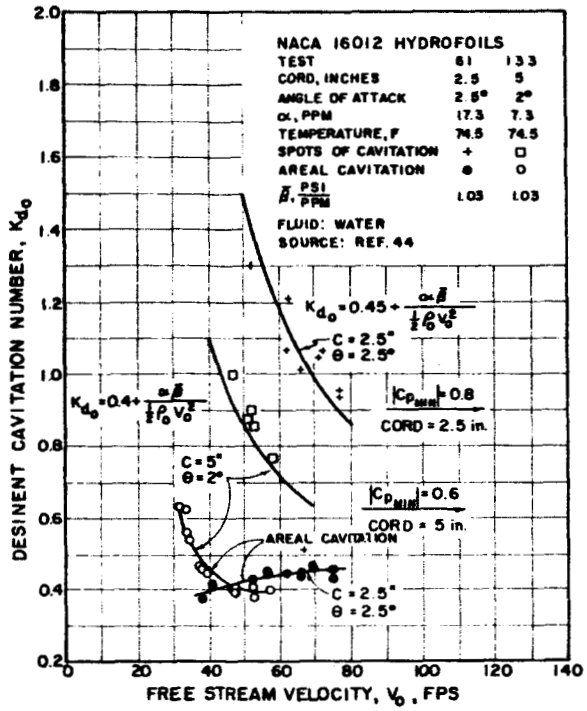

Figure 4.8 Two Types of Cavitation on 2.5-in. and 5-in. NACA 16012 Hydrofoils

The critical angle of attack is that angle at which the change of $|C_{p_{min}}|$ with angle becomes very large. The critical angle of attack for the NACA 16012 hydrofoils is about 1.5 degrees. [62]

Oshima [64] developed a relation, from boundary-layer gas-nuclei interaction considerations, which allows predicting the Reynolds number variation in K_{i_o} for flow past axially symmetric bodies. Calculations of the turbulent boundary-layer growth on the test bodies were combined with the suggestions of Daily and Johnson [58], concerning nuclei growth and turbulence effects to predict the scaling of cavitation inception as observed on the axisymmetric bodies referred to previously. Oshima's formula appears to agree fairly close with some selected experimental data. However, before definite conclusions can be formed about this work, additional experimental investigations (with liquids other than water) are necessary.

Knapp [65], in 1952, derived a formula which is similar to Oshima's formula. However, Oshima was able to show that Knapp's formula is a special case of his theory.

The inception of cavitation on isolated surface irregularities imbedded in a turbulent boundary layer was investigated experimentally and theoretically by Holl [66] and [60]. Holl was able to show how the effect of a small roughness element (of height, h) on a smooth surface may greatly increase the inception cavitation number (see Figure 4.9). In terms of the inception cavitation number, Kr_o, of

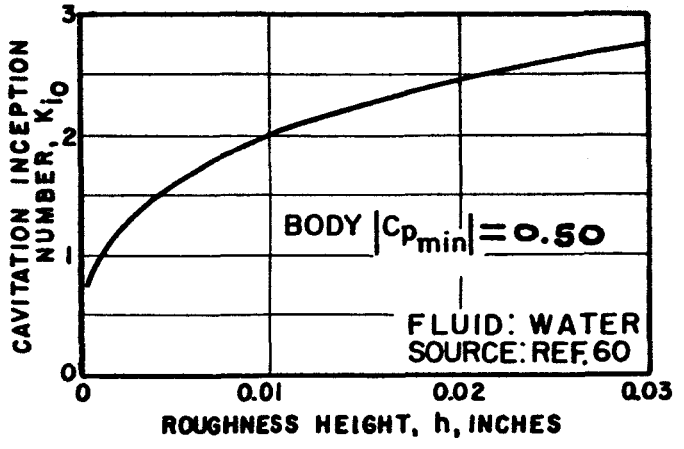

Figure 4.9 Calculation Effect of Relative-Roughness Size for a Particular Flow

the roughness element and the pressure coefficient of the smooth body, the inception cavitation number of the roughened body is

$$K_{i_o} = -C_p + (1-C_p) K_{r_o} . \qquad (4.8)$$

The roughness is most detrimental when placed at the minimum pressure-point of the parent body, that is, when $C_p = C_{p_{min}}$.

Holl [66] determined how K_{r_o} varied with the ratio of the height of a roughness element, h, to the boundary-layer thickness, δ, for different velocity-profile shapes and two different shapes of roughness elements. The velocity-profile shape was expressed by the boundary-layer shape parameter $H = \frac{\delta^*}{\theta}$, where δ^* is the displacement thickness and θ the momentum thickness. Two families of cylindrical roughness elements having constant cross section were studied. One family had a circular-arc cross section. The other family had a triangular cross section. The results of this study are shown in Figure 4.10.

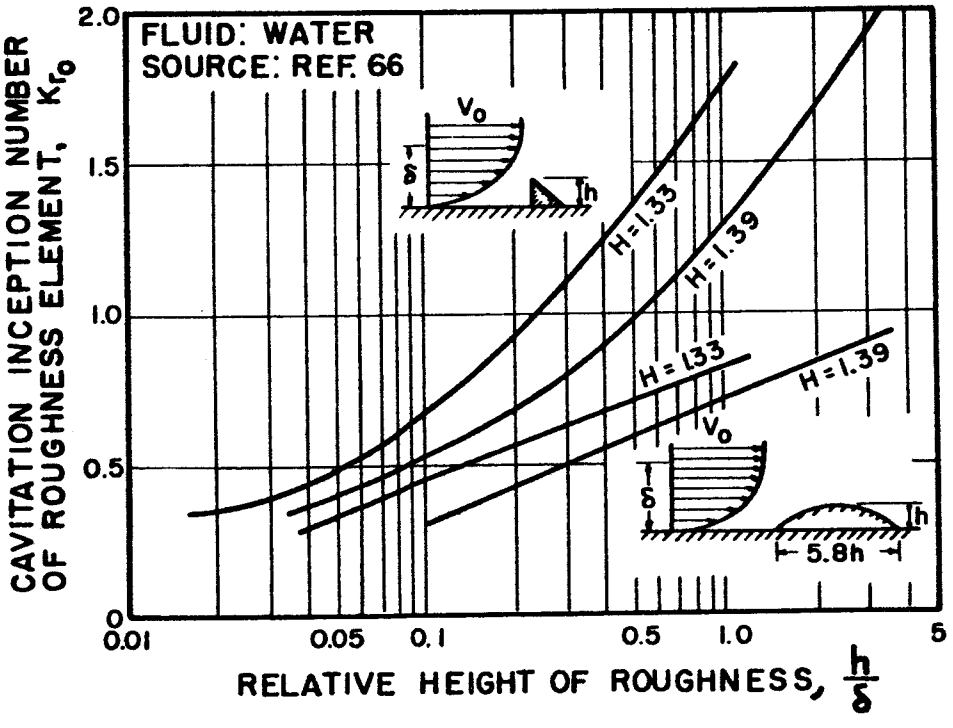

Figure 4.10 Cavitation Inception on Roughness Elements in Boundary-Layer Flows

The seriousness of roughness effects in producing cavitation inception scale effects is illustrated by the following example. [66] Consider a body with $C_{p_{min}} = -0.50$ of such proportions and tested at such a speed (V_o = 50 fps) that δ = 0.048 in. As Figure 4.9 shows, the effects for the sharp roughness of Figure 4.10 (and a fairly-normal turbulent boundary layer of H = 1.33) are considerable. A 102% ($K_{i_o} - |C_{p_{min}}| / |C_{p_{min_s}}| \times 100$) increase in K_{i_o} occurs for a 0.001 in. high roughness and much larger effects are easily possible.

B. Separated Flows Past Non-Streamlined Bodies

If the flow past a body is decelerated too rapidly, the boundary-layer separates and the pressure distribution along the boundary is no longer a true indication of the minimum pressure in the field. Unfortunately, there is no exact method of obtaining the minimum pressure coefficient in the flow field in terms of the measured boundary pressure. Nevertheless, some experimental studies of cavitation inception have been reported.

Most of the available test data pertain to sharp-edged disks (Figure 4.11) and zero caliber ogives, i.e. cylinders with a flat cutoff end facing the flow (Figure 4.12). The most striking difference, as compared to the behavior of streamlined bodies, lies in the magnitude of the changes in the desinent cavitation number, which varies by a factor of two for a change in Reynolds number by a factor of ten. This appears to be at least twice the largest change observed with most of the streamlined bodies (excepting the Joukowski hydrofoil data shown in Figure 4.5). Furthermore, the

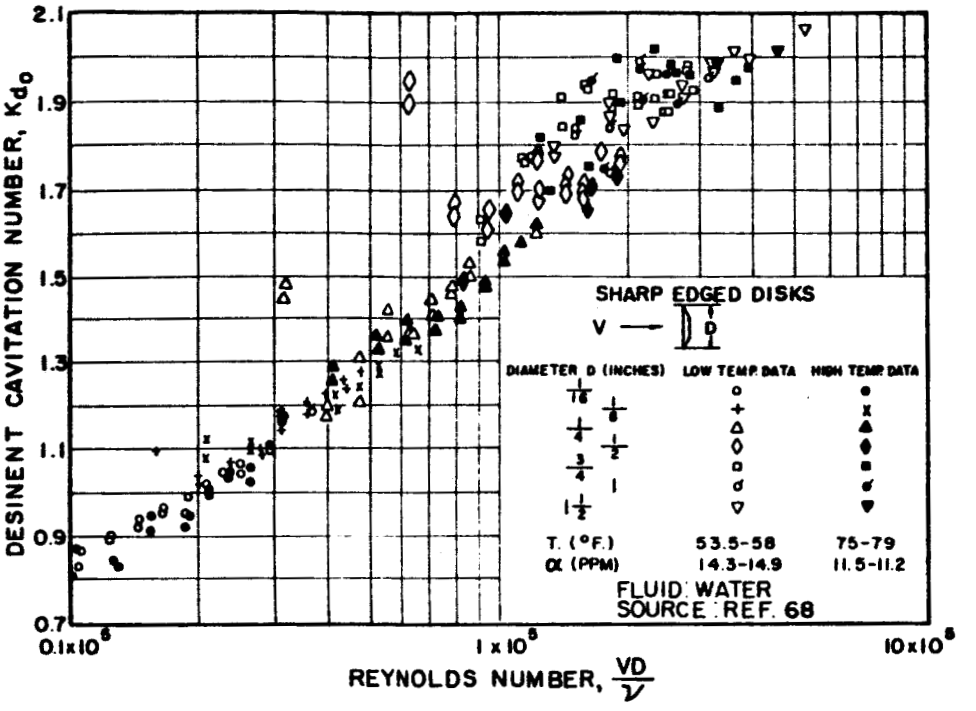

Figure 4.11 Desinent Cavitation Number as a Function of Reynolds Number for Water Flowing Past Sharp-Edged Disks

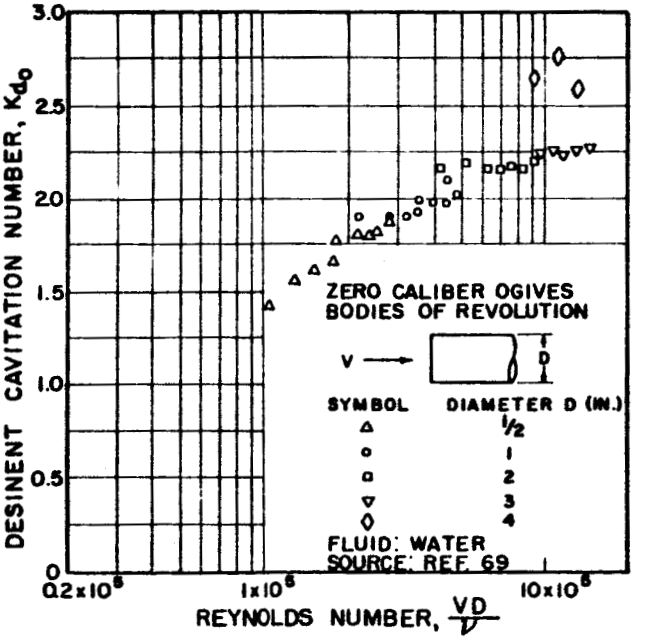

Figure 4.12 Desinent Cavitation Number as a Function of Reynolds Number for Water Flowing Past Zero-Caliber Ogives

cavitation number of bluff bodies (i.e., separated flow) continues to increase with increasing Reynolds number. In this respect the test points of the zero-caliber ogives (Figure 4.12) seem to continue the sharp disk dat (Figure 4.11) without a break or indication of leveling off.)

C. Flow in Venturi-Type Nozzles

The venturi-type nozzle has proved to be an effective shape for studying cavitation. This is due to the fact that a wide range of flow conditions are easily obtained. Thus, studies can be made for various degrees of cavitation under different pressure distributions.

In the experiments cited above (Kermeen, McGraw, and Parkin [53], no consistent effect of air content, varied between 7 and 13 ppm, could be detected. This disagrees with the observations of Numachi and Kurokawa [70], McCormick [67], Crump [71], [72], and others. Crump [71] found a significant dependence of inception on total air content in experiments with a venturi nozzle having a diffuser angle of 5^{o}. He reports that in fully aerated fresh water, cavitation first appeared at the boundary in the form of a small vapor cavity. In deaerated fresh water, Crump found that cavitation first appeared in the form of individual bubbles which do not necessarily form at the boundary. Under these conditions, bubbles formed and disappeared downstream under ambient tensions as high as four atmospheres. Furthermore, he found that higher tensions were required as the velocity was increased.

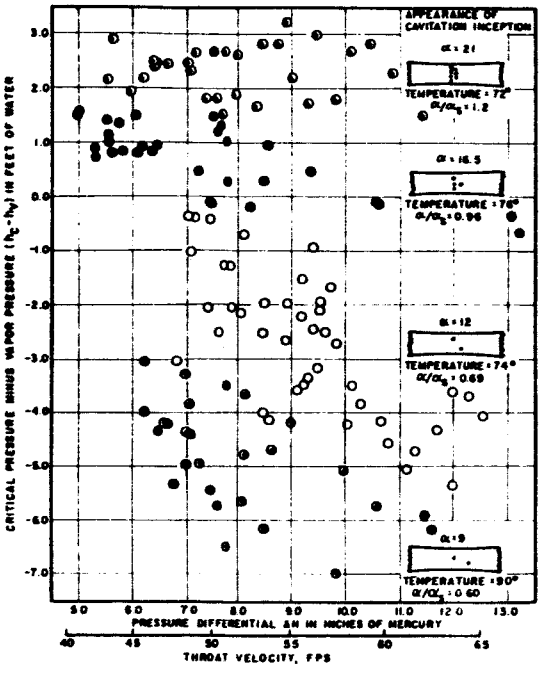

Figure 4.13 Critical Pressures for the Inception of Cavitation in Fresh Water of Varying Air Content

Figure 4.13 shows that in the undersaturated liquid it was possible to obtain tensions as the relative air content α/α_s was reduced. Results in a nozzle with an abrupt expansion, however, show opposite trends in the pressures required for inception; [72] although here, too, tensions were obtained. Comparable results for sea water are shown in Figure 4.14; in this case, bursts of cavitation were observed at pressures well above vapor pressure. While the trends in these experiments were fairly definitive, the very large scatter of results is indicative of the need for understanding the behavior and distribution of nuclei; i.e, the mechanisms by which nuclei are stabilized and the characterization of nuclei content; e.g., a "spectrum," or description of number and distribution in size. [82]

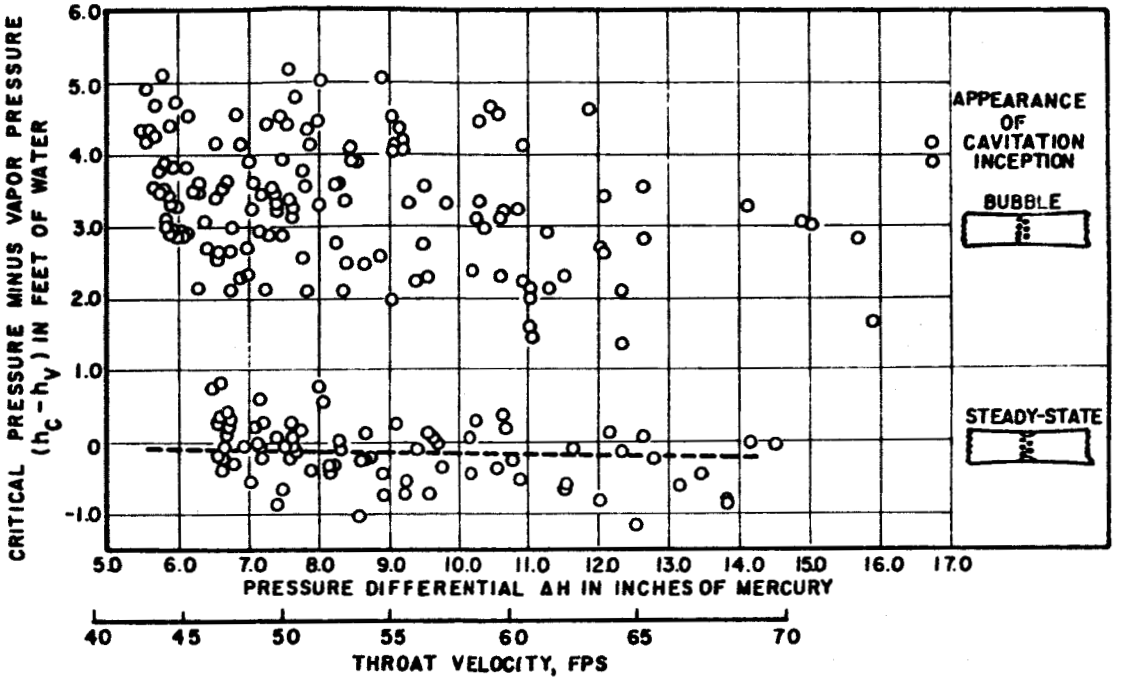

Figure 4.14 Critical Pressures for the Inception of Cavitation in Sea Water

Williams and McNutly [73] investigated the effect of an additive (sodium nitrate dissolved in distilled water) on cavitation inception. The incipient cavitation number was found to increase (cavitation to become easier) with an increase in the percentage (from 0 to 0.4% by weight) of dissolved sodium nitrate.

The flow of liquid nitrogen through a venturi test section has been investigated by Ruggeri and Gelder [75]. Just prior to incipient cavitation, the minimum local wall pressure was significantly less than the vapor pressure corresponding to the stream liquid temperature. This pressure difference was called effective liquid tension. The temperatures and pressures measured within regions of well-developed cavitation were in thermodynamic equilibrium but were less than the temperature and the saturation vapor pressure of the approaching

stream. These differences increased with both stream velocity and extent of cavitation.

Figures 4.15 and 4.16 show a comparison of cavitation tests of liquid nitrogen and room-temperature water (Ruggeri and Gelder [74] in the same venturi. Nitrogen sustained nearly twice the effective tension as water. The incipient cavitation numbers for water were usually higher than those for nitrogen. This indicates a possibility that temperature effects the nuclei in the test section. However, the test of additional pure fluids could bring out this effect. Scale effects other than temperature can be seen in Figures 4.15 and 4.16.

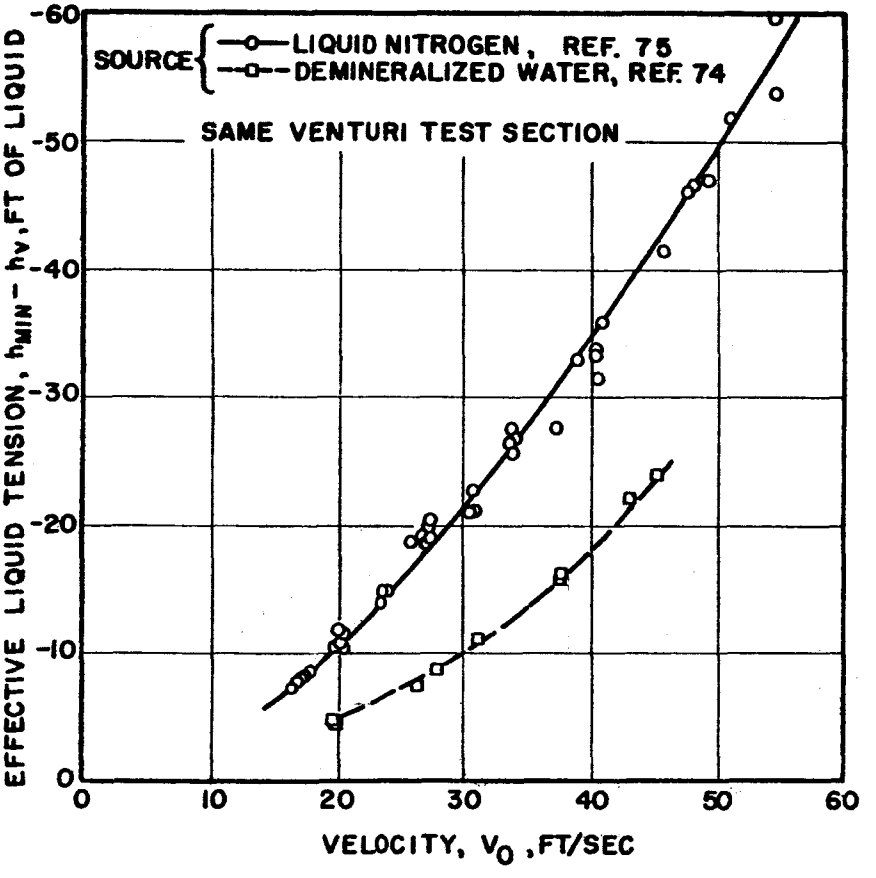

Figure 4.15 Comparison of Effective Liquid Tension Based on Visible Incipient Cavitation for Nitrogen and Water Flowing Through Same Venturi Model

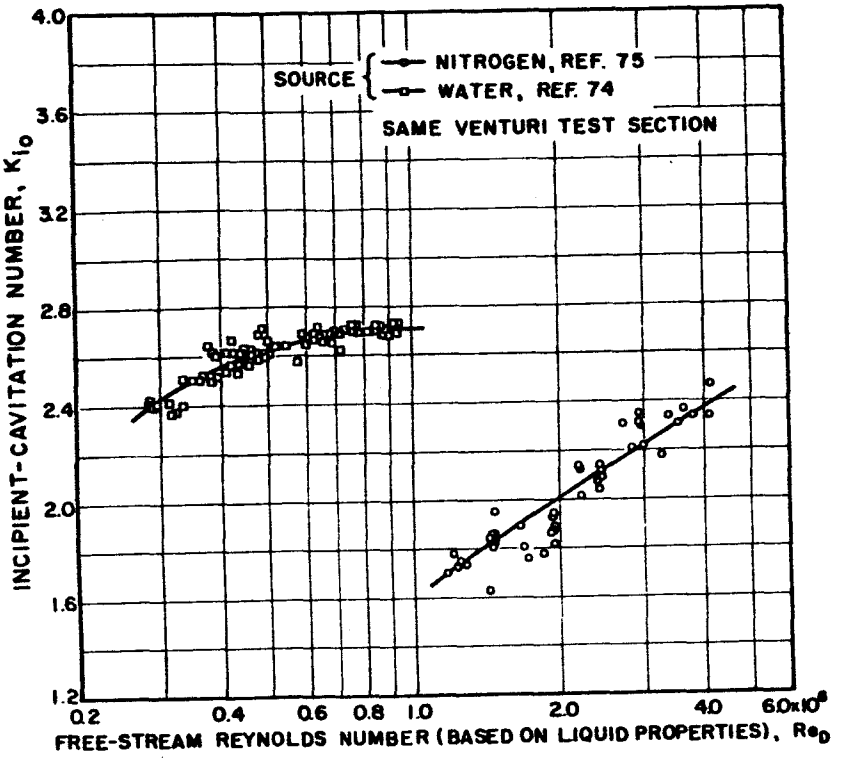

Figure 4.16 Comparison of Incipient Cavitation Number for Nitrogen and Water Flowing Through Same Venturi Model

Lehman and Young [45] investigated the pressures and cavitation numbers, near the location where incipient and desinent cavitation occurred, for water flowing through different convergent-divergent test sections. The results of this investigation are shown in Figures 4.17 and 4.18. The cavitation pressures measured near the plane of incipient and desinent cavitation were generally higher for the tests made using an abrupt contour test section.

Hammitt [76] made an investigation similar to the investigation made by Lehman and Young [45]. Hammitt observed no difference between the incipient and desinent cavitation numbers while studying the flow of water through a smoothly changing internal contour nozzle. This agrees fairly close with the investigation made by Lehman and Young on a similar shape nozzle. However, the abrupt

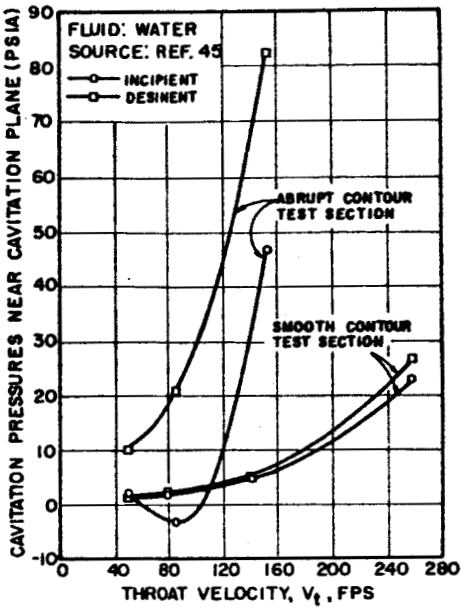

Figure 4.17 Cavitation Pressures Near Cavitation Planes As a Function of Stream Velocity at the Throat of a Venturi

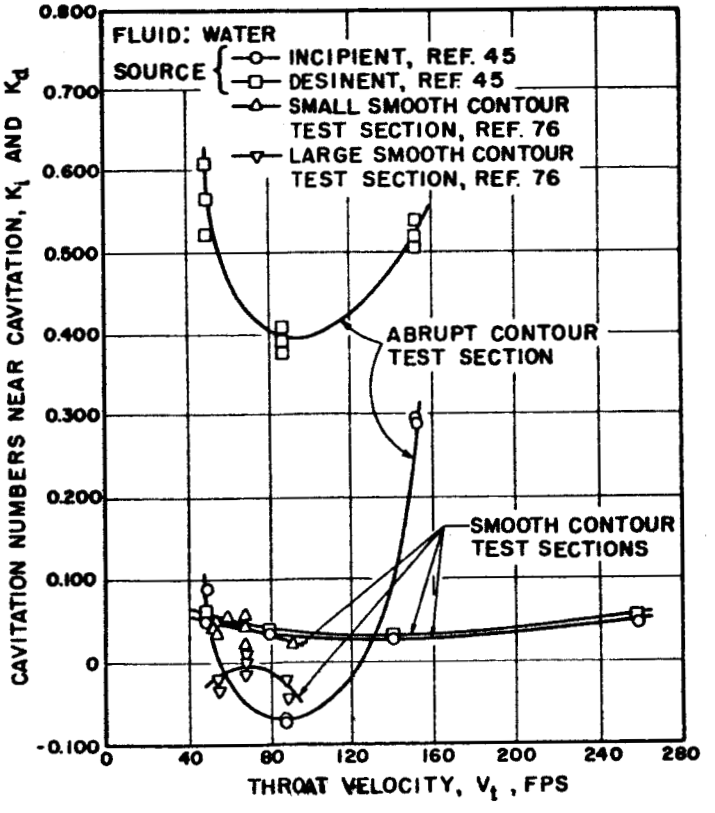

Figure 4.18 Comparison of Cavitation Numbers for Water Flowing Through Abrupt- and Smooth-Contour, Venturi Type, Test Sections

contour tested by Lehman and Young indicates that the conditions at the plane of cavitation are a function of the pressure distribution prior to cavitation.

D. Flow Through Orifices

The jets flowing from orifices into filled conduits (sudden enlargements) represent cases of extreme separation where, in addition to expansion and diffusion of the main jet, there is the generation of secondary flow and countless small eddies and vortices. The pressures within the eddies will be appreciably below that of the surrounding fluid, particularly when the velocity of orifice efflux is high. These low pressures can quite easily reach the vapor pressure of the fluid and there exist the possibility of cavitation.

The effect of cavitation on the discharge coefficient of orifices has received some attention [78], [79]. However, only the investigation of the flow of pure fluids through orifices will be reported at this time.

Jacobs and Martin [77] investigated the flow of water, liquid hydrogen, and liquid nitrogen through sharp-edged orifices. They were unable to produce cavitation as long as pure liquid entered the orifices. With liquid nitrogen, the pressures at the venae contractae were as much as 170 inches of liquid below the vapor pressure, while with liquid hydrogen the pressures at the venae contractae were as much as 192 inches of liquid below the vapor pressure. These were the lowest pressures attainable with their apparatus.

Jacobs and Martin observed that the only way cavitation could be produced was to have two-phase flow entering the orifices. In many tests even when two-phase flow entered the orifices, cavitation symptoms were not evident.

E. Flow Through Conduits

Mikol and Dudley [80] investigated the conditions at which cavitation inception occurs for the flow of Freon-12 through small bore copper and glass tubes. The point of inception of cavitation was observed to move by discrete jumps rather than in a continuous manner as operating conditions were changed. This was probably due to the gradual and uniform pressure gradient in the tube. In venturi test the inception site is fixed within rather close limits by the nonuniform and sharper pressure gradients imposed by the geometry. No such shift has been reported in any venturi test.

Mikol and Dudley observed that the tube material had the most important influence on the incipient cavitation number. The incipient cavitation number for the glass tube was nearly twice that for the copper tube. This result is in agreement with the nucleation theory expectation that a metal surface should provide many more nucleation sites than a glass surface.

Fauske and Min [81] investigated the flow of slightly sub-cooled Freon-11 through apertures and short tubes. They used a modified cavitation number to establish a criterion for determining single-phase or two-phase flow regimes in short tubes. The modified cavitation number is,

$$\bar{K}_o = \frac{2g\,\Delta P}{\rho_o V_o^2}\left(\frac{L_1}{D}\right) \qquad (4.9)$$

where ΔP is the pressure difference, $p_o - p_e$ for two-phase flow or $p_o - p_b$ for single-phase flow. Figure 4.19 indicates that for modified cavitation number below 10 the fluid exhibits completely metastable single-phase flow. When the modified cavitation number exceeds 14, two-phase flow exists. In the range of $\bar{K}_o$ between 10 and 14, unstable transitional flow occurs.

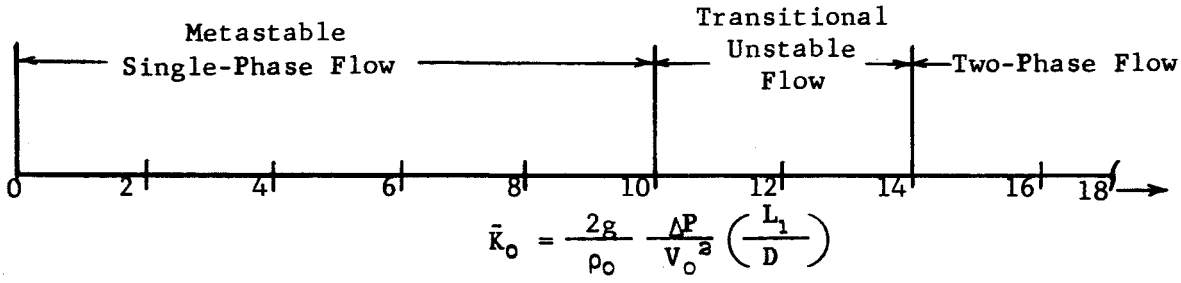

Figure 4.19 Correlation Number Determining the Occurrence of Single- and Two-Phase Flow Regimes. [81]

4.6 Conclusions

The preceding discussions are primarily an attempt to point out some of the knowns and unknowns about cavitation. For a constant cavitation number, both the time of exposure to the region of pressure below the vapor pressure (underpressure) and the amount of this underpressure, are functions of velocity. It may not be unreasonable to assume that the gross cavitation pattern is largely controlled by the nucleation process. It is conceivable that the nucleation process may depend upon time of exposure to underpressure and absolute value of this underpressure in such a way that the effects are not cancelled for

constant cavitation number. With systematic experimental studies of different liquids flowing through various pressure distributions, it may be possible to obtain a reasonably correct K_{i_o} value or trend for an arbitrary body and liquid by means of some relations between underpressure and relaxation time (time fluid remains at pressures below the vapor pressure before cavitation occurs). Also, a method is needed to accurately predict the conditions at the position where cavitation starts for limited and profuse cavitation.

In the literature reviewed there is a total absence of experiments related to the cavitation phenomenon for flow in bends. Most of the conduits in hydraulic machinery where cavitation occurs are curved. There are no clear ideas as to what actually takes place under such conditions. What portion of the flow is actually vaporized is of interest. Also, whether compound liquids like petroleum oils, would behave similarly to water under cavitation conditions.

CHAPTER V

Bubble Dynamics Literature Survey

5.1 Introduction

Bubble dynamics is the study of bubble size and radial velocity as a function of time and all other variables effecting the size and radial velocity of the bubble. The primary variables are the type of liquid around the bubble, the temperature and pressure fields in that liquid and inside the bubble, and the type of gas inside the bubble. Here the single component liquid and bubbles containing only the vapor of this liquid will be considered.

The need for a knowledge of bubble dynamics resulted from problems in the fields of cavitation and boiling heat transfer. However, a study of bubble dynamics need not involve the method by which a bubble is formed. Experimental results of both are considered.

The goal for knowledge in bubble dynamics is to have a theory which will predict when a bubble will form, grow and collapse. The prediction of when a bubble will form must be related to the probability that certain pressure, temperature, and nuclei requirements be met at a given time and position. The bubble may form as a result of cavitation (pressure reduction) or heat transfer (temperature increase). The growth and collapse of a vapor bubble is the subject of the following sections. The subject is considered in two parts: 1. theoretical or analytical approach, 2. experimental approach.

5.2 Theoretical Studies of Bubble Dynamics

When a vapor bubble grows, latent heat of vaporization must be supplied at the vapor-liquid interface and the liquid will experience a drop in temperature. This would have a tendency to reduce the growth rate. A vapor bubble in a superheated liquid can be expected to grow without bound as long as there is superheat in the liquid to provide the heat of vaporization. Similarly, when a vapor bubble collapses, latent heat is given up by the vapor at the interface and the liquid will experience a rise in temperature.

In a subcooled liquid a bubble will collapse due to heat transfer effects and inertia effects. The contribution of each method is discussed by Florschuetz and Chao [83]. They define a parameter, B_{eff}, that can be used to determine the relative control heat transfer and inertia have over collapse.

There have been several methods applied to the analytical solution of the bubble dynamics problem. Some assumptions identical in all approaches are:

1. The bubble is spherical in shape.
2. The pressure field in the liquid is known.
3. The temperature field in the liquid is known.
4. The surface tension pressure is $2\frac{\sigma}{R}$
5. The liquid and vapor are pure.
6. Fluid motion is irrotational.
7. Viscosity effects are neglected.
8. The liquid is incompressible.
9. Thermal conductivities and specific heats are constant over this temperature range.

10. Bubble wall velocity equals the liquid velocity at the wall.

11. Bubble wall velocity is small compared to the sonic velocity in the liquid.

12. The vapor inertia is neglected.

13. The vapor pressure and temperature is uniform in the bubble.

It is obvious that these assumptions do not hold over the whole range of growth and collapse. The spherical shape is unstable at the point of collapse. There is a large temperature variation in the collapsing bubble and the specific heat and thermal conductivity cannot be considered constant. However, the errors made by using these assumptions are small and the resulting theories do correlate much of the experimental data.

When the assumptions listed are applied to the continuity equation and equation of motion, an equation for the motion of the radius of the vapor bubble wall is determined:

$$R\ddot{R} + \frac{3}{2}\dot{R}^2 = \frac{p_v(T) - p_\infty}{\rho_L} - \frac{2\sigma}{\rho_L R} \quad ** \qquad (5.1)$$

The analytical solutions to Equation (5.1) result from the viewpoint of the authors.

A. Plesset - Zwick Approach

Zwick [84] solves Equation (5.1) along with the heat equation

$$\rho C_{pl}\left\{\frac{\partial T}{\partial t} + \vec{V}\cdot\nabla T\right\} = k\nabla^2 T + \dot{q} \qquad (5.2)$$

and boundary conditions

**Dots represent derivatives with respect to time.

$$R^2 k \left.\frac{\partial T}{\partial r}\right|_{r=R(t)} = \frac{L_v}{3}\frac{d}{dt}\left[R^3 \rho_v(T)\right] \tag{5.3}$$

and

$$T(r,0) = T_o \ . \tag{5.4}$$

The mathematics of solving Equations (5.1), (5.2), (5.3), and (5.4) together are presented and the bubble growth rate is given for four phases of bubble growth. The phases are arbitrarily selected by Zwick and are called delay period, early phase, intermediate phase, and asymptotic phase. The phase classification depends upon the physical variables which may be neglected for a given range of values. Zwick uses the physical properties of water to explain which terms may be neglected.

Plesset and Zwick [85] give an alternate solution to Equation (5.2). They consider the temperature change in the liquid to be concentrated in a thin boundary layer around the bubble and treat the problem as a nonsteady heat diffusion problem. Then in reference [86] they use the temperature distribution of reference [85] to solve the bubble dynamics problem. They use the relationship

$$\frac{\rho_v(T) - \rho_\infty}{\rho_L} = A(T-100) \tag{5.5}$$

where A is a constant and T from reference [85] is

$$T = T_o - \frac{\bar{D}}{k}\eta(t) - \left(\frac{\bar{D}}{\pi}\right)^{1/2} \int_0^t \frac{R^2(x)\left(\frac{\partial T}{\partial r}\right)_{r=R(x)}}{\left\{\int_x^t R^4(y)\,dy\right\}^{1/2}}\,dx \tag{5.6}$$

$\eta(t)$ is the heat source per unit volume and $\bar{D} = k/\rho C$.

Plesset and Zwick [87] give the asymptotic solution for a vapor bubble in a superheated liquid. The solution is the same as the one given in reference [86], but this analytical approach is compared with experimental data. The bubble growth rate is proportional to the square root of time:

$$R = R_o \left(\frac{2}{\pi\mu}\right)\left(\frac{kt}{3}\right)^{1/2} \tag{5.7}$$

Plesset [88] discusses the validity of some of the assumptions made in the analytical solution given. He gives expressions to be used in assessing the error resulting from assuming that the vapor pressure is uniform and that the wall velocity is the liquid velocity. These expressions give a very good feel for the order of magnitude of the terms involved.

B. Forster - Zuber Approach

Forster [89] gives a mathematical solution to the heat transfer Equation (5.2) with no heat generation (i.e., $\dot{q} = 0$). He assumes that the motion of the bubble wall $R = R(t)$ is a known function. The boundary conditions are either constant temperature or vanishing heat flux. He gets an approximate solution of the original problem by solving

$$dT = \frac{dQ(x)}{4\pi\sqrt{\pi a}\, R^2(\xi)\sqrt{t-x}}\left\{1 - \sqrt{\pi}\,\frac{\sqrt{a(t-x)}}{R(\xi)}\exp\left[\frac{a(t-x)}{R^2(\xi)}\right]\operatorname{erf}\left[\frac{\sqrt{a(t-x)}}{R(\xi)}\right]\right\}$$

where $R(\xi)$ is an appropriate mean value $= \sqrt{R(x)\,R(t)}$. He explains that the second term in this equation vanishes at $x = t$; and when dT becomes small, neglecting the second term will result in small

error. Therefore this term is neglected and the resultant solution is

$$T(t) = \frac{L_v \rho_v}{C_{fg} \rho_L (\pi a)^{1/2}} \int_0^t \frac{R^2(x)\, \dot{R}(x)}{R(x)\, R(t) \sqrt{t-x}}\, dx \tag{5.8}$$

Forster and Zuber [90] solve equation (5.1) by using the Clausius-Clapeyron relation

$$P_v - P_\infty = \frac{L_v}{T(v_v - v_L)} \left(T_{vs} - T_{\infty s}\right) \tag{5.9}$$

Then $T_{vs} - T_{\infty s}$ is found from the solution of (5.8). In addition, when $R > R_0$ the terms $R\ddot{R} + \frac{3}{2}\dot{R}^2 + \frac{2\sigma}{\rho L_v R}$ may be neglected when compared to the other terms in the equation. These terms are the hydrodynamic terms. For a growing vapor bubble in a superheated liquid the solution of Equation (5.1) with (5.8) and (5.9) need be completed only for a time interval from zero to one millisecond and then the hydrodynamic terms may be neglected. This solution also gives the bubble growth rate proportional to the square root of time.

Zuber [91] considers the problem of bubble dynamics in both a superheated and a subcooled liquid. He starts with a heat balance

$$\bar{h}(T_0 - T_s) = L_v \rho_v \frac{dR}{dt} \tag{5.10}$$

for a uniformly superheated liquid. The heat transfer coefficient, $\bar{h}$, was determined from the one dimensional transient heat conduction problem.

$$a \frac{\partial^2 T}{\partial z^2} = \frac{\partial T}{\partial t} \tag{5.11}$$

Then

$$\bar{h}\,(T_o - T_s) = k\left(\frac{\partial T}{\partial z}\right)_{z=0} \approx \frac{k(T_o - T_s)}{\sqrt{\pi a t}} \tag{5.12}$$

The solution of (5.10) and (5.12) agrees satisfactorily with experiment. In the nonuniform temperature field, Equation (5.10) must have a heat transfer term for heat from the vapor interface to the bulk liquid:

$$L_v \rho_v \frac{dR}{dt} = k\frac{T_o - T_s}{\sqrt{\pi a t}} - q_b \tag{5.13}$$

The term q_b must be picked for the average bubble in the non-uniform temperature field and cannot be used to predict the growth rate of any given bubble.

In a subcooled liquid reference [91] gives the results of Bosnjakovic and Jacob:

$$L_v \rho_v \frac{dR}{dt} = -\frac{\pi}{2} k \frac{T_s - T_L}{\sqrt{\pi a t}} \tag{5.14}$$

The bubble will reach a maximum radius

$$R_m = \frac{b}{\pi} \frac{(T_w - T_s) C_{pl} \rho_L}{L_v \rho_v} \sqrt{\pi a t_m} \tag{5.15}$$

and then collapse. Here b is a constant for any given temperature-pressure field. This analysis may be used with experimental data by taking the experimental point where $R = R_m$ and $\dot{R} = 0$ and drawing the theoretical collapse curve from this point. The growth is determined by integrating backward in time from this point.

C. Birkhoff, Margulies, and Horning

The above authors in [92] assume the solution of Equation (5.2) to be of the form

$$T(r,t) = f(s) \tag{5.16}$$

where

$$s = r/(at)^{1/2}. \tag{5.17}$$

This implies that the bubble growth rate is $K_1(\alpha t)^{\frac{1}{2}}$. K_1 is a dimensionless parameter. Equation (5.2) with (5.16) and (5.17) gives

$$f''(s) + \left\{ s - \frac{2}{s} - \frac{(\rho_L - \rho_v) K_1^2}{\rho_L s^2} \right\} f'(s) = 0. \tag{5.18}$$

The solution to Equation (5.2) is then of the form

$$T(r,t) = A - B \cdot F_K(s). \tag{5.19}$$

A and B are constants and $F_K(S)$ is defined:

$$F_K(s) = \int_s^\infty x^{-2} \exp\left\{ -\frac{x^2}{4} - \frac{K_1^3(\rho_L - \rho_v)}{2x\,\rho_L} \right\} dx. \tag{5.20}$$

For one particular range of the dimensionless parameter, K_1, this solution gives the result

$$R = \left(\frac{12}{\pi}\right)^{1/2} \frac{\rho_L C_{pl}}{\rho_L L} (T_{ws} - T_\infty)(at)^{1/2}. \tag{5.21}$$

This is the asymptotic growth rated equation determined by Plesset and Zwick for a uniformly superheated liquid. However, other ranges of K_1 give other asymptotic solutions.

D. Bankoff and Mikesell

Reference [93] considers Equation (5.1) where p_v and p_∞ are constant (the Rayleigh solution) and compares it with experiment. Then the authors solve the same equation allowing p_∞

to vary the way it would in cavitating flow. The analytical solution of Equation (5.1) with p_v constant is used to fit the experimental data.

E. Scriven Approach

Scriven [94] considers the growing vapor bubble in an infinite medium of uniform superheat. He considers the growth to be controlled entirely by the transport of heat and matter across the bubble boundary. He states that the solutions presented above are valid only over restricted ranges of pressure and superheat. His solution is exact under the assumptions made and is adequate for all but the earliest stages of bubble growth. He lists assumptions which are substantially those of the beginning of this section. He arrives with Equations (5.1) and (5.2) by considering the continuity equation, equation of motion, and energy equation. The exact solution to Equations (5.1) and (5.2) results from neglecting the hydrodynamic terms. His exact solution reduces approximately to those of Forster-Zuber and Plesset-Zwick, depending on the growth constant, β^*. Where β^* is defined

$$R = 2\beta^* \sqrt{at} . \tag{5.22}$$

Figure 5.1 is a comparison of Scriver's solution and the approximate solutions:

$$R = \sqrt{\frac{2\Delta T\, k\, t}{\rho_v [L_v + (C_{p\ell} - C_{pv})\Delta T]}} , \quad \beta^* \to 0 \tag{5.23}$$

$$R = \left(\frac{12}{\pi}\right)^{1/2} \frac{\Delta T \sqrt{\rho_\ell C_{p\ell} k t}}{[L_v + (C_{p\ell} - C_{pv})\Delta T]} , \quad \beta^* >> 0 . \tag{5.24}$$

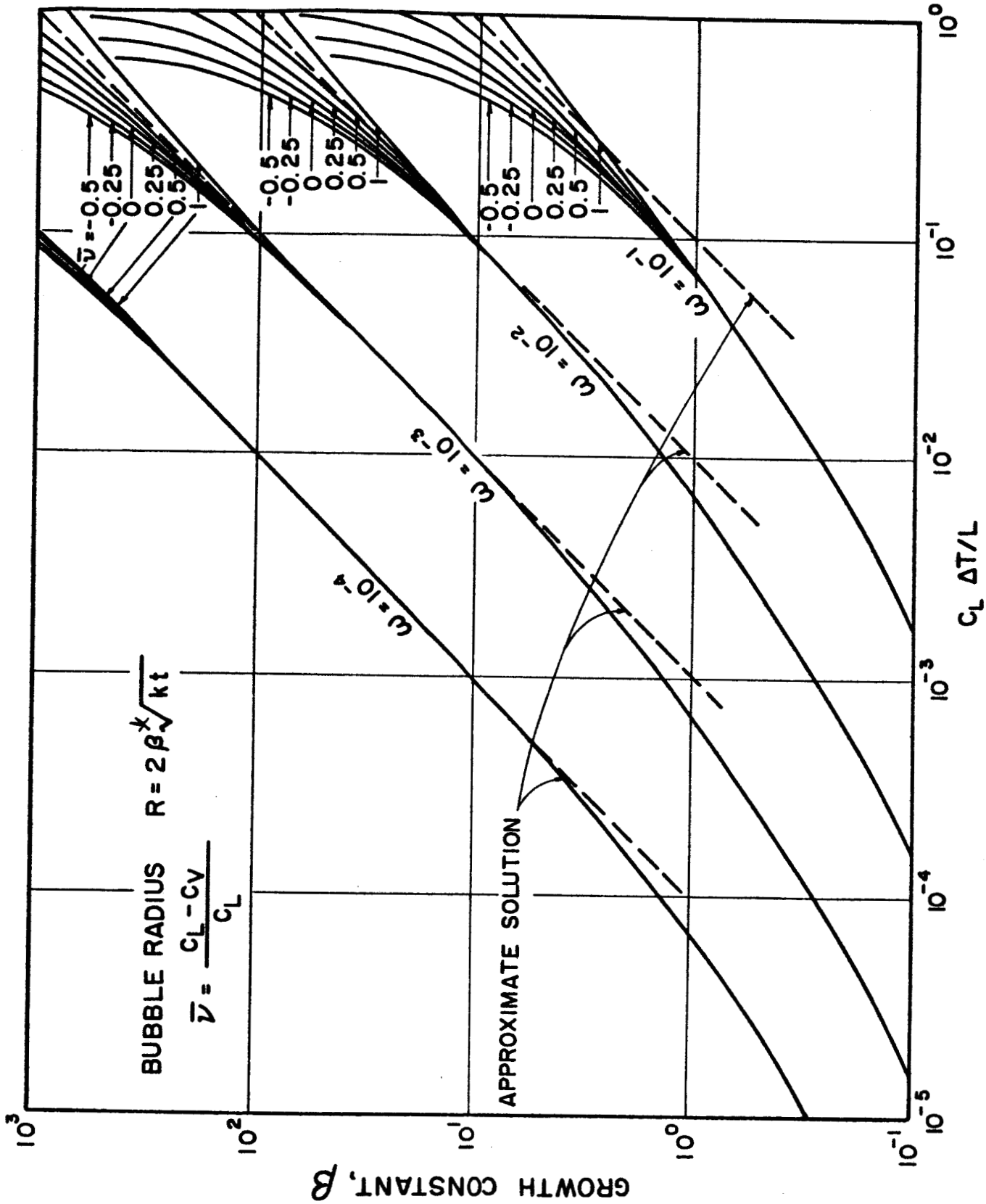

Figure 5.1 Scriven's Solution and Approximate Solutions Compared

Yang and Clark [95] solve Equation (5.2) neglecting the term $\bar{V} \cdot \bar{\nabla}T$. The solution is almost identical to that of Foster-Zuber but a coefficient of bubble growth given by Scriven is again introduced and the final solution depends on the selection of β^*. This development is compared in a chart like Figure 5.1 to the solutions of Scriven and Plesset-Zwick. Plesset and Zwick's solution is a closer fit to the solution of Scriven than is the theory of Yang and Clark.

At a conference on bubble dynamics [96] Forster and Zwick discussed the merits of their two respective theories. The general conclusion reached was that the Plesset-Zwick theory could be as accurate as desired, depending only on the order of approximation; but that the first order approximation in effect reduced the boundary layer to a thickness of zero and thus eliminated the convection term. The Plesset-Zwick solution requires the evaluation of twenty-two coefficients while the Forster-Zuber solution requires only two.

5.3 Experimental Studies of Bubble Dynamics

The two most prominent uses for the bubble growth and collapse rate theories are:

1. Using the information to predict the growth and collapse of a bubble in a cavitating stream of liquid.
2. Using the information for a method of correlating the heat transfer data in boiling heat transfer.

A. Cavitation

The cavitation problem was investigated experimentally by Plesset [97]. He assumes the vapor pressure and surface tension to be constant in Equation (5.1) and solves that equation for a controlled variable liquid pressure. He shows that the change in temperature in the liquid is approximately 1.8 degree F; and, therefore, the heat transfer problem need not be solved. The theory does a very good job of predicting the growth and collapse rates for a large bubble radius but is lacking in the early growth and late collapse stages.

B. Boiling Heat Transfer

Dergarabedian [98] performed an experimental study of the growth of vapor bubbles in superheated water. Both the Plesset-Zwick and the Forster-Zuber solutions were sufficient in correlating the growth rate.

Florschuetz and Chao [83] performed experiments in subcooled water and ethyl alcohol under approximate zero gravity conditions and found that the data did fit the theories of Plesset-Zwick and Forster-Zuber for inertia controlled collapse but did not fit for some heat transfer controlled collapse.

Engelberg-Forster and Greif [99] correlated boiling heat transfer data in terms of Δp (i.e., $p_v - p_\infty$) taken from Equation (5.1) and found one form of correlation that fit their experimental data. The equation is

$$\bar{q}_b = C_{p_\ell}\left(\frac{k}{25}\right)\Delta p\,(T_w - T_s)\left\{\frac{\rho_\ell^3 C_{p_\ell}^2 \pi a\, T_s^2 \Delta p^2}{N L_v^2 \rho_v^2}\right\}^{1/5}\left(\frac{N C_{p_\ell}}{k}\right)^{1/3}. \qquad (5.25)$$

Costello and Tuthill [100] experimented with superheated water under the effects of acceleration and found that only Equation (5.25) was satisfactory in correlating their data.

Gunther [101] gave some interesting experimental results for growth and collapse rates of vapor bubbles, but these results were not compared to any analytical solutions.

Forster and Zuber [102] show that the product of bubble radius and radial velocity is a constant and formulate a Reynolds number for flow in the superheated liquid near a heating surface. This Reynolds number becomes:

$$Re = \frac{\rho_L}{N}\left\{\frac{(T_{vs} - T_{\infty s})\, C_{pL}\, \rho_L \sqrt{\pi a}}{L_v \rho_v}\right\}^2. \tag{5.26}$$

They use this Reynolds number in correlating boiling heat transfer data and get:

$$\bar{q} = k(T_w - T_L)\sqrt{\frac{N\, Re\, \Delta P}{2\sigma \rho_L}}\sqrt[4]{\frac{\Delta P}{\rho_L}}\; Re^m Pr^n \tag{5.27}$$

For n-pentane, benzene, ethanol, and water this correlation reduces to

$$Nu = 0.0015\, Re^{0.62} Pr^{0.33}. \tag{5.28}$$

Equations (5.27) and (5.28) gave good experimental fits for the data of these liquids.

Zuber and Fried [103] state that in pool boiling the Forster-Zuber correlation (Equation (5.27)) is valid for cryogenic fluids. It is also shown that the correlation Equation (5.25) is identical to Equation (5.28).

Reference [104] discusses the fact that the growth rate in a hydrogen bubble chamber is proportional to the square root of time and that the growth rates of bubbles agrees with the theories of Plesset-Zwick and Birkoff-Margulies-Horning.

Staniszewski [105] experimented with water and ethanol at pressures of 14.7, 28, and 40 psia. His conclusions were that none of the present theories could be used in the correlation of his data.

Bankoff and Mason [106] give experimental verification of the fact that the latent heat of vaporization transported into the liquid by a vapor bubble cannot be neglected in subcooled boiling if accurate correlation is to result. The preceeding correlations could only adjust coefficients or exponents for better fit. There was no physical parameter in these correlations which truly represented this phenomena.

5.4 Summary

The analytical solution of the bubble dynamics has apparently been completed and solutions to any desired accuracy are available. The type of liquid is important in these solutions only in determining the terms that may be neglected without sacrificing accuracy.

The best pool boiling heat transfer correlation equations are based on the parameters involved in the bubble dynamics solution. The prediction of the growth and collapse of vapor bubbles in cavitating flow can be successfully accomplished with the equations governing bubble dynamics.

CHAPTER VI

Progress on the Single-Phase Conduit Models

6.1 Introduction

The purpose of this chapter is to give a detailed presentation of the analytical progress which has been made on single phase conduit models since Interim Report No. 64-1.

6.2 Application of Exact, Two-Dimensional, Viscous Solution to the Case of a Rigid Pipe

In Interim Report No. 64-1 an exact solution of Equation (2.5) was presented for the case of axisymmetric flow. The general solution showed the Laplace transformed radial and axial velocities to be of the form

$$V_r = -\left[B\beta J_1(\beta r) + A\Gamma J_1(kr)\right] e^{\Gamma z} \tag{6.1}$$

and

$$V_z = \left[B\Gamma J_0(\beta r) + Ak J_0(kr)\right] e^{\Gamma z} \tag{6.2}$$

where Γ, β, and k are related by

$$\Gamma^2 = k^2 + \frac{s}{\nu} = \beta^2 + \frac{s^2}{c_0^2 + \frac{4}{3}\nu s} . \tag{6.3}$$

The first approach to applying this solution to rigid pipe flow was made by assuming the term $A\alpha J_1(Kr)$ in Equation (6.1) was negligible. This led to the zeroth mode propagation constant

$$\Gamma_0 = \frac{s}{\mathcal{L}_0} \quad . \tag{6.4}$$

We will now proceed with a more exact analysis which yields a zeroth mode propagation constant that agrees very well with experimental results, whereas that of Equation (6.4) does not.

For a rigid pipe we require that both the radial and axial velocities go to zero at the pipe wall. Applying these conditions to Equations (6.1) and (6.2) yields

$$0 = B\beta J_1(\beta r_0) + A\Gamma J_1(kr_0) \tag{6.5}$$

and

$$0 = B\Gamma J_0(\beta r_0) + Ak J_0(kr_0). \tag{6.6}$$

Solving for A from Equation (6.6) and substituting into Equation (6.5) gives

$$k\beta \frac{J_1(\beta r_0)}{J_0(\beta r_0)} = -\Gamma^2 \frac{J_1(kr_0)}{J_0(kr_0)} \quad . \tag{6.7}$$

In our first analysis we found that $\beta_0 = 0$. For this more exact analysis we will assume instead that it is very small, thus we may approximate $J_1(\beta_0 r_0)$ and $J_0(\beta_0 r_0)$ by small argument values. Therefore assume

$$J_1(\beta_0 r_0) = \frac{\beta_0 r_0}{2} \tag{6.8}$$

and

$$J_0(\beta_0 r_0) = 1. \tag{6.9}$$

Substitution of Equations (6.8) and (6.9) into (6.7) gives

$$\beta_o^2 = 2\Gamma_o^2\left\{\frac{J_1(k_o r_o)}{k_o r_o J_o(k_o r_o)}\right\} \tag{6.10}$$

or, by substituting Equation (6.10) into (6.3) we have

$$\Gamma_o = \left\{\frac{\frac{s^2}{c_o^2 + 4/3\nu s}}{1 - \frac{2J_1(k_o r_o)}{k_o r_o J_o(k_o r_o)}}\right\}^{1/2} \tag{6.11}$$

where $k_o \approx i\sqrt{s/\nu_o} = \xi$. Equation (6.11) is now a more exact expression for the zeroth mode propagation constant. Figure 6.1 shows a theoretical comparison between the results obtained from using the approximate Γ_o from Equation (6.4) and the more exact value from Equation (6.11). The figure represents the dimensionless ratio of pressure amplitude to piston velocity amplitude for the case of a rigid conduit with a constant pressure reservoir at one end and an oscillating piston at the other end. Note the difference in damping and in the resonance peak between the two curves. In Chapter IX of this report, experimental studies are described which verify the accuracy of the propagation constant given by Equation (6.11) for the range of parameters of the test.

6.3 Effect of Nonlinear Terms

In Section 2.7 we discussed, to some extent, the problems associated with analytical investigations of fluid conduits where some consideration must be made of the nonlinear terms of the equations of motion. At this time we will present a solution of the governing equations for Case 1 of Section 2.7, i.e., the case

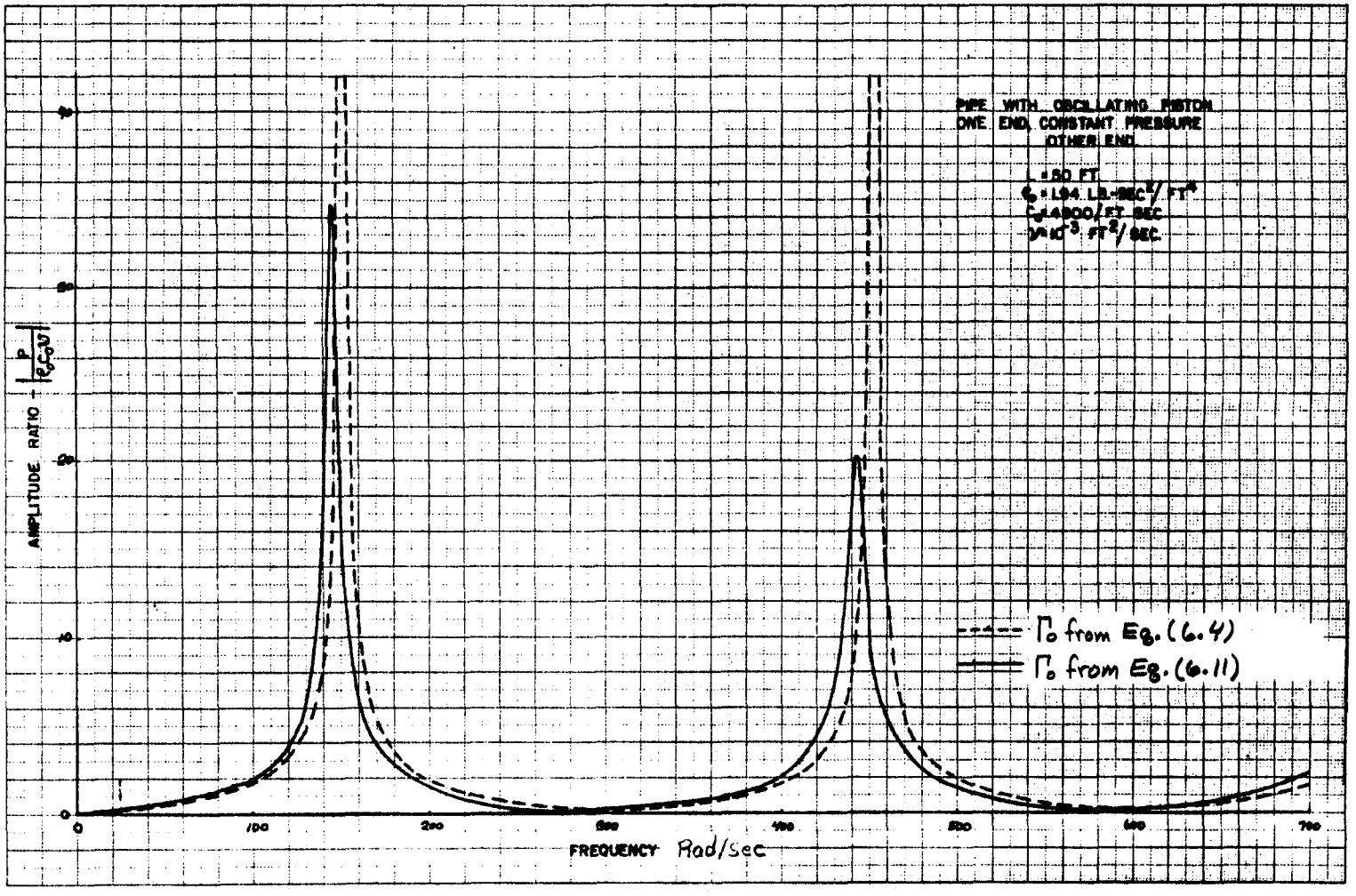

Figure 6.1 Theoretical Amplitude Ratio vs. Frequency Comparison for Different Values of Γ_0

where there is a large steady flow component but the perturbation or unsteady flow components are small. We assume for the fluid velocity (axisymmetric flow)

$$\bar{v} = r\, v_{r_1} + k(v_{z_0} + v_{z_1}) = \bar{v}_0 + \bar{v}_1 \tag{6.12}$$

where v_{z_0} represents the stady axial velocity component, v_{r_1} represents the radial unsteady velocity component and v_{z_1} is the axial unsteady component. $\bar{v}_0$ is the steady vector velocity and $\bar{v}_1$ is the unsteady vector velocity. Making our usual assumption of a semi-compressible fluid, i.e., a fluid whose density is time but not spatially dependent, we may write for the equation of motion (calling v_{z_0} simply v_0)

$$\frac{\partial \bar{v}_1}{\partial t} + v_0 \frac{\partial \bar{v}_1}{\partial z} = -\frac{\nabla p}{\rho_0} + \nu \left\{ \frac{4}{3} \nabla(\nabla \cdot \bar{v}_1) - \nabla \times (\nabla \times \bar{v}_1) \right\} \tag{6.13}$$

and for the continuity relation (including equation of state)

$$\frac{\partial p}{\partial t} + \rho_0 c_0^2 \nabla \cdot \bar{v}_1 = 0 . \tag{6.14}$$

It is convenient at this point to separate the velocity as

$$\bar{v}_1 = \nabla \varphi_1 + \nabla \times \bar{\psi}_1 \tag{6.15}$$

where φ_1 represents a scalar field and $\bar{\psi}_1$ a vector field. If we now take first the divergence and then the curl of Equation (6.13) we have, respectively

$$\frac{\partial \nabla \cdot \bar{v}_1}{\partial t} + \nabla \cdot \left(v_0 \frac{\partial \bar{v}_1}{\partial z} \right) = -\frac{\nabla^2 p}{\rho_0} + \frac{4}{3} \nu \nabla^2 (\nabla \cdot \bar{v}_1) \tag{6.16}$$

and

$$\frac{\partial \nabla \times \bar{v}_1}{\partial t} + \nabla \times \left(v_0 \frac{\partial \bar{v}_1}{\partial z} \right) = -\nu \nabla \times \left[\nabla \times (\nabla \times \bar{v}_1) \right] \tag{6.17}$$

or, since $\nabla \cdot \bar{v}_1 = \nabla^2 \varphi_1$ and $\nabla \times \bar{v}_1 = -\nabla^2 \psi_1$, $(\bar{\psi}_1 = \theta \psi_1)$ we may rewrite Equations (6.16) and (6.17) as

$$\frac{\partial \nabla^2 \varphi_1}{\partial t} + \nabla \cdot \left(v_0 \frac{\partial \bar{v}_1}{\partial z} \right) = -\frac{\nabla^2 p}{\rho_0} + \frac{4}{3} \nu \nabla^2 (\nabla^2 \varphi_1) \tag{6.18}$$

and

$$-\frac{\partial \nabla^2 \psi_1}{\partial t} + \nabla \times \left(v_0 \frac{\partial \bar{v}_1}{\partial z} \right) = \nu \nabla^2 (\nabla^2 \psi_1). \tag{6.19}$$

At this point we must make some considerations of the terms in Equations (6.18) and (6.19). Physically, φ_1 is a scalar potential for the plane wave propagation and ψ_1 is a function associated with the vorticity field. In order to be able to easily work with the terms $\nabla \cdot (v_0 \, \partial \bar{v}_1 / \partial z)$ and $\nabla \times (v_0 \, \partial \bar{v}_1 / \partial z)$, we need to assume that v_0 is constant even though mathematically it is some function of r.

What we are going to do is assume that v_0 is constant over the cross-section so far as Equation (6.18) is concerned. Since ψ_1 is associated with the vorticity, this indicates that it will have a significant value only near the wall where we can assume v_0 is zero. Thus, so far as Equation (6.19) is concerned $v_0 = 0$. We may now reduce Equations (6.18) and (6.19) to

$$\frac{\partial \varphi_1}{\partial t} + v_0 \frac{\partial \varphi_1}{\partial z} = -\frac{p}{\rho_0} + \frac{4}{3} \nu (\nabla^2 \varphi_1) \tag{6.20}$$

and

$$\frac{\partial \psi_1}{\partial t} = -\nu \nabla^2 \psi_1 . \tag{6.21}$$

Applying the Laplace transformation to Equations (6.14), (6.20) and (6.21) and solving we obtain

$$\hat{\varphi}_1 = J_0(\beta r)\left\{A_1 e^{\Gamma_1 z} + A_2 e^{\Gamma_2 z}\right\} \tag{6.22}$$

and

$$\hat{\psi}_1 = J_1(kr)\left\{B_1 e^{\Gamma_1 z} + B_2 e^{\Gamma_2 z}\right\} \tag{6.23}$$

where $\hat{\varphi}_1$ and $\hat{\psi}_1$ are the transforms of φ_1 and ψ_1. Also Γ_1 and Γ_2 are solutions of

$$\Gamma^2 - \frac{\Gamma v_0}{\frac{c_0^2}{s} + \frac{4}{3}\nu} - \beta^2 - \frac{s}{\frac{c_0^2}{s} + \frac{4}{3}\nu} = 0 \tag{6.24}$$

and furthermore

$$K^2 = \Gamma^2 + \frac{s}{\nu} . \tag{6.25}$$

Now for the transformed velocities, we have

$$v_r = -\beta J_1(\beta r)\left\{A_1 e^{\Gamma_1 z} + A_2 e^{\Gamma_2 z}\right\} + J_1(kr)\left\{\Gamma_1 B_1 e^{\Gamma_1 z} + \Gamma_2 B_2 e^{\Gamma_2 z}\right\} \tag{6.26}$$

and

$$v_z = J_0(\beta r)\left\{A_1 e^{\Gamma_1 z} + A_2 e^{\Gamma_2 z}\right\} + K J_0(kr)\left\{B_1 e^{\Gamma_1 z} + B_2 e^{\Gamma_2 z}\right\} . \tag{6.27}$$

Zeroth Mode Transfer Equations for Rigid Pipe

We want to proceed now to develop the transfer equations for a rigid pipe which has a steady flow component v_0 plus a perturbation component $v_1(t)$ which is an average for the cross-section. For the zeroth mode of propagation, we proceed with the application of boundary conditions to Equations (6.26) and (6.27) which require the velocity to be zero at the pipe wall. If this is carried out, the results are identical to those of Section 6.2 given by Equation (6.10), thus

$$\beta_0^2 = 2\Gamma_0^2 \left\{ \frac{J_1(k_0 r_0)}{k_0 r_0 J_0(k_0 r_0)} \right\}. \qquad (6.10)$$

Substitution of Equation (6.10) into (6.24) yields a quadratic in Γ (zeroth mode only)

$$\Gamma^2 \left\{ 1 - \frac{2J_1(k_0 r_0)}{k_0 r_0 J_0(k_0 r_0)} \right\} - \Gamma \left\{ \frac{v_0}{\frac{c_0^2}{s} + \frac{4}{3}\nu} \right\} - \left\{ \frac{s}{\frac{c_0^2}{s} + \frac{4}{3}\nu} \right\} = 0. \qquad (6.28)$$

Solving for Γ from Equation (6.28) gives

$$\Gamma_{1,2} = \frac{b \pm \sqrt{b^2 + 4ad}}{2a} = \Gamma_a \pm \Gamma_b \qquad (6.29)$$

where

$$a = \left\{ 1 - \frac{2J_1(k_0 r_0)}{k_0 r_0 J_0(k_0 r_0)} \right\} \qquad (6.30)$$

$$b = \left\{ \frac{v_0}{\frac{c_0^2}{s} + \frac{4}{3}\nu} \right\} \qquad (6.31)$$

and

$$d = \left\{ \frac{s}{\frac{c_o^2}{s} + \frac{q}{3}\nu} \right\}. \tag{6.32}$$

If the relation for axial velocity is averaged over the cross-section and the averaged pressure is calculated from the continuity relation we obtain

$$V(z) = C_1 e^{\Gamma_1 z} + C_2 e^{\Gamma_2 z} \tag{6.33}$$

and

$$P(z) = -\frac{\rho_o c_o^2}{s}\left\{ \Gamma_1 C_1 e^{\Gamma_1 z} + \Gamma_2 C_2 e^{\Gamma_2 z} \right\}. \tag{6.34}$$

Applying the conditions $V_1(s)$ and $P_1(s)$ at $z=0$ leads to the transfer equations given by

$$V_2(s) = e^{\Gamma_a L}\left\{ V_1(s)\cosh\Gamma_b L - \frac{P_1(s)}{\Gamma_b Z_c'}\sinh\Gamma_b L - \frac{\Gamma_a}{\Gamma_b}\sinh\Gamma_b L \right\} \tag{6.35}$$

and

$$P_2(s) = e^{\Gamma_a L}\left\{ P_1(s)\left[\frac{\Gamma_a}{\Gamma_b}\sinh\Gamma_b L + \cosh\Gamma_b L\right] - \right.$$
$$\left. - Z_c' V_1(s)\left[\Gamma_a\cosh\Gamma_b L + \Gamma_b\sinh\Gamma_b L\right] + Z_c'\left[\frac{\Gamma_a^2}{\Gamma_b}\sinh\Gamma_b L + \Gamma_a\cosh\Gamma_b L\right]\right\} \tag{6.36}$$

where

$$Z_c' = \frac{\rho_o c_o^2}{s}. \tag{6.37}$$

Equations (6.35) and (6.36) are now the desired transfer equations relating the variables of a four-terminal fluid conduit such as shown in Figure 2.5. It is important to note that if we let $v_o=0$

then these relations reduce identically to the standard form as given by Equations (2.23) and (2.24).

Figure 6.2 displays a plot of the frequency response Log $\left[V_1(o)/V_1(L)\right]$ for a pipe with constant pressure at $z=0$ and a "disturbance generator" at $z=L$. $V_1(o)$ is the transformed velocity at $z=0$ and $V_1(L)$ is the transformed velocity at $z=L$. Note that the greater U_o (mean steady velocity) the less the disturbance effect.

6.4 Effect of System Body and Vibration Forces

Now consider the effects which system body and vibration forces have upon the fluid contained within the system. Writing the first-order equation of motion for a viscous fluid, including a body force term, we have in vector form

$$\frac{\partial \bar{v}}{\partial t} = \frac{\bar{F}}{\rho_o} - \frac{\nabla p}{\rho_o} + \nu\left\{\frac{4}{3}\nabla(\nabla\cdot\bar{v}) - \nabla\times(\nabla\times\bar{v})\right\} \tag{6.38}$$

where $\bar{F}$ represents the vector body force acting on the fluid and may be a function of both space and time. Assume that $\bar{v}$ is representable as

$$\bar{v} = \nabla\varphi + \nabla\times\bar{\psi}, \tag{6.39}$$

also

$$\nabla\cdot\bar{v} = \nabla^2\varphi \tag{6.40}$$

and

$$\nabla\times\bar{v} = \nabla(\nabla\cdot\bar{\psi}) - \nabla^2\bar{\psi}. \tag{6.41}$$

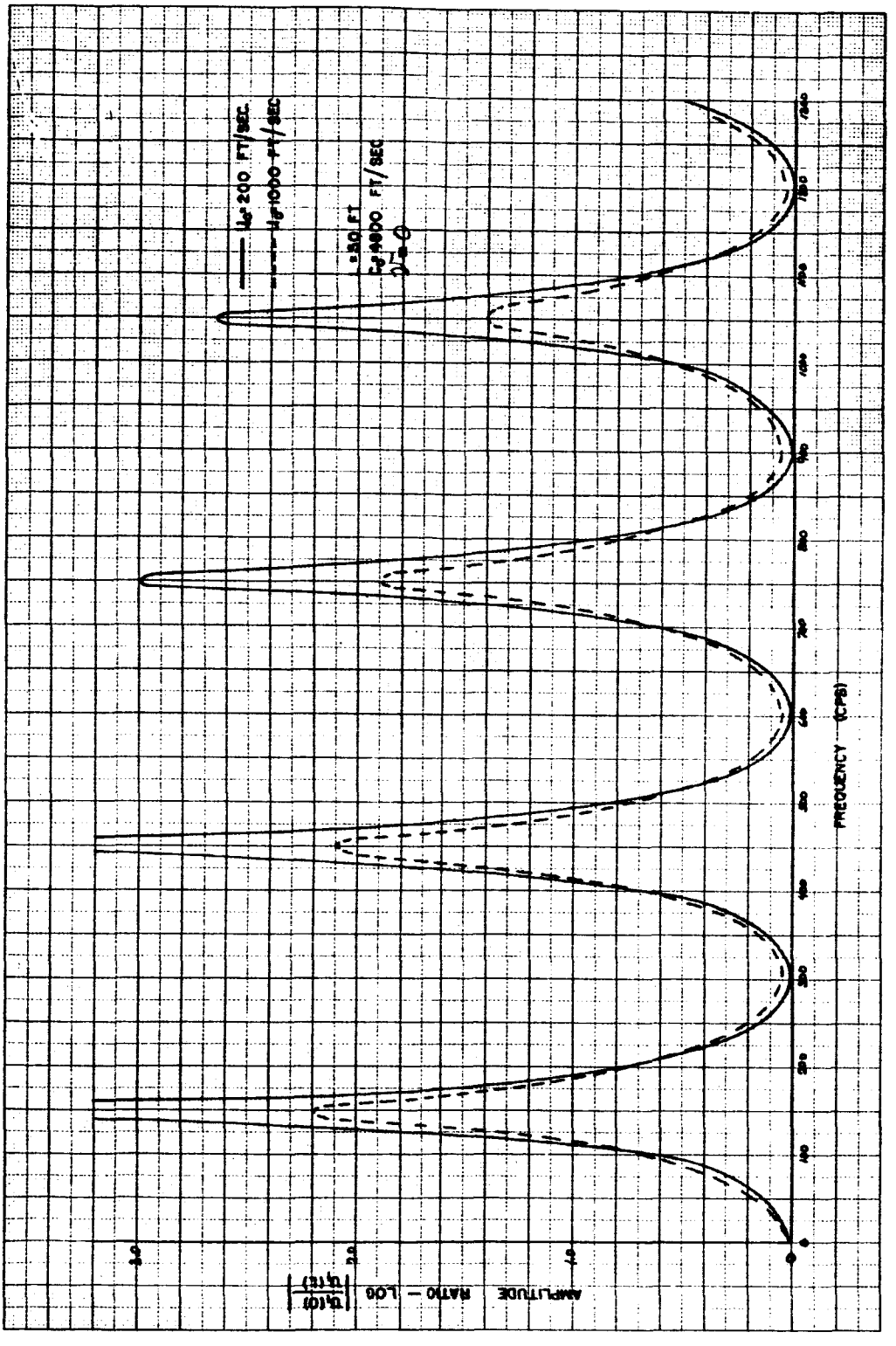

Figure 6.2 Amplitude Ratio vs. Frequency for Nonlinear Model.

Taking the divergence of Equation (6.38) gives

$$\frac{\partial \nabla\cdot\bar{v}}{\partial t} = \frac{1}{\rho_o}\left\{\nabla\cdot\bar{F} - \nabla\cdot(\nabla p)\right\} + \frac{4}{3}\nu\nabla\cdot\left\{\nabla(\nabla\cdot\bar{v})\right\} \tag{6.42}$$

or, introducing Equation (6.40) yields

$$\frac{\partial \nabla^2\varphi}{\partial t} = \frac{1}{\rho_o}\left\{\nabla\cdot\bar{F} - \nabla^2 p\right\} + \frac{4}{3}\nu\nabla^2(\nabla^2\varphi). \tag{6.43}$$

Similarly, taking the curl of Equation (6.38) and substituting Equation (6.41), we have (assuming axisymmetric flow)

$$\frac{\partial \nabla^2\bar{\psi}}{\partial t} = \nu\nabla^2(\nabla^2\bar{\psi}) + \frac{\nabla\times\bar{F}}{\rho_o}. \tag{6.44}$$

<u>Only if</u> we can now represent $\bar{F}$ as

$$\bar{F} = \nabla\varphi_f + \nabla\times\bar{\psi}_f \tag{6.45}$$

are we able to obtain a solution to Equations (6.43) and (6.44) in this manner. If $\bar{F}$ <u>is not</u> representable as in Equation (6.45) then we must use some other method. We are mainly interested in the case where $\bar{F}$ represents some time varying body force which is a result of boundary motion. If $\bar{F}$ is only time variant then it may not be expressed as in Equation (6.45).

Conceptually there are two separate types of problems which may be considered under the heading of time variant body forces. The first type involves conduit systems in which vibrations cause motion of the conduit walls. The second type deals with those systems which are subject to some type of external time variant gravitational field. We will discuss only the first case at this time even though the second case has also been work out (it will be presented at a later date.)

Case Where the System Boundary is Moving (Vibrating)

Consider a fluid conduit in which the walls are undergoing some axial motion as shown in Figure 6.3 $v_c(t)$ is the velocity which

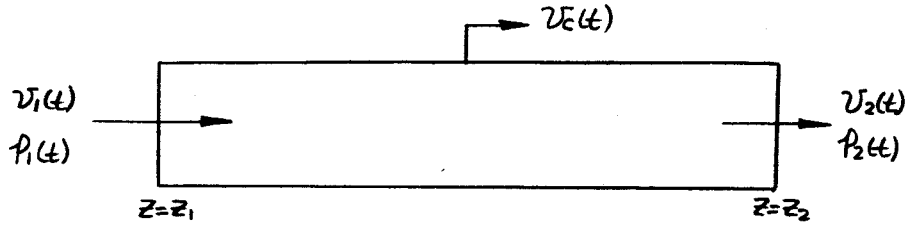

Figure 6.3 Fluid Conduit with Axial Vibration

the conduit wall attains as a result of the time variant body force. In order to obtain a solution, we will apply boundary conditions to a general solution without body forces in such a manner that the fluid has the velocity $v_c(t)$ at the wall. Thus, we are not considering there to be a body force but rather a boundary motion.

In order to avoid some mathematical difficulties, we will only discuss the zeroth mode for a rigid pipe at this time; thus we may reduce Equation (6.38) for this case to

$$\frac{\partial v}{\partial t} = -\frac{1}{\rho_0}\frac{\partial p}{\partial z} + \nu\left\{\frac{\partial^2 v}{\partial r^2} + \frac{1}{r}\frac{\partial v}{\partial r}\right\}. \tag{6.46}$$

We will assume that for this mode the pressure is only a function of axial position so that in Equation (6.46) it represents a forcing function. A general solution in the Laplace domain is

$$V(r,z,s) = h(z,s)\, J_0\left(ir\sqrt{\frac{s}{\nu}}\right) - \frac{1}{\rho_0 s}\frac{\partial P}{\partial z}. \tag{6.47}$$

Applying the boundary condition $V(r_o, s) = V_c(s)$ gives

$$h(z,s) = \frac{V_c(s) + (1/\rho_o s)\, \partial P/\partial z}{J_o(i r_o \sqrt{s/\nu})} . \tag{6.48}$$

Substituting (6.48) into (6.47) yields

$$V(r,z,s) = V_c(s) \frac{J_o(r\xi)}{J_o(r_o\xi)} + \frac{1}{\rho_o s} \frac{\partial P}{\partial z} \left\{ \frac{J_o(r\xi)}{J_o(r_o\xi)} - 1 \right\} . \tag{6.49}$$

We may now derive our standard transfer equations. If we average Equation (6.49) and combine the result with the continuity equation averaged over the cross-section, we obtain a second-order ordinary differential equation whose solution gives the propagation constant as

$$\Gamma_o = \frac{(s/c_o)}{\left\{ 1 - \dfrac{2 J_1(r_o\xi)}{\xi r_o J_o(r_o\xi)} \right\}^{1/2}} , \quad \xi = i\sqrt{s/\nu} \tag{6.50}$$

which is almost identical to the form given by Equation (6.11) for the zeroth mode. The corresponding transfer equations are

$$V_2(s) = V_1(s) \cosh\Gamma_o L - \frac{P_1(s)}{Z_c \Gamma} \sinh\Gamma_o L + V_c(s) f(s) \left(1 - \cosh\Gamma_o L\right) \tag{6.51}$$

and

$$P_2(s) = P_1(s) \cosh\Gamma_o L - Z_c \Gamma V_1(s) \sinh\Gamma_o L + Z_c \Gamma_o V_c(s) f(s) \sinh\Gamma_o L \tag{6.52}$$

where

$$f(s) = \frac{2 J_1(r_o\xi)}{r_o\xi\, J_o(r_o\xi)} \tag{6.53}$$

and Z_c is defined by Equation (2.26). Notice from Equations (6.51) and (6.52) that the effect of the system adds to each of the standard form transfer equations a term which is proportional to $V_c(s)$. If we put $V_c(s)=0$, then the equations reduce to the standard form for a conduit with no vibration.

As a matter of interest, apply the above transfer relations to the case of a rigid conduit which is closed at one end and has a constant pressure source at the other end. We also specify that the conduit experiences an axial sinusoidal vibration such that its transformed velocity is $V_c(s)$, Figure 6.4.

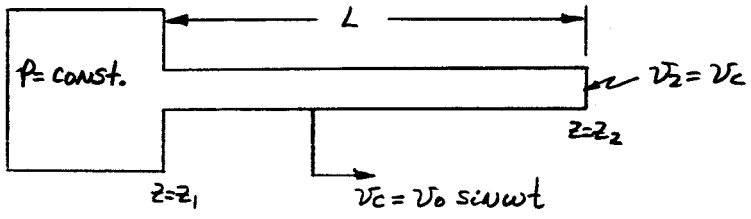

Figure 6.4 Conduit Model with Axial Sinusoidal Vibration

Applying Equations (6.51) and (6.52) in this case, we may obtain

$$\frac{P_2(s)}{V_c(s)} = Z_c\left\{f(s)\sinh\Gamma_0 L - \tanh\Gamma_0 L\left[1-f(s)\left(1-\cosh\Gamma_0 L\right)\right]\right\}. \qquad (6.54)$$

Equation (6.54) is now the transfer relation for the ratio of transformed pressure at the closed end to the vibration velocity. This example is similar to the problem of a vibrating piston in one end of a stationary pipe with a constant pressure at the other end; however, the relation here is considerably more complex.

Two different experimental models are planned with which to verify the vibrating conduit model presented in this section, see Chapter IX.

6.5 Lumped Parameter Models

In Section 2.5 we discussed the applicability of lumped parameter models in solving conduit problems. It was stated that these models are valid if the frequencies involved are less than about one-eighth of the first critical frequency of the lumped element. This restriction suggests a very convenient method of obtaining such a model if the corresponding distributed parameter model is known.

Similarity Between Lumped and Distributed Models

Consider now the transfer relations (2.23) and (2.24) for the case of low frequency, i.e., frequency low enough for a lumped model to be valid. This means that $\Gamma_o L < \pi/16$ so that we may approximate $\cosh \Gamma_o L$ and $\sinh \Gamma_o L$ by the first terms of their series expansions, thus

$$P_2(s) = P_1(s)\left(1 + \frac{\Gamma_o^2 L^2}{2}\right) - \left(Z_c \Gamma_o L\right) V_1(s) \tag{6.55}$$

and

$$V_2(s) = V_1(s)\left(1 + \frac{\Gamma_o^2 L^2}{2}\right) - \left(\frac{\Gamma_o L}{Z_c}\right) P_1(s) \, . \tag{6.56}$$

By a critical comparison of Equations (6.55) and (6.56) with the relations for the fundamental lumped model, Equations (2.41) and

(2.42), we see that by neglecting some of the small order terms the equations will be equivalent if

$$sI_v + R(v) = Z_c \Gamma_0 L \tag{6.57}$$

and

$$s C_v = \frac{\Gamma_0 L}{Z_c} \cdot \tag{6.58}$$

We have seen, Equation (2.26), that $Z_c = \rho_0 c_0^2 / s$, thus from Equation (6.58) we must have

$$sC_v = \frac{\Gamma_0 L}{\rho_0 c_0^2 \Gamma_0 / s} = \frac{sL}{\rho_0 c_0^2} = \frac{sL}{\chi} \tag{6.59}$$

which is correct, see Equation (2.35a). Considering now Equation (6.57) we see that we must have

$$sI_v + R(v) = \frac{\rho_0 c_0^2 \Gamma_0^2 L}{s} \cdot \tag{6.60}$$

Using the value of Γ_0 for the two-dimensional viscous model, Equation (6.11), we may rewrite Equation (6.60) as

$$sI_v + R(v) = \frac{\rho_0 sL}{\left\{1 - \frac{2 J_1(r_0 \xi)}{r_0 \xi J_0(r_0 \xi)}\right\}} \cdot \tag{6.61}$$

If we expand the right side of Equation (6.61) in a power series we have

$$sI_v + R(v) = \rho_0 sL \left\{1 + f + f^2 + \cdots\right\} \tag{6.62}$$

$$f(s) = \frac{2J_1(r_0\xi)}{r_0\xi\, J_0(r_0\xi)} . \tag{6.63}$$

From Equation (6.62) it is evident that we must have

$$R(v) = \rho_0 sL\left\{f + f^2 + \cdots\right\} . \tag{6.64}$$

We have now shown that the transfer equations for the fundamental lumped model and a low-frequency form of the distributed parameter model are approximately equivalent if R(v) is given by Equation (6.64). This result suggests, then, that we may obtain lumped parameter models from all of our existing distributed parameter models by simply writing them in approximate low-frequency form. This will yield forms which are mathematically much more tractable and which should be more easily inverted back to the time domain. It is anticipated that a number of example problems will be worked out using these models. If possible, the results will be experimentally checked. This may prove to be a rewarding area of study.

CHAPTER VII

Progress on Hydrodynamic Tunnel

7.1 Need for Hydrodynamic Tunnel

Considerable progress has been made in the development of a mathematical model which will describe the flow of a single-phase fluid through conduits (see Chapter VI). The development of a mathematical model which will handle single- and two-phase flow has been limited because of insufficient information about the cavitation properties of various liquids while flowing through different pressure distributions (see Chapter IV). In order to determine the conditions under which profuse and limited cavitation will start and the conditions which will cause these cavities to collapse, it will be necessary to construct a hydrodynamic tunnel. The flow of different fluids through various geometries will be studied to help determine these conditions. Given below is a list of the studies to be made using the hydrodynamic tunnel.

1. Determine the effect of acceleration or pressure distribution on relaxation time for limited- and profuse-cavitation occuring in venturi and elbow test sections.
2. Determine the conditions under which these cavities will collapse.

3. Determine the effect of flow patterns on the above items (1 and 2).

4. Determine the validity of solutions found to the continuity, momentum, and energy equations.

7.2 Discussion of Tunnel Design

The facility to be used in the study of bubble formation and collapse, for flowing fluids, is a closed-return hydrodynamic tunnel designed to handle cryogenic as well as ordinary liquids. The facility is shown schematically in Figure 7.1. The tunnel is designed to accommodate 18-inch-long venturi test sections and elbow test sections with various $\bar{R}/r_o$ ratios. It will be fabricated of 304 stainless steel except for the heat exchanger and test sections and has a total liquid capacity of about 5 U. S. gallons. The venturi test sections will be operated in a vertical position to help simulate actual flow patterns within a missle. A variable-speed pump-drive unit, which is capable of providing operational flow velocities from 15 to 100 feet per second in the test sections, will be used. The Centrifugal pump is a commercially available unit designed to handle liquid nitrogen. In order to reduce tunnel losses, only one test section will be installed at any time. Corner-turning vanes and flow straighteners will be used when uniform, steady, irrotational flow is desired at the test section.

The tunnel facility is designed to operate over a pressure range from 0 to 250 psia and a temperature range from 130 to -320 F. High pressure nitrogen gas will be used as the tunnel

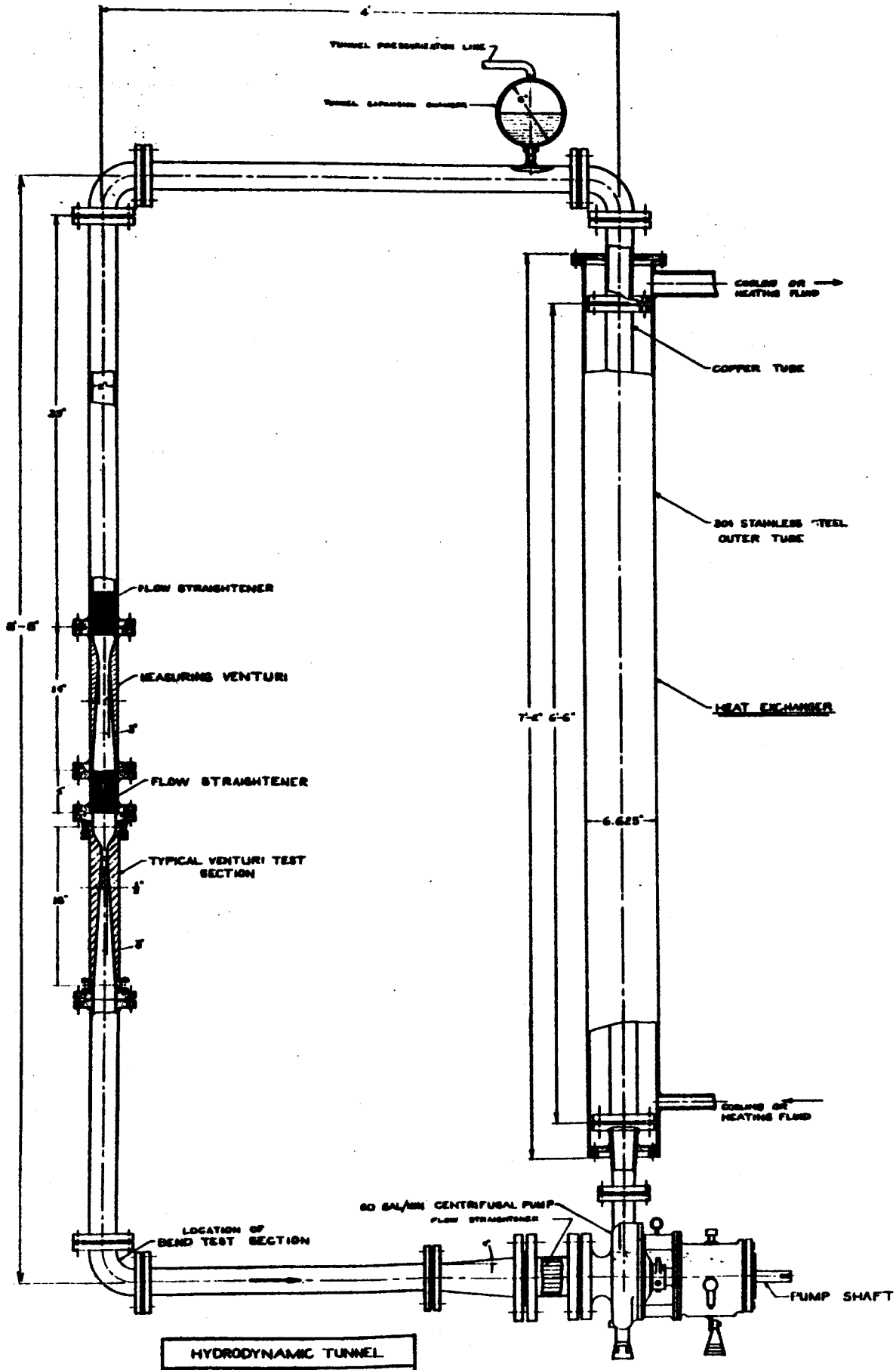

Figure 7.1 Hydrodynamic Tunnel.

pressurizing medium. Tunnel pressures less than atmospheric will be obtained by means of a vacuum system connected to the pressurizing line.

The heat exchanger consists of a double-pipe arrangement. The inner pipe will be fabricated of copper to provide a good heat transfer between the tunnel and the cooling or heating liquids. Provision has been made so that fins can be installed on the copper pipe if they are needed. The outer tube of the heat exchanger will be made of 304 stainless steel. An O-Ring seal will be used at the upper end of the heat exchanger to eliminate the formation of thermal stresses. A float type liquid level control valve will be used to control the coolant (liquid nitrogen) level when nitrogen is being studied in the tunnel.

The tunnel will be insulated with cork or some commercially available material which has a thermal conductivity of about 0.01 Btu/hr ft F. This will insure almost isothermal flow except through the pump and heat exchanger.

The free gas present in the tunnel will be controlled with a resorber. There is some question, however, of the optimum design of a resorber; if they are too "efficient", the amount of free gas, or nuclei, may be insufficient for purposes of modeling inception. Therefore, the tunnel will be operated without a resorber during initial testing.

CHAPTER VIII

Progress on Bubble Observation Chamber

The bubble observation chamber of Figure 8.1 has been constructed. All metal parts are type 304 stainless steel and the windows are made of one-quarter inch thick plexiglas.

The operating pressure range for the inner chamber is 0 to 30 psia. The transient pressure control inlet is connected to a large volume tank. At a point away from any gaseous flow in this tank, a static pressure tap with connections to a mercury manometer is used to measure the vapor pressure above the liquid nitrogen. The correction for the large temperature gradient in the gas is less than one-half inch of liquid nitrogen.

A strain gauge on a diaphragm was placed in the bubble chamber and is to be calibrated statically with the mercury manometer and the pressure in the vacuum jacket.

Two No. thirty-gauge copper-constantan thermocouples were placed in the inner chamber to measure the temperature at a distance from the bubbles and the temperature of either a heating element or the pressurized vapor. (The bubbles to be observed may be formed on a heating element or by forcing a vapor through the pressurized vapor inlet.)

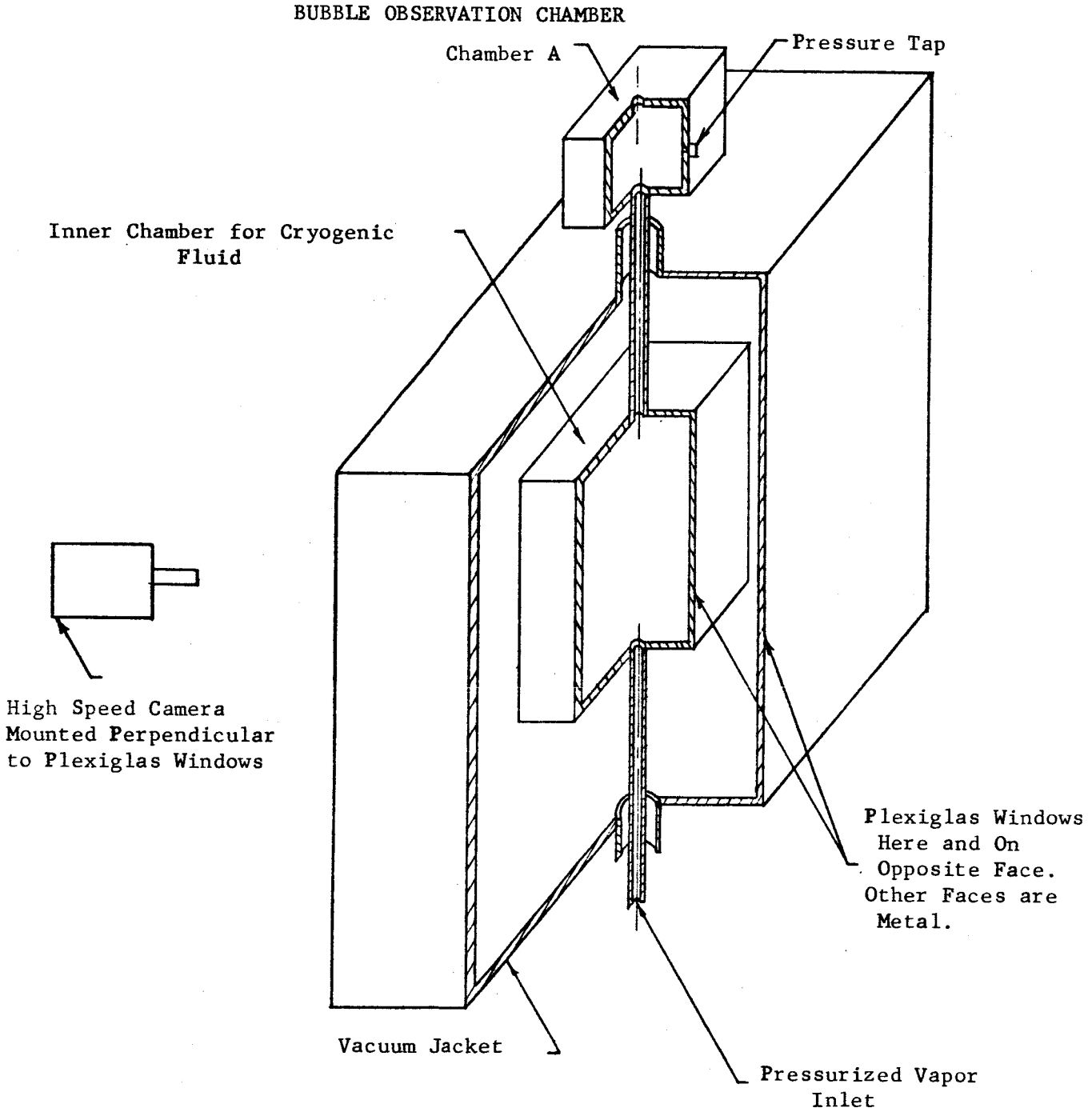
BUBBLE OBSERVATION CHAMBER
Chamber A
Pressure Tap
Inner Chamber for Cryogenic Fluid
High Speed Camera Mounted Perpendicular to Plexiglas Windows
Plexiglas Windows Here and On Opposite Face. Other Faces are Metal.
Vacuum Jacket
Pressurized Vapor Inlet

Figure 8.1

The plexiglas windows are sealed to the metal surfaces by pressure and teflon O-Rings. The seal between the vacuum jacket and the inner chamber is made by rubber plugs with holes in the center.

Complete calibration and reproducibility are being considered for manometers, strain gauges, thermocouples, camera speed, and length measurements.

CHAPTER IX

Experimental Studies on Single-Phase Conduit Models

9.1 Introduction

In the following material a description is given of the experimental work which is being conducted in association with the single phase part of the study. The material includes a discussion of experimental apparatus which has been constructed or is to be constructed.

9.2 Description of Existing Apparatus

For the purpose of implementation of the experimental studies, the following equipment has been constructed.

Oscillating Piston and Drive Unit

The oscillating piston and drive unit (Figure 9.1 and 9.2) was constructed to drive the two basic sets of experimental apparatus detailed below. The piston is driven by a hydraulic motor capable of speeds from nearly zero to 4000 rpm. The power supply (Figure 9.3) consists of a gear pump directly coupled to an electric motor and employs a flow divider valve for control of oscillator speed.

Simple Hydraulic Line Pulsation Unit

The first experimental setup (Figure 9.4) utilizes the drive unit to impose a true sinusoidal pressure transient on the fluid

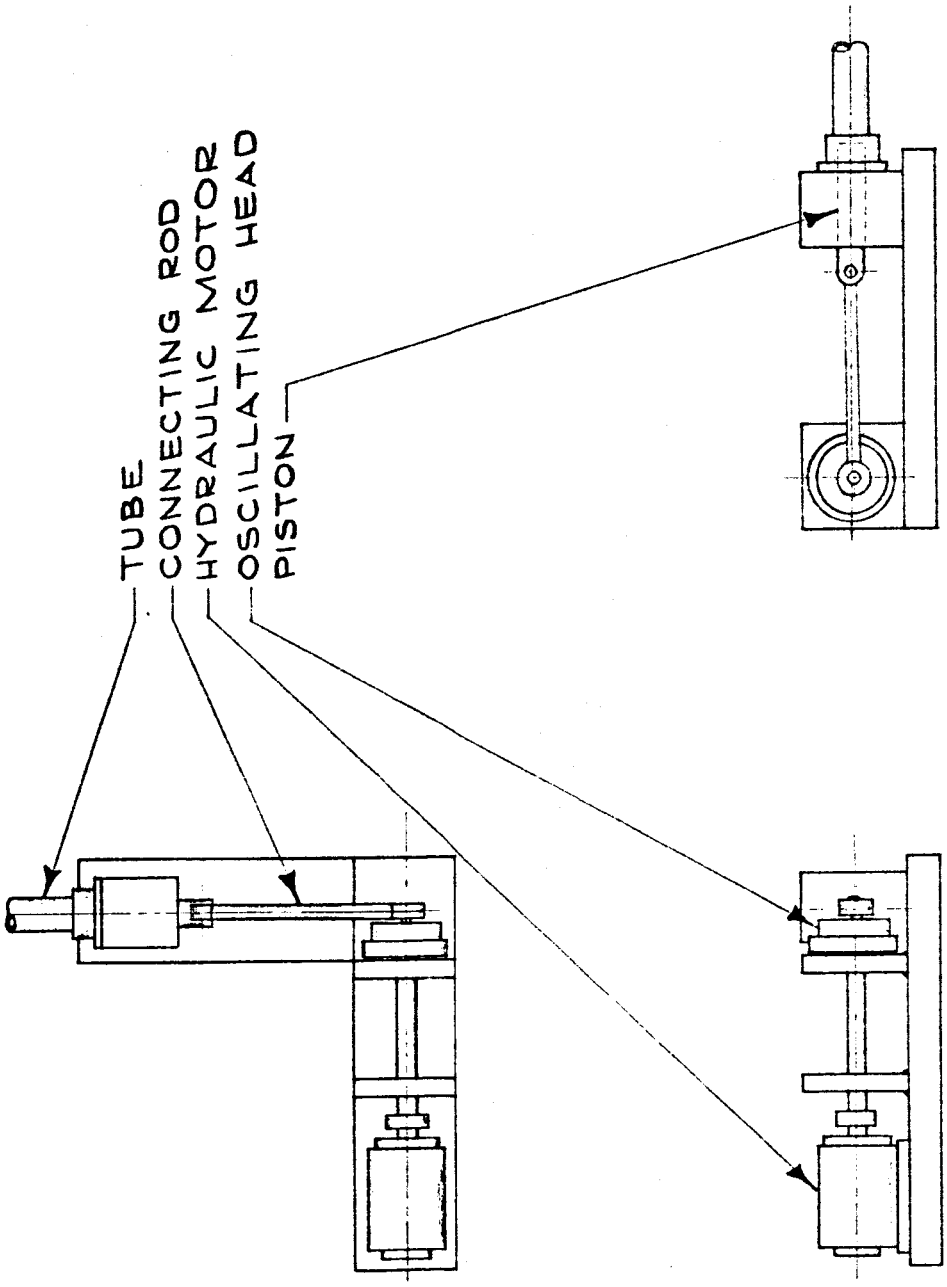

Figure 9.1 Oscillating Piston and Drive Unit

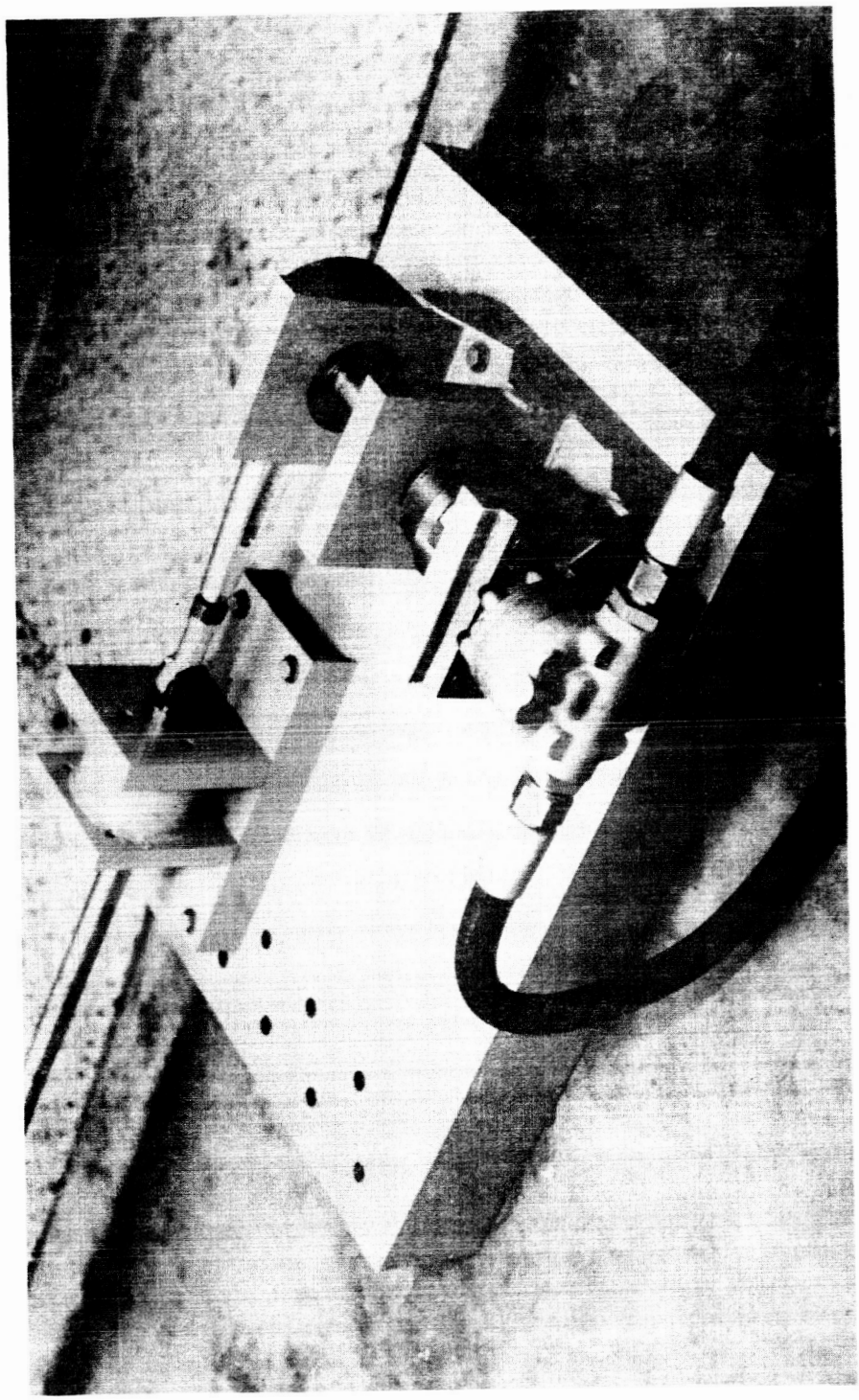

Figure 9.2 Oscillator Unit

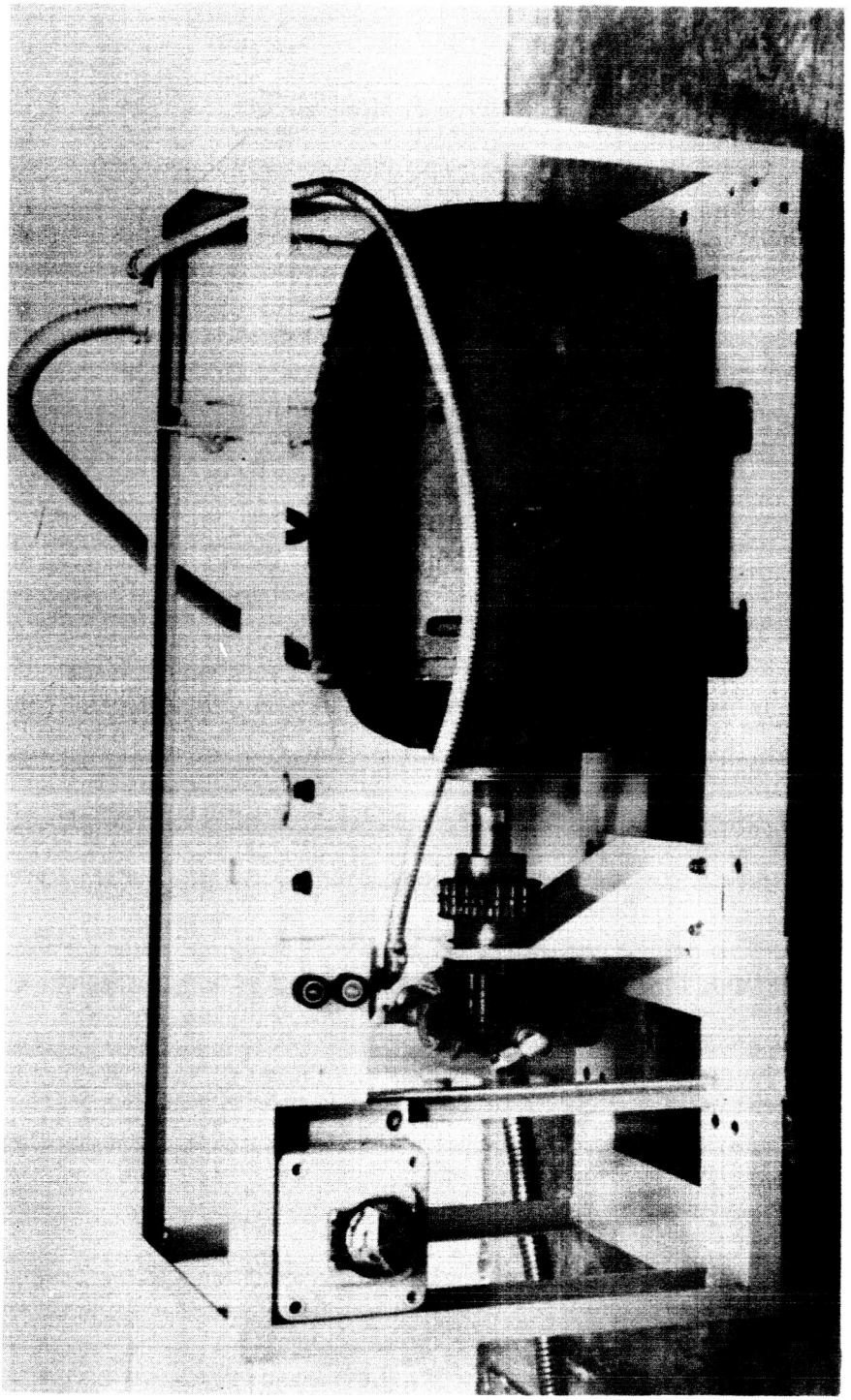

Figure 9.3 Hydraulic Power Supply

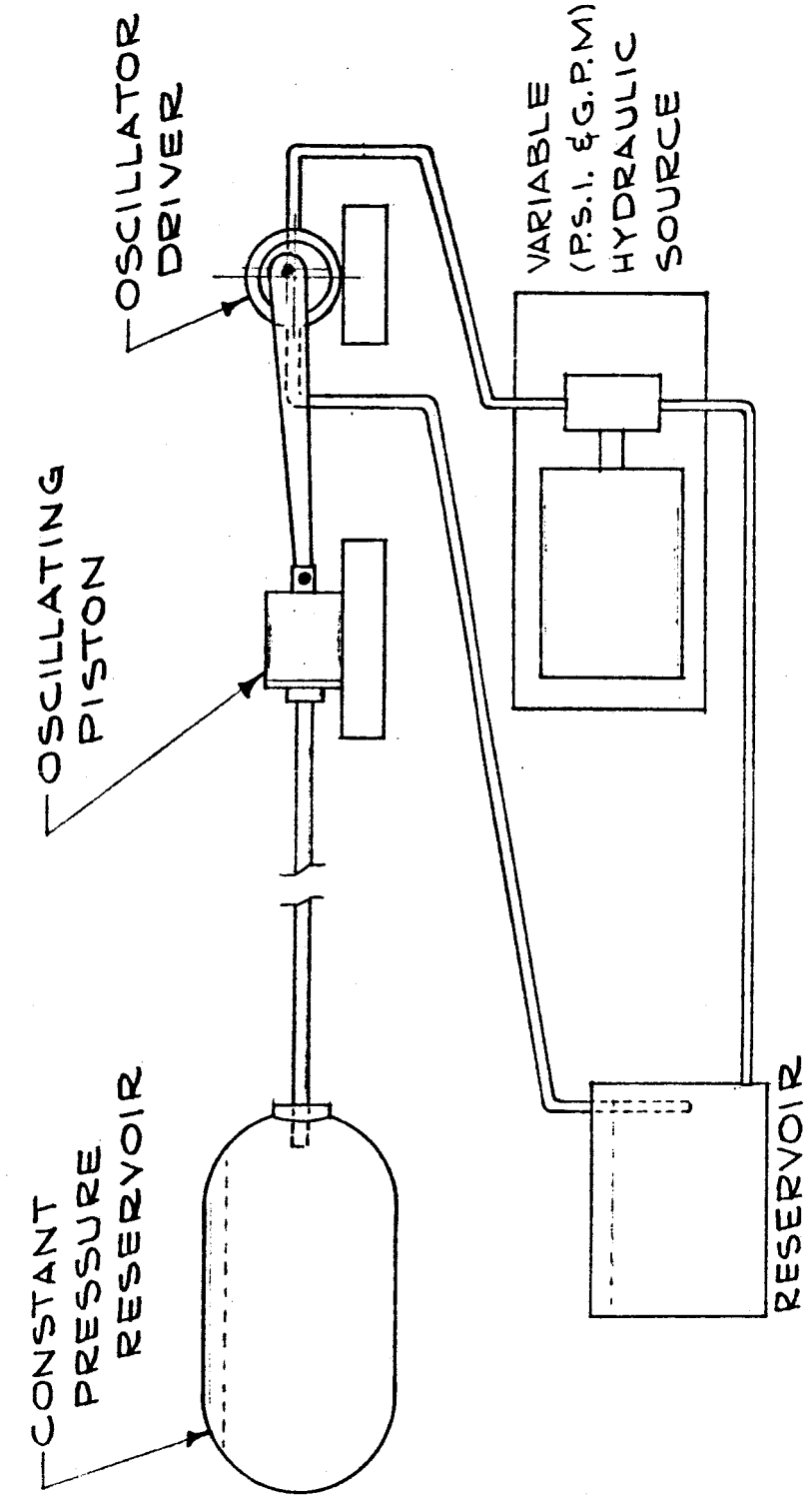

Figure 9.4 Conduit with Oscillator at One End and Constant Pressure Reservoir at Other End

contained in an eighty foot, one inch o.d., stainless steel line which terminates in the constant pressure reservoir (Figure 9.5). A 1000 pound cement pad is used to provide a firm base for the driver unit. Instrumentation has been provided to read out driver frequency, pressure at the pistonface, and reservoir pressure.

The Liquid Filled Vibrating Tube Unit I

The basic oscillating driver unit has been constructed so that it may be mounted in a vertical as well as a horizontal position. The vibrating tube unit I employs the driver, mounted in a vertical position with the base of a plexiglas tube attached as shown in Figure 9.6. This unit is intended to be used in determining system vibration effects both for single-phase and two-phase fluid studies. A variety of fluids are to be employed including Freon 11. Instrumentation is available to measure driver frequency and system fluid pressure at various points along the tube. This unit is now operational.

9.3 Experimental Results

The following is a description of the tests which have been performed using the test apparatus shown in Figure 9.4.

Verification of Two-Dimensional Conduit Model

The first series of tests was conducted in order to verify the two-dimensional viscous model represented by the transfer relations (Equations 2.23 and 2.24) and using the propagation factor given in Equation (6.11). Tests were conducted first with water as the operating fluid. The frequency of the driver unit

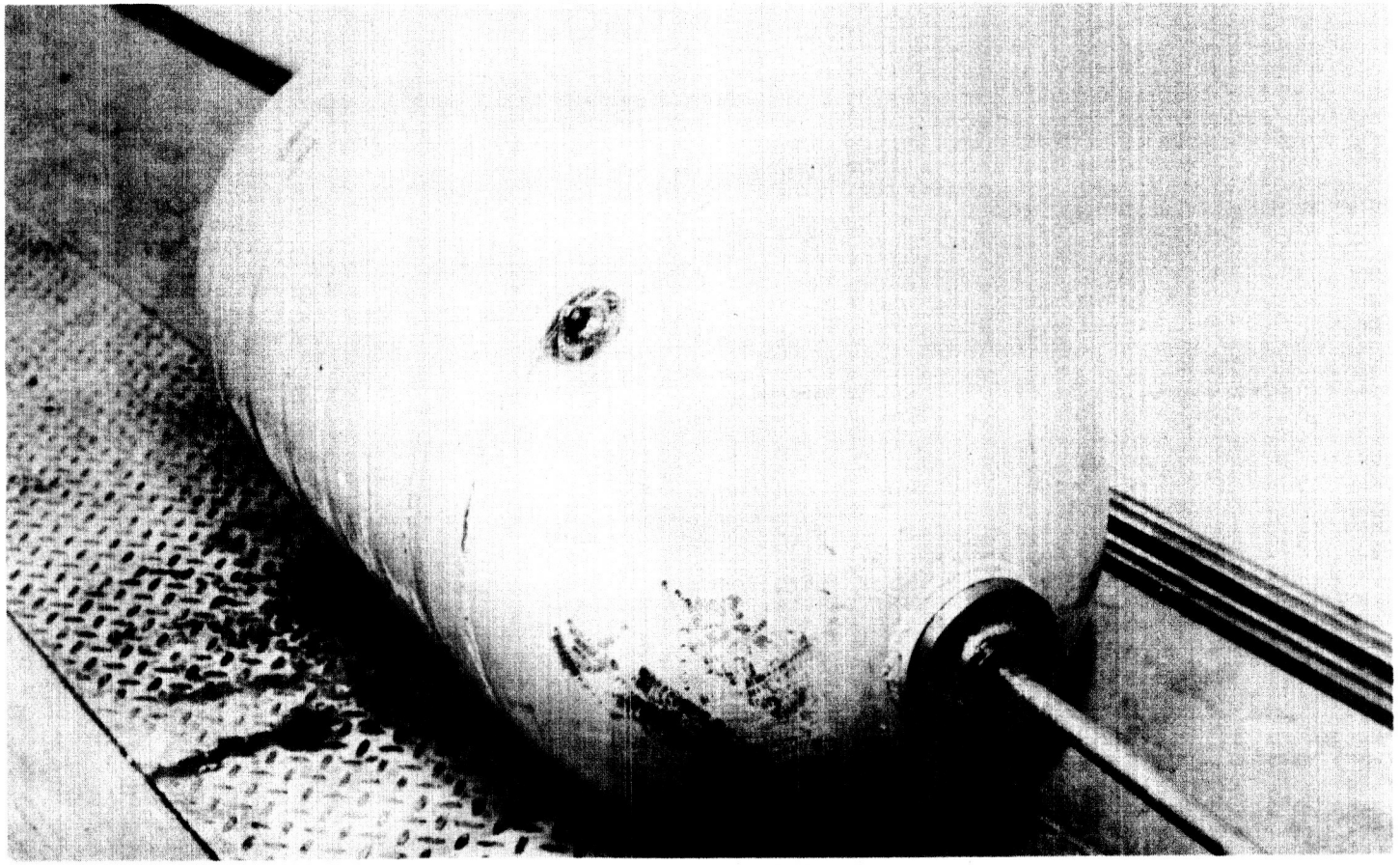

Figure 9.5 Constant Pressure Reservoirs

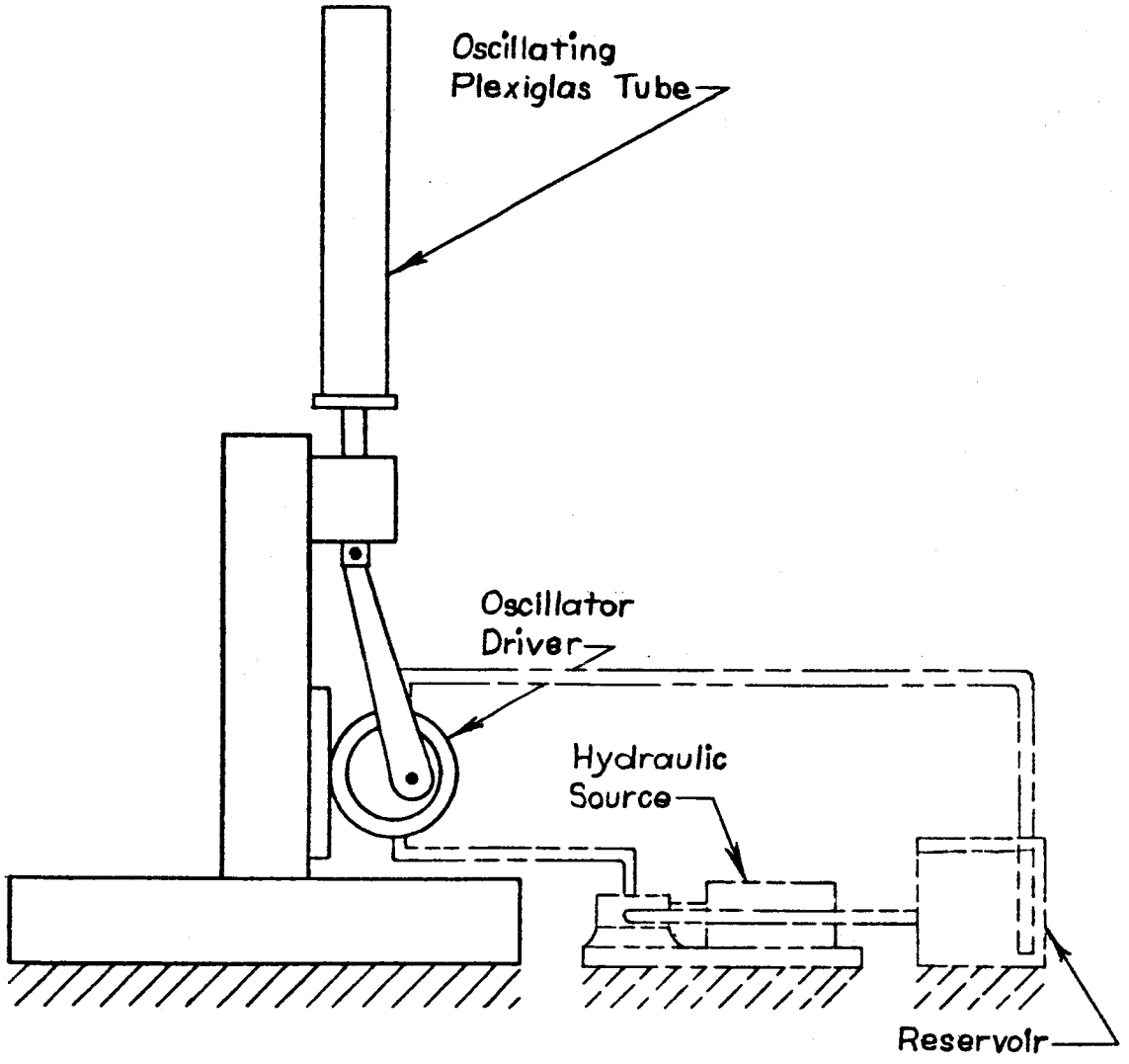

Figure 9.6 Vibrating Tube Unit I

was varied from 400 rpm to 3000 rpm and the pressure disturbance at the driver end was recorded. The pressure recording equipment consists of a pressure transducer with both single pin recorded and scope output. The recorder is used in the low rpm ranges to record the traces, and a camera fitted to the scope records the traces in the higher rpm ranges. The system static pressure was maintained at 500 psi, thus allowing up to 1000 psi peak-to-peak pressure variations. Figure 9.7 shows an experimental and theoretical plot for an experimental run made with a driver amplitude of .025 inches. The experimental data follows the theoretical predictions well in the region of the first resonant point, but there appears to be some discrepancy on the second resonant point. This difference stems from the fact that there is about a 2 per cent difference in the resonant frequencies between the experimental and theoretical data. This is a rather small experimental error and could easily be accounted for in the calculation of the effective speed of sound of the fluid. Since the tube walls are not perfectly rigid, Equation (2.43) was used in calculating the effective speed of sound. The values of χ, c_o, and E_t used in the calculations were obtained from a handbook and there is no assurance of their accuracy.

It is interesting to note that a common practice among writers reporting upon conduit studies is to correct their analytical value of the speed of sound to match their experimental data. This is mainly due to the lack of knowledge concerning accurate values of χ and c_o for many fluids. These constants

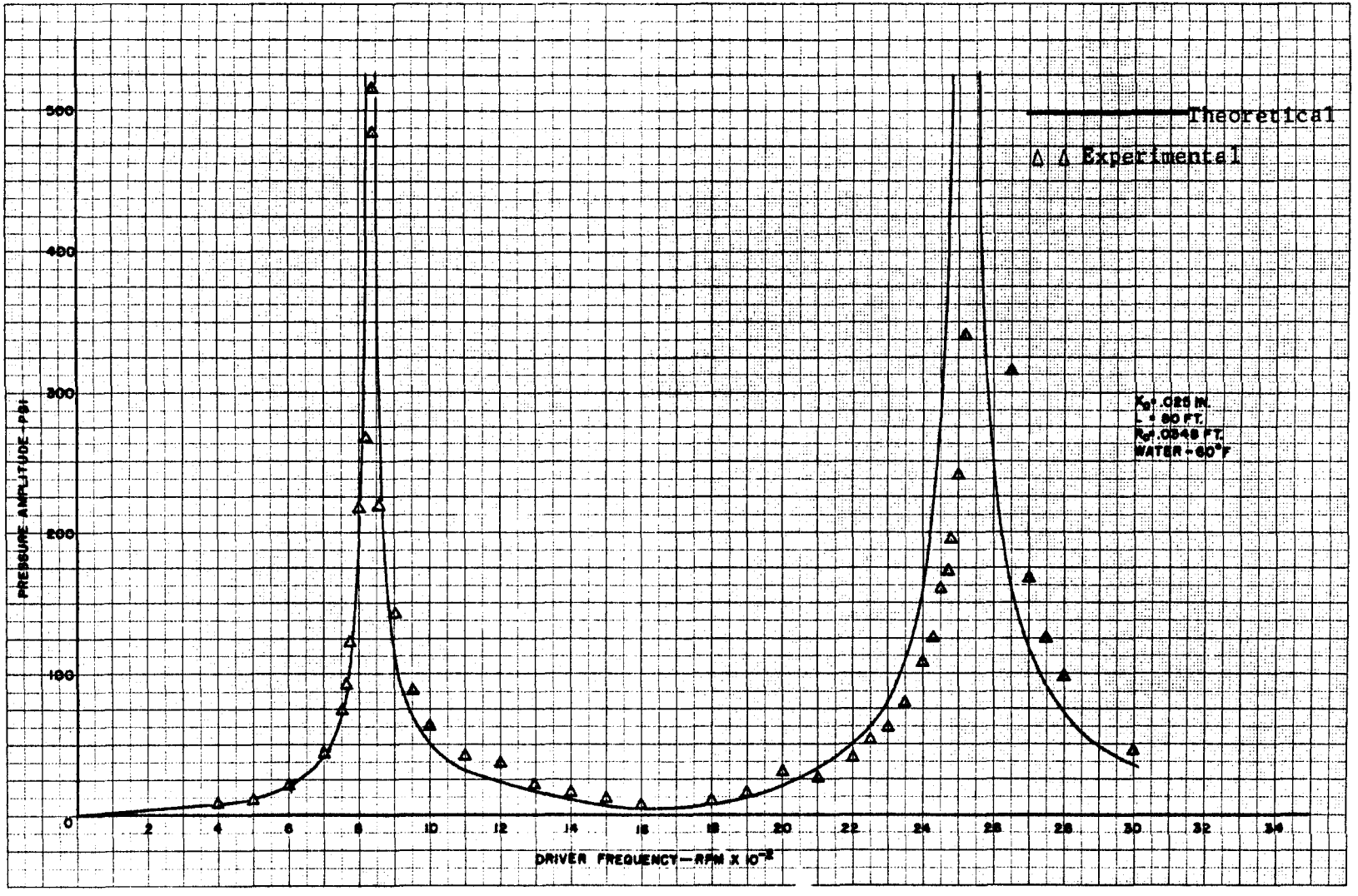

Figure 9.7 Theoretical and Experimental Pressure Amplitude vs. Driver Frequency for Setup in Figure 9.4

are difficult to determine and may vary drastically depending on the type of fluid, its additives, and other fluid parameters. For example, the kerosene obtained from one manufacturer may have quite different properties from that of another manufacturer.

Two phenomena which occurred during the tests are worthy of note at this point. The first was that frequency oscillations occurred in the hydraulic drive system when the system is operated very close to a resonant peak. This is apparently due to the great change in power per change of frequency near these points. Because of this, the resonant points must be approached very slowly in order to not induce this oscillation. It was found to be impossible to get the system to operate exactly at resonance. The other phenomena was the occurrence of a superimposed sine wave upon the main disturbance at certain frequencies. The exact cause of this superimposed disturbance has not yet been determined, but it is suspected that it may be the natural frequencies of the driver. Figure 9.8 shows typical pressure traces when this superimposed disturbance is not noticeably present. Figure 9.9, on the other hand, shows the main sine wave plus the superimposed wave. It was rather hard to determine the amplitude of the main disturbance from these traces so the peak-to-peak values were used. This gives values which are too high as may be seen from the points at 1200 and 2000 in Figure 9.7. Very similar results were obtained using the same experimental configuration but with a driver amplitude at .050 inches.

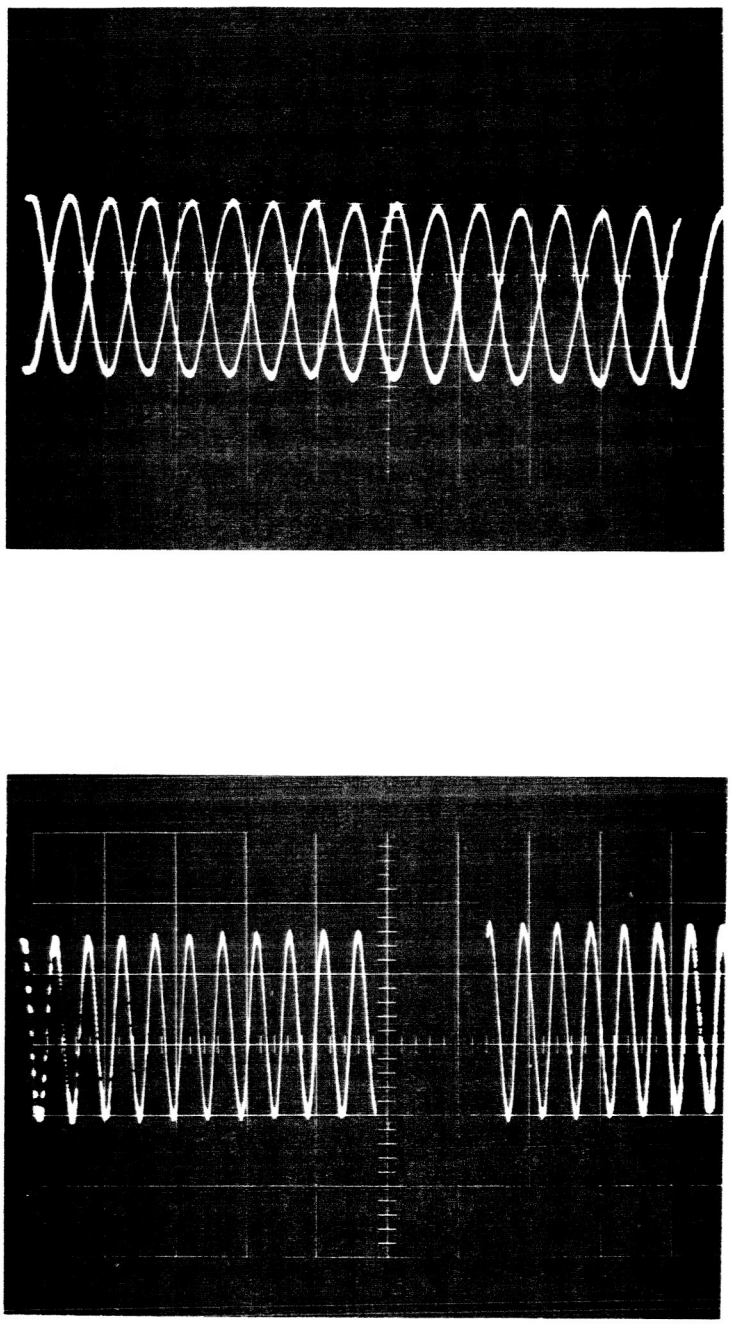

Figure 9.8 Typical Pressure Traces

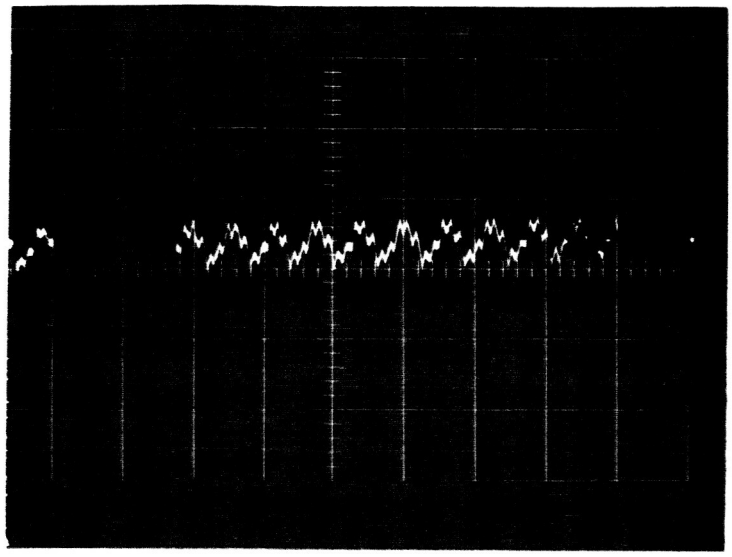

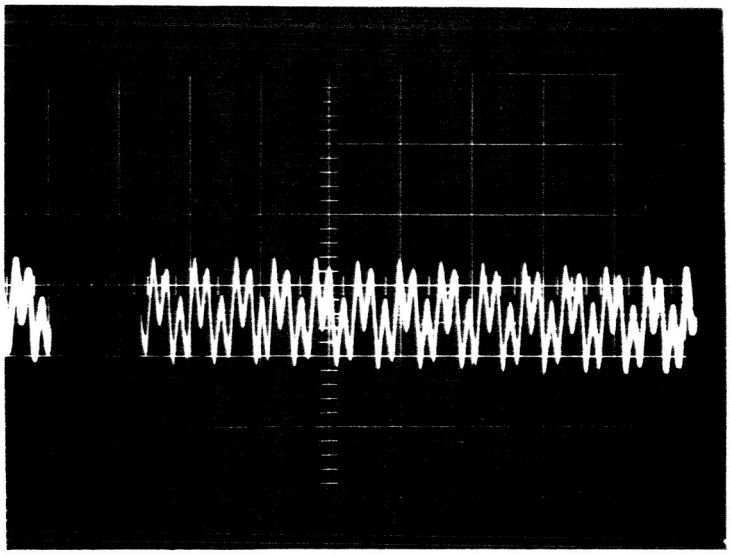

Figure 9.9 Typical Pressure Traces
With Superimposed Sine Wave

Again, using the first experimental setup with MIL-5606 hydraulic fluid as the media, a test was made with the .025 inch driver amplitude. All other conditions were similar to the previous tests. Figure 9.10 shows the pressure amplitude vs. driver frequency plot for the test. The plot of theoretical values shows good agreement with the experimental data.

As was predicted the more viscous fluid demonstrated a lesser pressure amplitude, particularly near the resonant point. Also, as anticipated by theory, the resonant frequencies were lowered slightly.

Tests With an Orifice in the Line

Two tests were conducted in which an orifice was situated in the conduit between the driver and the reservoir. The orifice diameter was 0.25 inches and the conduit diameter was 0.833 inches. Curve #1 (Figure 9.11) depicts the result with the orifice 5.87 feet from the driver. Curve #2 represents the result when the orifice was 74.75 feet from the driver. The conduit length was 80.0 feet. Analytical results have not yet been completed for this configuration.

9.4 Planned Equipment Construction and Modifications

Gear Box

Parts are being procured for the construction of a setup gear box with a ratio of 6.25:1 which is to be installed on the basic driver unit. This will make possible the investigation of higher frequencies. The box will be easily removeable so that low frequency phenomena can still be studied.

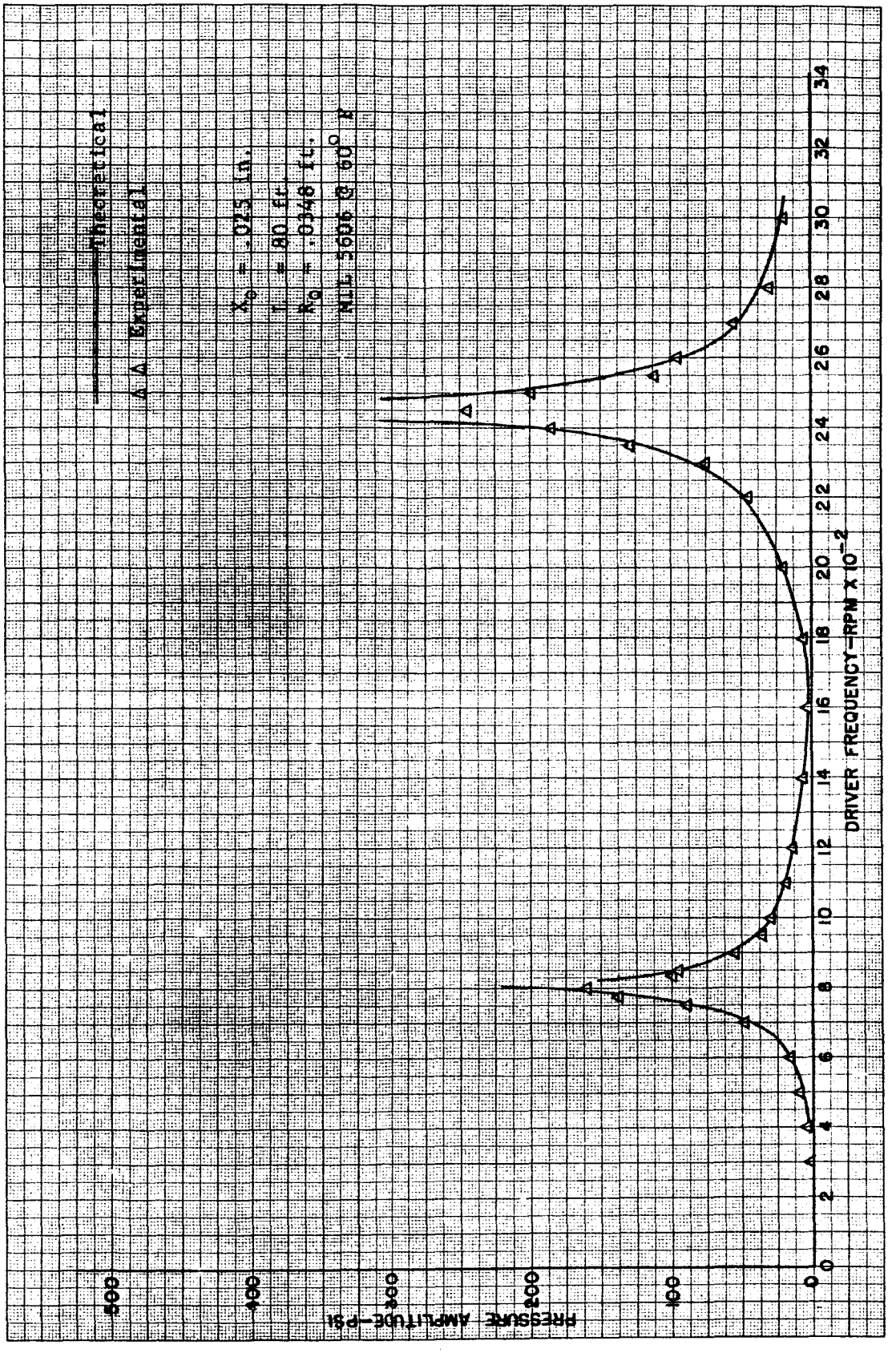

Figure 9.10 Theoretical and Experimental Pressure Amplitude vs. Driver Frequency for Setup in Figure 9.4

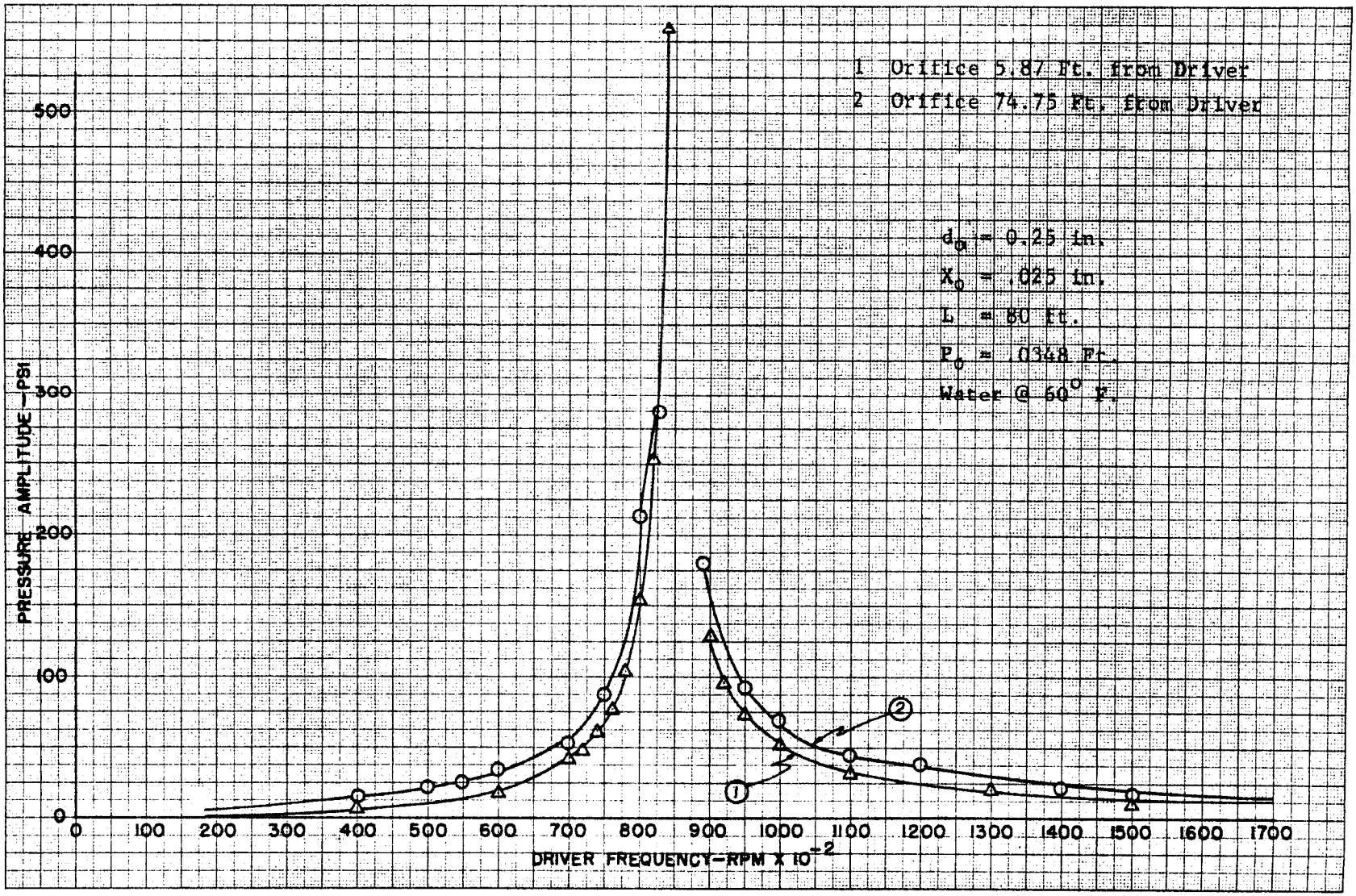

Figure 9.11 Experimental Pressure Amplitude vs. Driver Frequency for Setup of Figure 9.4 With Orifice in Line

Vibrating Tube Model II

Figure 9.12 shows vibrating tube model II which is being constructed to enable single-phase studies. Primarily it will be used to determine the validity of the analytical models associated with system vibration and body forces.

Steady Flow with Imposed Pulsation Model

Equipment has already been procured for modification of the driver unit to allow a net flow of fluid through apertures in the piston. This will enable experimental verification of the nonlinear model.

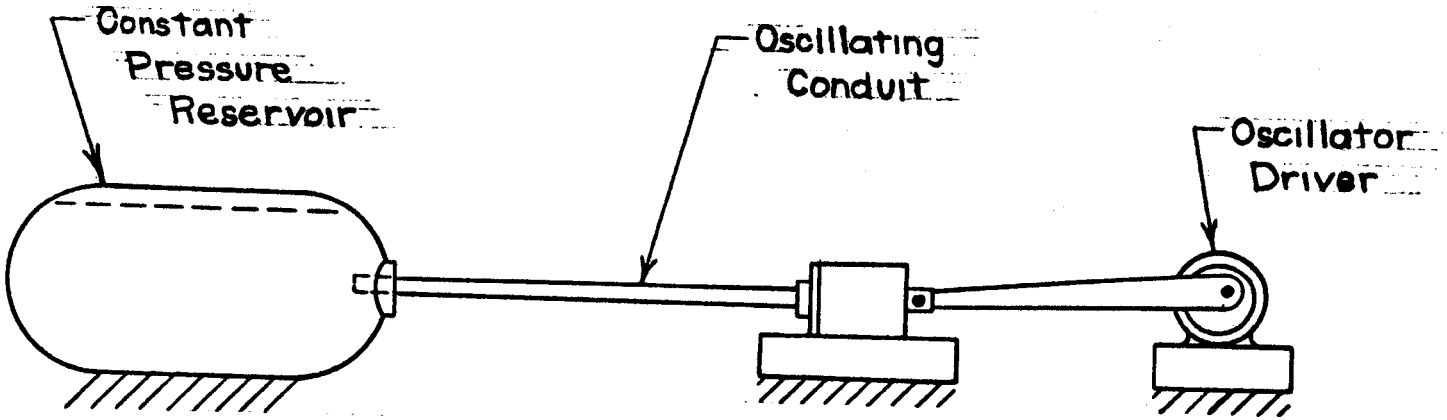

Figure 9.12 Vibrating Tube Model II

BIBLIOGRAPHY

References for Chapter II

1. Lass, H., Vector and Tensor Analysis, McGraw-Hill Book Co., Inc., 1950.

2. Schlichting, H., Boundary Layer Theory, McGraw-Hill Book Co., Inc., 1960.

3. Bird, R. B., W. E. Steward, and E. N. Lightfoot, Transport Phenomena, John Wiley and Sons, Inc., New York, 1960.

4. Joukowsky, N., "Water Hammer," Proceedings American Water Works Association, 1904, p. 341.

5. Allievi, Lorenzo, "Theory of Water Hammer," translated by E. E. Halmos, 1925. See "Symposium on Water Hammer," ASME publication, 1933, Second Printing, 1949.

6. Rich, G. R., Hydraulic Transients, McGraw-Hill Book Co., Inc., New York, 1955.

7. Paynter, H. M., "Section 20, Fluid Transients in Engineering Systems," from Handbook of Fluid Dynamics, by V. L. Streeter, Ed., McGraw-Hill Book Co., Inc., New York, 1961.

8. Walker, M. L., Jr., E. T. Kirkpatrick and W. T. Rouleau, "Viscous Dispersion in Water Hammer," Trans. ASME, Vol. 82, 1960, pp. 759-764.

9. Schuder, C. B. and R. C. Binder, "The Response of Pneumatic Transmission Lines to Step Inputs," Trans. ASME, Series D, Vol. 81, 1959, pp. 578-584.

10. Oldenburger, R. and R. E. Goodson, "Simplification of Hydraulic Line Dynamics by Use of Infinite Products," Trans. ASME, Series D, Vol. 86, 1964, pp. 1-10.

11. Schiesser, Boonshaft and Fuchs, Inc., "The Frequency Response of an Actuator Supplied by Two Long Hydraulic Lines," Trans. AIChE, 1964 Joint Automatic Control Conference, Stanford University.

Chapter II

12. Rouleau, W. T., "Pressure Surges in Pipelines Carrying Viscous Liquids," Trans. ASME, Vol. 82, 1960, pp. 912-920.

13. Sarlat, I. M. and T. L. Wilson, "Surge Pressures in Liquid Transfer Lines," Trans. ASME, Vol. 84, 1962, pp. 363-368.

14. Waller, E. J., "Response of Pipe Line Systems to Transient Flow Using the Generalized Impedance Method," Oklahoma Engineering Experiment Station Publication, Oklahoma State University, January, 1960.

15. Nichols, N. B., "The Linear Properties of Pneumatic Transmission Lines," ISA Trans., Vol. 1, January, 1962, pp. 5-14.

16. Iberall, A. S., "Attenuation of Oscillatory Pressures in Instrument Lines," Journal of Research, National Bureau of Standards, Vol. 45, July, 1950, pp. 85-108.

17. Brown, F. T., "The Transient Response of Fluid Lines," Trans. ASME, Series D, Vol. 84, 1962, pp. 547-553.

18. D'Souze, A. F. and R. Oldenburger, "Dynamic Response of Fluid Lines," Trans. ASME, September, 1964, pp. 589-598.

19. Watson, G. N., A Treatise on the Theory of Bessel Functions, Cambridge University Press, Cambridge, 1958, pp. 77-83, Appendix, p. 78, p. 498.

20. Blackburn, J. F., Gerhard Reethof and J. L. Shearer, Fluid Power Control, The M.I.T. Press, Cambridge, Mass., 1960.

21. Aseltine, J. A., Transform Method in Linear System Analysis, McGraw-Hill Book Co., Inc., New York, 1958.

22. Waller, E. J., L. E. Hove and W. D. Bernhart, "Liquidborne Noise Reduction," Volumes I, II and III, Engineering Report, Oklahoma State University, 1963.

23. Pipes, L. A., "The Matrix Theory of Four-Terminal Networks," Philosophical Magazine, Vol. 30, 1940, pp. 370-395.

24. Bergeron, Waterhammer in Hydraulics and Wave Surges in Electricity, ASME Publication, 1961.

Chapter II

25. Technical Documentary Report No. APL TDR 64-109, "Research Investigation of Hydraulic Pulsation Concepts," October, 1964.

26. Lamb, H., "On the Velocity of Sound in a Tube, as Affected by the Elasticity of the Walls," Manchester Memoirs, Vol. XLII (1898) No. 9, pp. 1-16.

27. Jacobi, W. J., "Propagation of Sound Waves Along Liquid Cylinders," Journal of the Acoustical Society of America, Vol. 21, 1949, pp. 120-127.

28. Morgan, G. W. and J. P. Kiely, "Wave Propagation in Viscous Liquid Contained in a Flexible Tube," Journal of the Acoustical Society of America, Vol. 26, May, 1954, pp. 323-328.

29. Lin, T. C. and G. W. Morgan, "Wave Propagation Through Fluid Contained in a Cylindrical, Elastic Shell," Journal of the Acoustical Society of America, Vol. 28, November, 1956, pp. 1165-1176.

30. Skalak, R., "An Extension of the Theory of Water Hammer," Trans. ASME, Vol. 78, 1956, pp. 105-116.

31. Regetz, J. D., Jr., "An Experimental Determination of the Dynamic Response of a Long Hydraulic Line," NASA Technical Report D-576, December, 1960, pp. 1-38.

32. Shapiro, A. H., Compressible Fluid Flow, The Ronald Press Company, New York, 1953.

33. Goodson, R. E., Viscous and Boundary Effects in Fluid Lines, University Microfilms, Inc., Ann Arbor, Michigan, Ph.D Thesis, January, 1963.

34. Thurston, G. B. and C. E. Martin, Jr., "Periodic Fluid Flow Through Circular Orifices," Journal of the Acoustical Society of America, Vol. 25, January, 1953, pp. 26-31.

References for Chapter III

35. Gouse, S. W., Jr., "An Introduction to Two-Phase Gas-Liquid Flow," AD-No. 603659, June, 1964.

36. Kepple, R. R. and Tung, T. V., "Two-Phase (Gas-Liquid) System: Heat Transfer and Hydraulics; An Annotated Bibliography," ANL-6734, July, 1963.

Chapter III

37. Gouse, S. W. Jr., "An Index to the Two-Phase Gas-Liquid Flow Literature - Part I," AD-No. 411512, May, 1963.

38. Maurer, G. W., "Bibliography on Two-Phase Heat Transfer," WAPD-TM-249, 1960.

39. Maung-Myint, M., "A Literature Survey of Two-Phase Flow of Gas and Liquid," S. B. Thesis, M.I.T., 1959.

40. Gouse, S. W., Jr. and G. A. Brown, "A Survey of the Velocity of Sound in Two-Phase Mixtures," ASME Paper No. 64-WA/FE-35, December, 1964.

41. Martinelli, R. C. and D. B. Nelson, "Prediction of Pressure Drop During Forced-Circulation Boiling of Water," Trans. ASME, Vol. 70, 1948, pp. 695-702.

42. Gouse, S. W., Jr., "Two-Phase Gas-Liquid Flow Oscillations: Preliminary Survey," AD-No. 603652, July, 1964.

References for Chapter IV

43. Strasberg, M., "Undissolved Air Cavities as Nuclei," Cavitation in Hydrodynamics (Proc. Nat. Phys. Lab. Symposium), Paper 6, Her Majesty's Stationery Office, London, 1956.

44. Holl, J. W., "An Effect of Air Content on the Occurrence of Cavitation," Trans. ASME, Series D, Journal of Basic Engineering, Vol. 82, 1960, pp. 941-946.

45. Lehman, A. F. and J. O. Young, "Experimental Investigations of Incipient and Desinent Cavitation," Trans. ASME, Series D, Journal of Basic Engineering, Vol. 86, 1964, pp. 275-284.

46. Kermeen, R. W., "Some Observations of Cavitation on Hemispherical Head Models," Report E-35.1, Hydrodynamics Laboratory, California Institute of Technology.

47. Eisenberg, P., "On the Mechanism and Prevention of Cavitation," The David W. Taylor Model Basin Report 712, July, 1950.

48. Havey, E. N., Wm. D. McElroy, and A. H. Whiteley, "On Cavity Formation in Water," Journal of Applied Physics, Vol. 18, February, 1947, pp. 162-172.

Chapter IV

49. Johnson, V. E., Jr., "Mechanics of Cavitation," Journal of the Hydraulics Division, ASCE, Vol. 89, No. HY 3, Proc. Paper 3530, May, 1963, pp. 251-275.

50. Noltingk, B. E., "Cavitation Produced by Ultrasonics," Proceedings Physical Soc. (B)., London, Vol. 63, 1950, pp. 674-685.

51. Schweitzer, P. H. and V. G. Szebehely, "Gas Evolution in Liquids and Cavitation," Journal of Applied Physics, Vol. 21, December, 1950, pp. 1218-1224.

52. Knapp, R. T., "Cavitation and Nuclei," Transactions of the ASME, Vol. 80, 1958, pp. 1315-1324.

53. Kermeen, R. W., J. T. McGraw, and B. R. Parkin, "Mechanism of Cavitation Inception and the Related Scale-Effects Problem," Trans. ASME, Vol. 77, 1955, pp. 533-541.

54. Robertson, J. M., "Cavitation in Hydraulic Structures: Scale Effects Involved in Cavitation Experiments," Journal of the Hydraulics Division, ASCE, Vol. 89, No. HY 3, Proc. Paper 3520, May, 1963, pp. 167-180.

55. Holl, J. W. and G. F. Wislicenus, "Scale Effects on Cavitation," Trans. ASME, Series D, Journal of Basic Engineering, Vol. 83, 1961, pp. 385-398.

56. Schlichting, H., Boundary Layer Theory, McGraw-Hill Book Company, Inc., 1960.

57. Knapp, R. T. and A. Hollander, "Laboratory Investigations of the Mechanism of Cavitation," Trans. ASME, Vol. 70, 1948, pp. 419-435.

58. Daily, J. W. and V. E. Johnson, Jr., "Turbulence and Boundary-Layer Effects on Cavitation Inception from Gas Nuclei," Trans. ASME, Vol. 78, 1956, pp. 1695-1706.

59. Parkin, B. R., "Scale Effects in Cavitation Flow," Ph.D Dissertation, California Institute of Technology, 1952.

60. Holl, J. W., "The Effect of Surface Irregularities on Incipient Cavitation," Ph.D. Dissertation or TM 5.3410-03, Ordnance Research Laboratory, The Pennsylvania State University, 1958.

Chapter IV

61. Calehuff, G. L. and Wislicenus, G. F., "ORL Investigations of Scale Effects on Hydrofoil Cavitation," TM 19.4212-03, Ordnance Research Laboratory, The Pennsylvania State University, February, 1956.

62. Abbott, I. H., A. E. von Doenhoff, and L. S. Stivers, Jr., "Summary of Airfoil Data," NACA Report 824, 1945.

63. Parkin, B. R. and J. W. Holl, "Incipient-Cavitation Scaling Experiments for Hemispherical and 1.5 Caliber Ogive-Nosed Bodies," Report NOrd 7958-264, Ordnance Research Laboratory, The Pennsylvania State University, May, 1954.

64. Oshima, R., "Theory of Scale Effects on Cavitation Inception on Axially Symmetric Bodies," Trans. ASME, Series D, Journal of Basic Engineering, Vol. 83, 1961, pp. 379-384.

65. Knapp, R. T., "Cavitation Mechanics and Its Relation to the Design of Hydraulic Equipment," Engineering, Vol. 173, 1952, pp. 566-

66. Holl, J. W., "The Inception of Cavitation on Isolated Surface Irregularities," Trans. ASME, Series D, Journal of Basic Engineering, Vol. 82, 1960, pp. 169-183.

67. McCormick, B. W. Jr., "On Cavitation Produced by a Vortex Trailing From a Lifting Surface," Trans. ASME, Series D, Journal of Basic Engineering, Vol. 84, 1962, pp. 369-379.

68. Kermeen, R. W. and B. R. Parkin, "Incipient Cavitation and Wake Flow Behind Sharp-Edged Disks," Report 85-4, Hydrodynamics Laboratory, California Insistute of Technology, August, 1957.

69. Robertson, J. M., J. H. McGinley, and J. W. Holl, "On Several Laws of Cavitation Scaling," La Houille Blanche, September, 1957, p. 540.

70. Numachi, F. and T. Kurokawa, "Über den Einfluss des Luftgehaltes auf die Kavitationsentstehung," [On the Effect of Air Content on the Appearance of Cavitation], Werft-Reederei-Hafen, Vol. 20, 1939.

Chapter IV

71. Crump, S. F., "Determination of Critical Pressures For the Inception of Cavitation in Fresh and Sea Water as Influenced by Air Content of the Water," The David W. Taylor Model Basin, Report 575, October, 1949.

72. Crump, S. F., "Critical Pressures for the Inception of Cavitation in a Large-Scale Numachi Nozzle as Influenced by the Air Content of the Water," The David W. Taylor Model Basin, Report 770, July, 1951.

73. Williams, E. E. and P. McNulty, "Some Factors Affecting the Inception of Cavitation," Cavitation in Hydrodynamics (Proc. Nat. Phys. Lab. Symposium) Paper 2, Her Majesty's Stationery Office, London, 1956.

74. Ruggeri, R. S. and T. F. Gelder, "Effects of Air Content and Water Purity on Liquid Tension at Incipient Cavitation in Venturi Flow," National Aeronautics and Space Administration, TN D-1459, March, 1963.

75. Ruggeri, R. S. and T. F. Gelder, "Cavitation and Effective Liquid Tension of Nitrogen in a Tunnel Venturi," National Aeronautics and Space Administration, TN D-2088, February, 1964.

76. Hammitt, F. G., "Observation of Cavitation Scale and Thermodynamic Effects in Stationary and Rotating Components," Trans. ASME, Series D, Journal of Basic Engineering, Vol. 85, 1963, pp. 1-16.

77. Jacobs, R. B. and K. B. Martin, "Cavitation Problems in Cryogenics," Trans. ASME, Series D, Journal of Basic Engineering, Vol. 82, 1960, pp. 756-757.

78. Numachi, F., M. Yamabe, and R. Ōba, "Cavitation Effect on the Discharge Coefficient of the Sharp-Edged Orifice Plate," Trans. ASME, Series D, Journal of Basic Engineering, Vol. 82, 1960, pp. 1-11.

79. Ball, J. W. and W. P. Simmons, "Progress Report on Hydraulic Characteristics of Pipeline Orifices and Sudden Enlargements Used for Energy Dissipation," Bureau of Reclamation, Hydraulics Branch, Report No. Hyd.-519, December, 1963.

80. Mikol, E. P. and J. C. Dudley, "A Visual and Photographic Study of the Inception of Vaporization in Adiabatic Flow," Trans. ASME, Series D, Journal of Basic Engineering, Vol. 86, 1964, pp. 257-264.

Chapter IV

81. Fauske, H. K. and T. C. Min, "A STudy of the Flow of Saturated Freon - 11 Through Apertures and Short Tubes," ANL-6667, January, 1963.

82. Eisenberg, P., "A Brief Survey of Progress on the Mechanics of Cavitation," The David W. Taylor Model Basin Report 842, June, 1953.

References for Chapter V

83. Florschuetz, L. W. and B. T. Chao, "On the Mechanics of Vapor Bubble Collapse," Trans. ASME, Paper Number 64-HT-23.

84. Zwick, S. A., "The Growth and Collapse of Vapor Bubbles," AD-54059, December, 1954.

85. Plesset, M. S. and S. A. Zwick, "A Nonsteady Head Diffusion Problem with Spherical Symmetry," Journal of Applied Physics, Vol. 23, 1952, p. 95.

86. Plesset, M. S. and S. A. Zwick, "On the Dynamical of Small Vapor Bubbles in Liquids," Journal of Mathematics and Physics, Vol. 33, 1955, p. 308.

87. Plesset, M. S. and S. A. Zwick, "The Growth of Vapor Bubbles in Superheated Liquids," Journal of Applied Physics, Vol. 25, 1954, p. 493.

88. Plesset, M. S., "Bubble Dynamics," AD-298566, February, 1963.

89. Forster, H. K., "Diffusion in a Moving Medium with Time-Dependent Boundaries," A.I.Ch.E. Journal, Vol. 4, 1957, p. 535.

90. Forster, H. K. and Zuber, N., "Growth of a Vapor Bubble in a Superheated Liquid," Journal of Applied Physics, Vol. 25, 1954, p. 474.

91. Zuber, N., "The Dynamics of Vapor Bubbles in Nonuniform Temperature Fields," International Journal of Heat and Mass Transfer, Vol. 2, 1961, p. 83.

Chapter V

92. Birkhoff, G., R. S. Margulies, and W. A. Horning,"Spherical Bubble Growth," The Physics of Fluids, Vol. 1, 1958, p. 201.

93. Bankoff, S. G. and R. D. Mikesell,"Bubble Growth Rates in Highly Subcooled Nucleate Boiling," Chemical Engineering Progress Symposium Series, No. 29, Vol. 55, 1959, p. 95.

94. Scriven, L. E., "On the Dynamics of Phase Growth," Chemical Engineering Science, Vol. 10, 1959, p. 1.

95. Yang, W. and J. A. Clark, "On the Application of the Source Theory to the Solution of Problems Involving Phase Change. Part I - Growth and Collapse of Bubbles," Trans. ASME, Journal of Heat Transfer, 1964, p. 207.

96. "Summary of Conference on Bubble Dynamics and Boiling Heat Transfer Held at the Jet Propulsion Laboratory June 14 and 15, 1956," AD-118586.

97. Plesset, M. S., "The Dynamics of Cavitation Bubbles," Journal of Applied Mechanics, September, 1949, p. 277.

98. Dergarabedian, P., "The Rate of Growth of Vapor Bubbles in Superheated Water," Journal of Applied Mechanics, 1953, p. 537.

99. Engelberg-Forster, K. and R. Greif, "Heat Transfer to a Boiling Liquid-Mechanism and Correlation," Trans. ASME, Journal of Heat Transfer, 1959, p. 43.

100. Costello, C. P. and W. E. Tuthill, "Effects of Acceleration on Nucleate Pool Boiling," Chemical Engineering Progress Symposium Series, No. 32, Vol. 57, p. 189.

101. Gunther, F. C., "Photographic Study of Surface Boiling Heat Transfer to Water with Forced Convection," Trans. ASME, 1951, p. 115.

102. Forster, H. K. and N. Zuber, "Dynamics of Vapor Bubbles and Boiling Heat Transfer," A.I.Ch.E. Journal, Vol. 1 1955, p. 531.

103. Zuber, N. and E. Fried, "Two-Phase Flow and Boiling Heat Transfer to Cryogenic Liquids," American Rockets Society Journal, September, 1962, p. 1332.

Chapter V

104. Progress in Cryogenics Vol. 2, K. Mendelssohn (Editor), 1960.

105. Staniszewski, B. M., "Nucleate Boiling Bubble Growth and Departure," AD-227262, August, 1959.

106. Bankoff, S. G. and J. P. Mason, "Heat Transfer From the Surface of a Steam Bubble in Turbulent Subcooled Liquid Stream," A.I.Ch.E. Journal, March, 1962, p. 30.

ADDITIONAL REFERENCES

Chapter II

107. Abbott, M. R., "Axially Symmetric Steady Motion of a Viscous Incompressible Fluid: Some Numerical Experiments," February, 1963. (AD 407-510)

108. Abbott, M. R., "Solution of Non-Linear Wave Equation," May, 1962. (AD 283-590)

109. Aerospace Information Division Library of Congress, "Use of Variational Methods in Problems of Vibration of Liquid and Liquid-filled Bodies," December, 1962. (AID Report 62-203) (AD 292-340)

110. Babenko, G. S., and A. M. Smirnov, "Effect of the Viscosity of Liquids in Hydraulic Piping on its Dynamic Properties," Automation and Remote Control, Vol. 24, Part 1, January, 1963, pp. 106-109.

111. Barn, M. L., A. T. Matthews, and H. H. Bleich, "Forced Vibrations of an Elastic Circular Cylindrical Body of Finite Length Submerged in an Acoustic Fluid," June, 1962. (AD 286-905)

112. Beatty, R. E., Jr., "Boundary Layer Attenuation of Higher Order Modes in Rectangular and Circular Tubes," Journal of the Acoustical Society of America, Vol. 22, November, 1950, pp. 850-854.

113. Bennett, M. D., "Pressure Response in a Long Tube Which is Closed at One End," Aero-Thermodynamics, SC-4646(RR), November, 1951, pp. 1 and 3-22.

114. Biot, M. A., "Propagation of Elastic Waves in a Cylindrical Bore Containing a Fluid," Journal of Applied Physics, Vol. 23, September, 1952, pp. 997-1005.

115. Blackstock, David T., "Approximate Equations Governing Finite-Amplitude Sound in Thermoviscous Fluids," May, 1963, General Dynamics Corporation. (AD 415-442)

Chapter II

116. Blackstock, D. T., "Propagation of Plane Sound Waves of Finite Amplitude in Nondissipative Fluids," Journal of the Acoustical Society of America, Vol. 34, January, 1962, pp. 9-30.

117. Blokhintzev, D., "The Propagation of Sound in an Inhomogeneous and Moving Medium I," Journal of the Acoustical Society of America, Vol. 18, October, 1946, pp. 322-328.

118. Bochner, S., "Almost Periodic Solutions of the Inhomogeneous Wave Equation," Proc. National Academy Science, Vol. 46, Part 2, 1960, pp. 1233-1236.

119. Browder, J. E., "On Non-Linear Wave Equations," Mathematics Zeitschr, Vol. 80, 1962, pp. 249-264.

120. Brown, F. T., S. E. Nelson, "Step Responses of Liquid Lines With Frequency-Dependent Effects of Viscosity," Trans. ASME, Paper No. 64-WA/FE-6, pp. 1-7.

121. Chang, S. S. L., "Transient Effects of Supply and Connecting Conduits in Hydraulic Control Systems," Franklin Institute Journal, Vol. 262, 1956, pp. 437-452.

122. Cohen, Hirsh and Yih-O-Tu, "Viscosity and Boundary Effects in the Dynamic Behavior of Hydraulic Systems," Trans. ASME, Series D, Vol. 84, 1962, pp. 593-601.

123. Contractor, D. N., "The Reflection of Waterhammer Pressure Waves from Minor Losses," Trans. ASME, Paper No. 64-WA/FE-16, pp. 1-7.

124. Eckart, C., "Vortices and Streams Caused by Sound Waves," Physical Review, Vol. 73, 1948, pp. 68-76.

125. Elrod, H. G., Jr., "The Theory of Pulsating Flow in Conical Nozzles," Trans. ASME, Vol. 85, Part E, March, 1963, pp. 1-6.

126. Ezekiel, F. D., "The Effect of Conduit Dynamics of Control-Valve Stability," Trans. ASME, Vol. 80, 1958, pp. 904-908.

127. Fay, R. D., "Waves in Liquid-Filled Cylinders," Journal of the Acoustical Society of America, Vol. 24, No. 5, September, 1952, pp. 459-462.

Chapter II

140. Paynter, H. M. and F. D. Ezekiel, "Water Hammer in Nonuniform Pipes as an Example of Wave Propagation in Gradually Varying Media," Trans. ASME, Vol. 80, 1958, pp. 1585-1595.

141. Rich, G. R., "Water-Hammer Analysis by the Laplace-Mellin Transformation," Trans. ASME, Vol. 67, 1945, pp. 361-376.

142. Richardson, E. G., and E. Tyler, "The Transverse Velocity Gradient Near the Mouths of Pipes in Which an Alternating or Continuous Flow of Air is Established," The Proceedings of the Physical Society, Vol. 42, No. 231, December, 1929, pp. 1-15.

143. Rohmann, C. P. and E. C. Grogan, "On the Dynamics of Pneumatic Transmission Lines," Trans. ASME, Vol. 79, 1957, pp. 853-874.

144. Rouleau, W. T. and F. J. Young, "Distortion of Short Pulses in Tapered Tube Pulse Transformers. Part I - Inviscid Liquid," Trans. ASME, 64-WA/FE-11, pp. 1-6.

145. Rouleau, W. T. and F. J. Young, "Distortion of Short Pulses in Tapered Tube Pulse Transformers. Part II - Inviscid Liquid," Trans. ASME, Paper No. 64-WA/FE-12, pp. 1-6.

146. Sabersky, Rolf H., "Effect of Wave Propagation in Feed Lines on Low-Frequency Rocket Instability," Jet Propulsion, Vol. 24, 1954, pp. 172-174.

147. Schiesser, Boonshaft and Fuchs, Inc., "The Frequency Response of an Actuator Supplied by Two Long Hydraulic Lines," Trans. AIChE, 1964 Joint Automatic Control Conference, Stanford University.

148. Schuder, C. B. and G. C. Blunck, "The Driving Point Impedance of Fluid Process Lines," ISA Transactions, January, 1963, Vol. 2, Part 1, pp. 39-45.

149. Sexl, Theodor, "Uber den von E. G. Richardson's entdeckten 'Annulareffekt'," Z. Phys., Vol. 61, 1930, pp. 349-362.

150. Sibley, W. A. and W. G. Oakes, "Dynamic Characteristics of a Liquid Filled Tube," American Rocket Society Publication, November, 1956, pp. 5953-5987.

151. Skalak, R., "An Extension of the Theory of Water Hammer," Trans. ASME, Vol. 78, 1956, pp. 105-116.

Chapter II

152. Thomson, W. T., "Transmission of Pressure Waves in Liquid Filled Tubes," Proceedings of First U.S. Congress of Applied Mechanics, pp. 927-933.

153. Thurston, G. B., "Periodic Fluid Flow Through Circular Tubes," Journal of the Acoustical Society of America, Vol. 24, November, 1952, pp. 653-656.

154. Uchida, S., "The Pulsating Viscous Flow Superposed on the Steady Laminar Motion of Incompressible Fluid in a Circular Pipe," ZAMP, Vol. VII, 1956, pp. 403-422.

Chapter IV - Cavitation

155. Ball, J. W., "Cavitation Characteristics of Gate Valves and Globe Valves Used as Flow Regulators Under Heads Up to About 125 Feet," Trans. ASME, Vol. 79, 1957, pp. 1275-1283.

156. Ball, J. W., "Hydraulic Characteristics of Gate Slots," ASCE, Journal of the Hydraulics Division, Vol. 85, No. HY10, 1959, pp. 81-114.

157. Briggs, J. L., "The Maximum Superheating of Water as a Measure of Negative Pressure," Journal of Applied Physics, Vol. 26, 1955, pp. 1001-1003.

158. Briggs, J. L., "Limiting Negative Pressure of Water," Journal of Applied Physics, Vol. 21, 1950, pp. 721-722.

159. Brown, F. R., "Cavitation in Hydraulic Structures: Problems Created by Cavitation Phenomena," Journal of the Hydraulics Division, ASCE, Vol. 89, January, 1963, pp. 99-115.

160. "Cavitation in Hydrodynamics," Proc. Symposium Natl. Phys. Lab., London, 1956.

161. "Cavitation in Hydraulic Structures: A Symposium," Proc. Amer. Soc. Civ. Engrs., Vol. 71, September, 1945, pp. 999-1068.

162. "Cavitation in Hydrodynamics," Proceedings, Symposium of the National Physical Laboratory, London, September 14-17, 1955.

Chapter IV - Cavitation

163. Daily, J. W., "Cavitation Characteristics and Infinite-Aspect - Ratio Characteristics of a Hydrofoil Section," Trans. ASME, Vol. 71, 1949, pp. 269-284.

164. Dean, R. B., "The Formation of Bubbles," Journal of Applied Physics, Vol. 15, 1944, pp. 446-451.

165. Eisenberg, P., "Modern Developments in the Mechanics of Cavitation," Applied Mechanics Reviews, Vol. 10, 1957, pp. 85-89.

166. Eisenberg, P., "Cavitation," International Science and Technology, February, 1963, pp. 72-84.

167. Eisenberg, P. and M. P. Tulin, "Cavitation," Handbook of Fluid Dynamics, McGraw-Hill Book Company, Inc., 1961.

168. Fisher, J. C., "The Fracture of Liquids," Journal of Applied Physics, Vol. 19, 1948, pp. 1062-1067.

169. Fox, F. E. and K. F. Herzfeld, "Gas Bubbles with Organic Skin as Cavitation Nuclei," Journal of the Acoustical Society of American, Vol. 26, 1954, pp. 984-989.

170. Harvey, E. N., K. W. Cooper, and A. H. Whiteley, "Bubble Formation from Contact of Surfaces," Journal of the American Chemical Society, Vol. 68, Part 2, 1946, pp. 2119-2120.

171. Harvey, E. N., D. K. Barnes, W. D. McElroy, A. H. Whiteley, D. C. Pease, and K. W. Cooper, "Bubble Formation in Animals," Journal of Cellular and Comparative Physiology, Vol. 24, 1944, pp. 23-44.

172. Harvey, E. N., D. K. Barnes, W. D. McElroy, A. H. Whiteley, and D. C. Pease, "Removal of Gas Nuclei From Liquid s and Surfaces," Journal of the American Chemical Society, Vol. 67, 1945, pp. 156-157.

173. Hunsaker, J. C., "Cavitation Research," Mechanical Engineering, Vol. 57, 1935, pp. 211-216.

174. Jakobsen, J. K., "On the Mechanism of Head Breakdown in Cavitating Inducers," Trans. ASME, Series D, Journal of Basic Engineering, Vol. 86, 1964, pp. 291-305.

Chapter IV - Cavitation

175. Jarman, P. D. and K. J. Taylor, "Light Emission from Cavitating Water," Brit. Journal of Applied Phys., Vol. 15, 1964, pp. 321-322.

176. Numachi, F., R. Kobayashi, and S. Kamiyama, "Effect of Cavitation on the Accuracy of Herschel - Type Venturi Tubes," Trans. ASME, Series D, Journal of Basic Engineering, Vol. 84, 1962, pp. 351-362.

177. Pease, D. C. and L. R. Blinks, "Cavitation From Solid Surfaces in the Absence of Gas Nuclei," Journal of Phys. Colloid Chem., Vol. 51, 1947, pp. 556-567.

178. Robertson, J. M., "Water Tunnels for Hydraulic Investigations," Trans. ASME, Vol. 78, 1956, pp. 95-104.

179. Rouse, H., "Cavitation in the Mixing Zone of a Submerged Jet," La-Houille Blanche, 1953, pp. 9-19.

180. Rouse, H. and J. S. McNown, "Cavitation and Pressure Distribution: Head Forms at Zero Angle of Yaw," State University Iowa Studies in Engr. Bull 32, 1948.

181. Rouse, H., "Cavitation and Pressure Distribution: Head Forms at Angles of Yaw," State University Iowa Studies in Engr. Bull. 42, 1962.

182. Sarosdy, L. R. and A. J. Acosta, "Note on Observations of Cavitation in Different Fluids," Trans. ASME, Series D, Journal of Basic Engineering, Vol. 83, 1961, pp. 399-400.

183. Stahl, H. A. and A. J. Stepanoff, "Thermodynamic Aspects of Cavitation in Centrifugal Pumps," Trans. ASME, Vol. 78, 1956, pp. 1691-1693.

184. Stepanoff, A. J., "Cavitation Properties of Liquids," Trans. ASME, Series A, Journal of Engineering for Power, Vol. 86, 1964, pp. 195-200.

185. Stiles, G. F., "Cavitation in Control Valves," Instruments and Control Systems, Vol. 34, 1961, pp. 2086-2093.

186. Strasberg, N., "The Influence of Air-Filled Nuclei on Cavitation Inception," David W. Taylor Model Basin Report 1078, May, 1957.

Chapter IV - Cavitation

187. Temperley, H. V. N. and L. L. G. Chambers, "The Behavior of Water Under Hydrostatic Tension," Proc. Physical Society, (London), Vol. 58, 1946, pp. 420-443.

188. Thomas, H. A. and E. P. Schuleen, "Cavitation in Outlet Conduits of High Dams," Trans. of the ASCE, Vol. 107, 1942, pp. 421-493.

189. Wang, P. K. C. and J. T. S. Ma, "Cavitation in Valve-Controlled Hydraulic Actuators," Trans. ASME, Series E Journal of Applied Mechanics, Vol. 85, 1963, pp. 537-546.

190. Ziegler, G., "Tensile Stresses in Flowing Water," Cavitation in Hydrodynamics, (Proc. Nat. Phys. Lab. Symposium), Paper 3, Her Majesty's Stationery Office, London, 1956.

Chapter IV - Ultrasonic Cavitation

191. Akulichev, V. A. and V. I. Il'ichev, "Spectral Indication of the Origin of Ultrasonic Cavitation in Water," Soviet Physics - Acoustics, Vol. 9, 1963, pp. 128-130 (English Translation).

192. Bondy, C. and K. Söllner, "On the Mechanism of Emulsification by Ultrasonic Waves," Trans. Faraday Society, Vol. 31, Part I, 1935, pp. 835-846.

193. Brown, B., "Ultrasonic Cavitation in Water," British Communications and Electronics, Vol. 9, Part 2, 1962, pp. 918-920.

194. Connolly, W. and F. E. Fox, "Ultrasonic Cavitation Thresholds in Water," Journal of the Acoustical Society of America, Vol. 26, 1954, pp. 843-848.

195. Gabrielli, I. and G. Iernetti, "Cavitation and Chemical Effects in Ultrasonic Stationary Fields," Acustica, Vol. 13, 1963, pp. 165-174.

196. Gaertner, W., "Frequency Dependence of Ultrasonic Cavitation," Journal of the Acoustical Society of America, Vol. 26, 1954, pp. 977-980.

Chapter IV - Ultrasonic Cavitation

197. Gallant, H., "Untersuchungen über Kavitationsblasen," Österreichische Ingenieur Zeitschrift, Vol. 5, 1962, pp. 74-83.

198. Galloway, W. J., "An Experimental Study of Acoustically Induced Cavitation in Liquids," Journal of the Acoustical Society of America, Vol. 26, 1954, pp. 849-857.

199. Goldsmith, H. A. and R. C. Heim, "New Way to Measure Ultrasonic Cavitation Intensity," Metal Engineering Quarterly, Vol. 2, No. 1, 1962, pp. 62-66.

200. Kozyrev, S. P., "Ultrasonic Apparatus for Testing Materials for Cavitation - Abrasive Wear," Industrial Laboratory, Vol. 29, No. 2, 1963, pp. 216-218.

201. Mellen, R. H., "Ultrasonic Spectrum of Cavitation Noise in Water," Journal of the Acoustical Society of America, Vol. 26, 1954, pp. 356-360.

202. Messino, D., D. Sette, and F. Wanderlingh, "Statistical Approach to Ultrasonic Cavitation," Journal of the Acoustical Society of America, Vol. 35, 1963, pp. 1575-1583.

203. Neppiras, E. A. and B. E. Noltingk, "Cavitation Produced by Ultrasonics: Theoretical Conditions for the Onset of Cavitation," Proc., Phys. Soc. (B), Vol. 64, 1951, pp. 1032-1038.

204. Numachi, F., "Transitional Phenomena in Ultrasonic Shock Waves Emitted by Cavitation on Hydrofoils," Trans. ASME, Series D, Journal of Basic Engineering, Vol. 81, 1959, pp. 153-166.

205. Sette, D. and F. Wanderlingh, "Nucleation by Cosmic Rays in Ultrasonic Cavitation," Physical Review, Vol. 125 No. 2, 1962, pp. 409-417.

206. Weissler, A., "A Chemical Method for Measuring Relative Amounts of Cavitation in an Ultrasonic Cleaner," IRE International Convention Record, Vol. 10, Part 6, 1962, pp. 24-30.

207. Willard, G. W., "Ultrasonically Induced Cavitation in Water: A Step-by-Step Process," Journal of the Acoustical Society of America, Vol. 25, 1953, pp. 669-686.

208. Wilson, R. W., "Influence of Physical Properties of Liquids on Severity of Cavitation Damage," Compressed Air and Hydraulics, Vol. 27, No. 319, 1962, pp. 382-385.